Stony Brook University

Study of Lipid Raft Formation in Model Membranes and Cells

A Dissertation Presented

by

Priyadarshini Pathak

to

The Graduate School

in Partial Fulfillment of the

Requirements

for the Degree of

Doctor of Philosophy

In

Chemistry

Stony Brook University

December 2012

Stony Brook University
The Graduate School

Priyadarshini Pathak

We, the dissertation committee for the above candidate for the
Doctor of Philosophy degree, hereby recommend
acceptance of this dissertation.

Dr. Erwin London – Dissertation Advisor
Professor, Department of Biochemistry and Cell Biology

Dr. Daniel Raleigh - Chairperson of Defense
Professor, Department of Chemistry

Dr. Carlos Simmerling- Third Member
Professor, Department of Chemistry

Dr. James Konopka- Outside Member
Professor, Department of Molecular Genetics and Microbiology

This dissertation is accepted by the Graduate School

Charles Taber
Interim Dean of the Graduate School

Abstract of the Dissertation

Study of lipid raft formation in model membranes and cells

by

Priyadarshini Pathak

Doctor of Philosophy

in

Chemistry

Stony Brook University

2012

Ordered membrane domains, (conventionally called lipid rafts) are tightly packed sphingolipid and cholesterol rich domains, proposed to co-exist with disordered domains, in the plasma membrane. In spite of many cellular functions allotted to rafts, their direct detection in cells has been difficult. Rafts may be too small to detect and this could easily be misinterpreted as their absence. For this reason, the contention that in the absence of detergent Triton X-100 (commonly used to isolate rafts), domains may not exist in the lipid mixture resembling the plasma membrane, was investigated. A novel FRET pair variation assay in which, FRET pairs with successively smaller interaction distances, were used to detect nanodomains and roughly estimate domain size. A lipid mixture in which rafts were claimed to be Triton induced was used. Domains were detected at physiological temperature even in the absence of Triton and their size gradually decreased with increase in temperature. In addition, Triton and transmembrane peptides increased domain size by coalescing smaller nanodomains and made detection easier.

Next, domain formation was studied in living cells. The outer membrane of the spirochete *Borrelia burgdorferi* contains microdomains enriched in (unusual) cholesterol glycolipids and

free cholesterol. To determine whether these recently discovered microdomains are ordered domains, the correlation between structure and domain forming abilities of sterols, characterized by our lab previously, was used in conjunction with a novel FRET assay. It was found that ordered domain favoring sterols were both necessary and sufficient for the formation of domains in living *B.burgdorferi* cells. Domains were also detected in untreated *B.burgdorferi* cells. This study provides evidence for the existence of lipid rafts in living cells. The sterol substitution strategy applied in this report may be extended to study domain formation in eukaryotic cells.

To my family,

with love and gratitude

Table of Contents

List of Tables

List of Figures

List of Abbreviations

10SLPC	1-palmitoyl-2-stearoyl-(10-doxyl)-phosphatidylcholine
10SLPC	10-spin labeled PC
Å	angtroms
A	area
ACGal	acylated cholesteryl galactoside
AFM	atomic force microscopy
B.b	*Borrelia burgdorferi*
BCR	B cell receptor
BSK-H	Barbour-Stoenner-Kelly-H
bSM	porcine brain sphingomyelin
bSM	brain sphingomyelin
CGal	cholesteryl galactoside
CHAPS	3-[(3-Cholamidopropyl)dimethylammonio]-1-propanesulfonate
Chol	cholesterol
DArPC	1,2-diarachaonylphosphatidylcholine
DLPC	dilaurylphosphatidylcholine
DOPC	1, 2- dioleoyl-sn-glycero-3-phosphatidylcholine
DOPE	1, 2- dioleoyl-sn-glycero-3-phosphatidylethanolamine
DPH	1,6-diphenyl-1,3,5-hexatriene
DPPC	1, 2- dipalmitoyl-sn-glycero-3-phosphatidylcholine
DRM	detergent resistant membrane
ε	molar extinction co-efficient
eSM	chicken egg sphingomyelin
eSM	egg sphingomyelin
ESR	electron spin resonance

F	donor /fluorophore fluorescence intensity in presence of acceptor/quencher
Fo	donor /fluorophore fluorescence intensity in absence of acceptor/quencher
FRET	fluorescence resonance energy transfer
G	gel
g	acceleration due to gravity
GM1	monosialotetrahexosylganglioside
GP	generalized polarization
GPI	glycosylphosphatidylinositol
GPMV	giant plasma membrane vesicles
GUV	giant unilamellar vesicles
HBSS	Hank's buffered salt solution
IgE	immunoglobulin E
LAURDAN	6-dodecanoyl-2-dimethylaminonaphthalene
Ld	liquid disordered
Lo	liquid ordered
LUV	large unilamellar vesicles
LW peptide	Acetyl-$K_2W_2L_8AL_8W_2K_2$-amide
MβCD	methyl beta cyclodextrin
MGalD	monogalactosyl diacylglycerol
MLV	multilamellar vesicles
NBD-DPPE	1,2-dipalmitoylphosphatidylethanolamine-N-(7-nitro-2-1,3-benzoxadiazol-4-yl)
ODRB	octadecyl rhodamine B
OspB	outer surface protein B
PBS	phosphate buffered saline
PC	phosphatidylcholine

PG	phosphatidylglycerol
POPC	1-palmitoyl-2-oleoyl-phosphatidylcholine
pyrene-DPPE	1,2-dipalmitoylphosphatidylethanolamine-N-(1-pyrenesulfonyl) ammonium salt
R_c	critical radius
R_{domain}	radius of domain
rhod-DOPE	1,2-dioleoylphosphoethanolamine-N-(Lissamine rhodamine B sulfonyl)
rhod-DOPE	rhodamine DOPE
Ro	Förster radius
SM	sphingomyelin
SNARE	soluble NSF attachment protein receptor
SUV	small unilamellar vesicles
TCR	T cell receptor
TEM	transmission electron microscopy
TEMPO	2,2,6,6-Tetramethylpiperidine 1-oxyl,
TIRF	total internal reflection fluorescence
Tm	melting temperature
TM	transmembrane
TMADPH	1-(4-trimethylammonium)-6-phenyl-1, 3, 5-hexatriene *p*-toluenesulfonate
T_{mid}	midpoint melting temperature
Tupper	upper temperature limit of facile domain detection
TX-100	Triton X-100

Acknowledgments

First of all, I sincerely thank my advisor and role model, Dr. Erwin London for his invaluable guidance and advice that I will cherish throughout my life. As an accomplished scientist, he is unique because his nature is a blend of both kindness and genius: a trait that in my opinion is very rarely found. I thank him for always finding time to answer all my questions with patience and for the hours of insightful discussions that helped me think of a problem from different perspectives. For me, he played the roles of mentor, advisor, and a mind reader of reviewers.

I thank my committee members Dr. Raleigh, Dr. Simmerling and Dr. Konopka for their helpful suggestions. I am grateful to Dr. Jorge Benach and Dr. Timothy LaRocca for their encouragement and support during our collaborative project. I thank all my lab mates for good company but especially Lindsay Nelson for always being there for me even after she graduated. I will always depend on her for instant help and genuine advice.

I thank my day care provider, Ms Lori Gillam for lovingly taking care of my daughter Radha and alleviating the myriad worries of a graduate student mom in the dissertation writing phase.

I cannot thank my in laws enough for their kind support and everything they did to make my life as a graduate student bearable. I thank my Mom and Dad for opening an avenue, right from my first science book and set to graduate school. I thank my mom who completely took care of me and my children during my writing phase. For every sacrifice she has made to raise me, and help me get where I stand now, I am sincerely grateful. I could achieve this due to her relentless encouragement over long distance calls during the hardest of all times in my graduate life, her positive, calm nature and tremendous patience and trust in me. I thank my sisters Monica and Rashmi for setting a good example, for their advice on perseverance and for always being there for me. Importantly, I thank my grandparents who I miss and remember every single day with love. Their four step study mantra: “read, think, understand and explain” will always guide me.

I thank my husband, Dr. Riwij Kulkarni, for his complete and sincere love and dedication to our family and my career. I would often come home from work to find a hearty meal ready and our kids snoring in bed, in spite of his three hour daily commute to work. This encouraged me to work harder. I also thank him for critical suggestions for parts of my dissertation. I thank my well behaved daughters Radha and Sharada for filling my life with immense happiness and love. For this and much more I dedicate my dissertation to my family.

Publications in Peer Reviewed Journals

1. LaRocca TJ*, **Pathak P***, Chiantia S, Toledo A, Dastgheib-Behesti K, Silvius JR, Benach JL and London E. **(* Equal contribution)**. Proving Lipid Rafts Exist: Lipid Raft Formation and Properties are Necessary and Sufficient for Membrane Domain Formation in Borrelia burgdorferi. (Submitted)

2. **Pathak P** and London E (2011) Measurement of Lipid Nanodomain (Raft) Formation and Size in Sphingomyelin/POPC/Cholesterol Vesicles Shows TX-100 and Transmembrane Helices Increase Domain Size by Coalescing Pre-Existing Nanodomains But Do Not Induce Domain Formation. Biophysical Journal 101 (2417-2425).

3. LaRocca TJ, Crowley JT, Cusack BJ, **Pathak P**, Benach J, London E, Garcia-Monco JC and Benach JL. (2010). Cholesterol lipids of Borrelia burgdorferi form lipid rafts and are required for the bactericidal activity of a complement-independent antibody. Cell Host Microbe 8 (331-342).

4. Omar Bakht, **Pathak P** and London E. (2007). Effect of the structure of lipids favoring disordered domain formation on the stability of cholesterol-containing ordered domains (lipid rafts): Identification of multiple raft-stabilization mechanisms. Biophysical Journal 93 (4307-4318).

Important Note: This dissertation only includes the data from experiments performed by Pathak P. It does not include data from experiments performed by other authors. Therefore, Chapter 4 may seem incomplete to some readers. All readers are kindly referred to the above publications for a complete manuscript.

Chapter 1

Introduction:

The plasma membrane is a protein-containing amphiphilic lipid bilayer that forms a selectively permeable enclosure to regulate the interaction between the cell and the extracellular environment. Plasma membrane lipids differ from each other in size and charge of the head groups as well as in length and saturation of their acyl chains (Figure 1.1A, 1.1B and 1.1C). This structural diversity may impact not only the asymmetric distribution of lipids across the two leaflets but also the formation of lipid domains in the plane of the membrane. (Figure 1.1 D) In model membrane vesicles, immiscibility of dissimilar lipids results in association of similar lipids with each other to form lipid domains. Moreover, since a majority of the plasma membrane lipids are unsaturated glycerophospholipids (that have at least one cis double bond), it is hypothesized that these lipids segregate from mixtures of saturated acyl chain lipids such as sphingolipids and flat, rigid sterols such as cholesterol, which can combine to form ordered membrane domains (1). These ordered domains are conventionally called lipid rafts to denote lipid-protein platforms floating in a sea of phospholipids (2). (Figure 1.2A)

It is commonly understood that proteins perform most of the membrane functions by serving as channels, receptors and transducers. Segregation of the plasma membrane into domains may facilitate protein function. Ordered domains may assist protein function by clustering interacting proteins into one domain or by segregating non-interacting proteins into different domains (3-5) (Figure 1.2A). In fact, various cellular processes such as signal transduction, viral and bacterial cell entry and lipid sorting have been linked to the formation of ordered domains in cell membranes (6-10). Despite their functional significance, proving the presence of ordered domains in cells in a direct, unambiguous manner has been a challenging task and whether and under what conditions they form is one of the remaining mysteries of the cell (11). Thus, to gain insights into the formation of ordered domains in cells, lipid mixtures that form phase separated membranes have been studied in simple model membranes.

Development of the raft model of the cell membrane:

Prior to the raft model, the plasma membrane was described using the fluid mosaic model (Figure 1.2B). Proposed in early 1970s, this model relied on electron microscopic observations which illustrated that the plasma membrane is a bilayer of lipids as well as on a study involving

the fusion of antibody labeled human and mouse cells which revealed that proteins from both cells mix and diffuse in the plane of the membrane upon fusion (12,13). Interestingly, the fluid mosaic model did not consider lipids to play any additional role in cellular function apart from forming a selective barrier controlling the passage of material across the cell membrane. Based on the research that followed, our portrayal of the distribution of lipids and proteins in the cell membrane has undergone a sea change. This has been largely based upon the study of physical properties of the lipid bilayer such as lipid phase behavior in model membranes (1,14-17) that helped explain observations that were not considered in the fluid mosaic model (9,18,19). This is discussed below.

Historically, the idea of lipid rafts as sorting platforms emerged from studies in epithelial cells. The membrane of epithelial cells that line our body cavities is polarized into two distinct regions: the apical region (facing the lumen or the cavity of the organ) and the basolateral region (facing the tissue or the neighboring cells). These two regions are separated by an intra membrane diffusion barrier called a tight junction (9,20). Owing to the tight junction, the lipids in apical and basolateral regions of the plasma membrane do not mix with each other as judged by the placement of a fluorescent lipid probe (21). The apical, (rather than the basolateral) membrane is enriched in glycosphingolipids (saturated acyl chains) (9) and is considered as an example of raft formation. The role of rafts as lipid as well as protein sorting platforms that may be employed during transportation of proteins from the Golgi was further highlighted by the observation that influenza virus hemaglutinin and GPI anchored proteins such as placental alkaline phosphatase are found in ordered membrane (sphingolipids and cholesterol rich) regions before migrating to the surface of the cell (19,22). Even though involvement of rafts in epithelial cell sorting is not completely clear (23,24), understanding the physical properties of lipid bilayers using model membranes based upon the observations in epithelial cells, has given us important insights into their possible formation in cell membranes.

Physical properties of a lipid bilayer:

1. Lipid phase behavior:

When added to water, most membrane lipids arrange into an amphipathic bilayer, with polar head groups facing the water and the nonpolar hydrophobic tails facing the center of the bilayer. Lipid bilayers can exist in a solid like ordered gel (G) state or a fluid like liquid disordered (Ld) state (Figure 1.3). Bilayers in the G state are composed of lipids that are tightly packed owing to strong Van der Waals interactions between their acyl chain atoms and have slow lateral diffusion rates. These bilayers are relatively thick due to their extended acyl chains (25). In contrast, the bilayers in Ld state are composed of lipids that are loosely packed due to weaker lipid-lipid interactions, are thinner due to less extended acyl chains and have faster lateral diffusion rates. Interestingly, there is a third state that was first described in the 1980s: the liquid ordered (Lo) state (26). Bilayers in the Lo state are made of tightly packed saturated lipids and cholesterol and have intermediate properties between those of G and Ld states. For example, similar to the Ld state, Lo state lipids have a high rate of lateral diffusion (27,28). However, similar to the G state, Lo state bilayers contain tightly packed lipids forming a thicker bilayer.

2. Phase transition:

Bilayers composed purely of a specific lipid undergo a melting transition at a characteristic lipid melting temperature, Tm (Figure 1.4A). At temperatures below its Tm, a lipid bilayer is in a tightly packed G state while at temperatures above Tm, the G state bilayer undergoes a phase transition into a loosely packed Ld state. Hence, Tm of a lipid is a measure of the stability of its gel state and depends on the chemical structure of its acyl chains (29).

Lipids with unsaturated acyl chains bend around the cis double bond to form a kink in the tail, tend to be loosely spaced next to one another in a bilayer and have a low gel to Ld Tm; whereas lipids with saturated acyl chains prefer to be packed tightly with each other in a bilayer and so have a high gel to Ld Tm. (Figure 1.4B and figure 1.4C) Most naturally occurring glycerophospholipids have at least one cis double bond and so are low melting lipids. For

example, POPC, a lipid with one saturated and one unsaturated acyl chain melts at a lower temperature than mostly saturated naturally occurring lipids such as sphingomyelin (SM) and glycosphingolipids which have saturated acyl chains (30,31) (Table 1) and (Figure 1.5).

3. Ordered and disordered phase co-existence:

High Tm lipids are partly immiscible with low Tm lipids (at temperatures below the Tm of the high Tm lipid and above the Tm of the low Tm lipid) because of their different acyl chain packing properties. This leads to gel and liquid disordered phase co-existence over a range of lipid compositions.

Similarly, low Tm lipids are partly immiscible with mixtures of high Tm lipids with cholesterol and ternary mixtures containing these lipids can phase separate into Ld and Lo phases that co-exist over a range of temperatures (14). (Figure 1.6A and figure 1.6B). An illustration of how acyl chain packing properties can lead to phase separation, comes from the observation that Ld state lipids are found in tubules having high membrane curvature and are sorted from Lo state lipids (32), which prefer not to reside in a curved membrane due to their tightly packed acyl chains

Detergent Resistant Membranes (DRM):

Lo and Ld domains in cells are proposed to co-exist and participate in many functions, especially by controlling protein-protein interactions. In order to study Lo domains and related processes in cells, their protein and lipid composition must be first evaluated. The composition provides information regarding the subset of proteins that may cluster together and gives important clues for Lo domain function. The simplest, most economical, and hence routinely used method to isolate rafts and raft associated molecules is to treat cells with detergents such as Triton-100 (TX-100) followed by isolation of the detergent resistant portions of the membrane on a sucrose gradient (19,33). The detergent insoluble portion that floats on the top (low density fraction) of a sucrose gradient is termed detergent resistant membrane (DRM) (19) .

1. Relationship between detergent resistance and lipid phase:

Similar to lipids, detergents are amphiphatic molecules with hydrophilic head groups and hydrophobic tails. TX-100 is a non-ionic detergent that exists in the form of monomers and micelles when dissolved in water. When added to a lipid bilayer (that is either in the form of a liposome or cell membrane), TX-100 micelles interact primarily with loosely packed Ld state lipids to form mixed detergent lipid micelles in a process termed as detergent solubilization (29). In contrast, lipids that are resistant to detergent (TX-100) solubilization are in the tightly packed G state (saturated acyl chain lipids such as phospholipids and sphingolipids). Lipid bilayers and associated proteins (for example, GPI-anchored proteins) in the tightly packed Lo state (saturated lipids plus cholesterol) are also resistant to solubilization by detergent (1). Hence, it was proposed that DRM may arise from the tightly packed lipids that, prior to detergent treatment, were in the Lo state (1) (Figure 1.7). To investigate this hypothesis, Lo domain formation was further explored using model membrane vesicles in the absence of detergent. A lipid anchored quencher that strongly partitions into Ld domains and a fluorophore that moderately partitions into Lo domains was used. At low temperature, in the presence of co-existing Lo and Ld domains, quencher is segregated from the fluorophore. (See Figure 1.8). At high temperature, Lo domains gradually melt and the probe segregation is lost. Therefore, quenching becomes strong. This temperature dependence of quenching was used to show that mixtures of high Tm lipid, low Tm lipid, and cholesterol formed co-existing Lo/Ld domains (14). Furthermore, the amount of membrane in Lo, estimated by fluorescence quenching was found to be similar to that gauged by detergent insolubility (14).

Taken together these studies showed that DRM are obtained only from those membranes that initially contain co-existing Lo/Ld domains. Therefore, rafts in eukaryotic cells may represent Lo domains co-existing with Ld domains present in the cell membrane, prior to extraction by detergent (1,14). This hypothesis has been supported and confirmed by many other subsequent studies (34-39). For example, using atomic force microscopy (AFM) (36,39,40) it was shown that TX-100 dissolves the Ld domains in bilayers containing co-existing Ld/G or Ld/Lo phases at room temperature. It was also proposed that the observed detergent insolubility of G and Lo

states may be the result of lipid-lipid interactions caused by tightly packed acyl chains outweighing lipid-detergent interactions at very low temperatures (29).

Thus when a detergent micelle encounters a bilayer consisting of co-existing Lo and Ld domains, it preferentially binds to the Ld region of loosely packed lipids thereby solubilizing them and leaving behind a tightly packed Lo region held intact with strong Van der Waals lipid interactions (4,29,41,42). Structurally, DRM are proposed to consist of a mixture of planar and vesicular membranes (19). The planar forms may be composed of a planar bilayer of Lo lipids surrounded by detergent monomers on the edge of the bilayer (37).

2. Different detergents that are used to prepare DRM:

Rafts from cell membranes are routinely isolated using different detergents. All detergents used for this purpose do not solubilize the membrane in a similar fashion; Hence there are differences in the amount and kinds of proteins (raft-associated versus non raft-associated) and lipids (saturated versus unsaturated) found in DRM obtained using various detergents (43-45). This compositional difference in DRM obtained using different detergents has led to the proposition that there could be different types of cholesterol containing rafts. For example, DRM obtained after treatment with detergents such as TX-100 and CHAPS are similar in composition (34). Whereas DRM obtained from detergents such as Lubrol WX, Brij 58, Brij 96, Brij 98 differ from those obtained by TX-100 in lipid and protein composition (45-48). In a recent study, DRM from intestinal microvillar brush border cell membranes were isolated using Brij 98 at 37^{o}C (49). This is in contrast to the cooling to 4 ^{o}C, required for TX-100 extraction of DRM. This study points towards the existence of rafts at physiological temperature and may contradict the proposition that rafts are low temperature artifacts.

In the natural world, a case in which detergent resistance involves a detergent other than TX-100 is the exposure of plasma membrane of hepatocytes (rat hepatocytes) to bile salts naturally produced by the liver. These salts include cholic acid (derived from cholesterol) which is a natural surfactant with the ability to dissolve lipids from the membrane. Therefore, the membrane that is exposed to bile must contain lipids that can protect themselves from the solubilizing action of bile (50). Interestingly, but not surprisingly, model membrane liposomes

made up of lipids that are found in the hepatocyte canalicular membrane such as SM and cholesterol were reported to be insoluble in bile detergents whereas those containing phosphatidylcholine (PC) lipids with unsaturated acyl chains were soluble. This study is in agreement of the fact that bile is actually composed mainly of PC lipids (51).

Detection and significance of rafts in cells

1. Some examples of detecting rafts in cells without the use of detergents:

A literature search for the last couple of years alone gives a number of articles that link diseases ranging from Alzheimer's to cigarette smoke induced lung damage to rafts (46,52,53). Numerous examples of such studies use detergent resistance as the only criterion for assigning raft-like properties. It has been pointed out that isolation of DRM from cells, although an important technique to identify Lo domain favoring proteins, does not confirm their presence in Lo domains prior to addition of detergent (29,33). As a result it has been suggested that conclusions about rafts be drawn based on multiple methods used in parallel (4,29,42). Since rafts are most often likely to be nanoscopic (i.e. submicroscopic) and may even be transiently produced by the cell when required, their detection in situ without perturbing their natural state is tricky. However, small rafts can be clustered together into larger ones, by cross linking raft associated proteins. This renders them easier to detect (54). This method, although indirect, very effectively describes how rafts may function in protein-protein interactions.

Nonetheless, it is important to detect rafts directly in the "resting" stage. Extensive research to make raft detection less ambiguous, has led to newer methods that can detect formation of very small ordered lipid microdomains, from the surrounding fluid state lipid. FRET is one such method that is now more often used for identification of Lo nanodomains in model membranes as well as in cells (55-58). For example, FRET between fluorescently labeled saturated and unsaturated lipid analogs showed the presence of co-existing Lo and Ld regions in the plasma membrane of living mast cells (57).

Studies also point towards raft involvement in the function of immune cells such as B cells and T cells. For example, FRET between lipid anchored CFP (probe for lipid rafts) and YFP labeled B cell receptors (BCR) shows that BCR form microclusters that co-localize within raft domains upon antigen binding (59). T cell antigen receptor (TCR) signaling foci are said to reside within lipid raft microdomains. It was shown that plasma membrane surrounding the TCR activation domain, isolated from Jurkat cells is composed of Lo domain supporting lipids such as SM, cholesterol as well as some PE and PS lipids (60). This supports lipid raft formation in cells and may also point towards domain formation in the inner leaflet due to the greater enrichment of PE and PS in the inner leaflet of mammalian cell plasma membranes.

Several other studies employing different biophysical methods to detect Lo domains in cells are noteworthy. Generalized polarization (GP) of Laurdan, (a fluorescent probe that partitions equally between Lo and Ld but has an environment sensitive spectrum) is a valuable tool for direct visualization of co-existing Lo/Ld domains in cells at 37^{o}C (61). In addition to imaging domains in model membrane liposomes and live cells, GP of Laurdan has been also used to image membrane order in living zebrafish embryos (62).

Another method that gives information regarding the stability and motion of raft domains in cells is to follow the lateral diffusion of a single Lo domain associated protein. One such study that measured diffusion of membrane proteins in mammalian cells showed that proteins diffuse more slowly when present in raft region as compared to non-raft regions in a cholesterol dependent manner (63). This supports the hypothesis that raft lipids are tightly packed and more ordered than the surrounding non-raft lipids.

Yet another method that is commonly used to study domain formation in model membranes is electron spin resonance (ESR). ESR spectra of spin-labeled lipids are sensitive to Lo and Ld lipid environments. When incorporated into live cells, the presence of Lo and Ld like components in the plasma membranes was demonstrated by measuring the rotational diffusion of the spin-labeled lipids (64).

Finally, studies using the lipidomics approach build upon earlier observations of lipid sorting in polarized epithelial cells. For example, details of lipid structural and compositional changes that occur during formation of polarized epithelium were studied using mass spectroscopy. It was

found that levels of glycosphingolipids, cholesterol, PE and plasmalogen increased during the transition from a non-polarized to a polarized epithelial morphology (65,66). Recently, comparison of mass spectrometric data from apical portion of MDCK cells and the envelope of influenza virus budding out of these cells showed higher levels of SM and cholesterol (Lo forming lipids) compared to the whole cell (67).

2. Some examples of the biological significance of rafts:

The role of lipid rafts in signal transduction in immune cells has been studied in great detail for the past decade using TX-100 based detergent extraction and other methods in order to specify interactions between raft and non-raft proteins. One example of raft function allotted to proteins by detergent is IgE signaling (7). During allergic response, T-cells produce cytokine interleukin (IL4) and interact with B-cells that produce antibodies such as IgE. The Fc region of IgE binds to FcεRI (a receptor on immune cell surface) (68). The IgE-FcεRI complexes are cross linked by oligomeric antigens followed by phosphorylation by tyrosine kinase, Lyn. This process eventually results in histamine production. Interestingly, Lyn is found in DRM only upon cross linking of IgE-FcεRI complexes, suggesting that Lyn is recruited into ordered domains that contain these complexes. In addition to Lyn, cross linking of FcεRI also brings ganglioside GM1 and GPI-anchored proteins (raft-associating proteins) into raft domains that are large enough to be seen by microscopy. (69). In contrast, the transmembrane phosphatase CD45 (which has the ability to dephosphorylate both Lyn and FcεRI) is present in the detergent soluble fraction (not in DRM). Because both Lyn and FcεRI are found in rafts and are segregated from CD45 which is found in non-raft domains, it was proposed that the raft environment protects the Lyn and FcεRI from becoming dephosphorylated by CD45 and that small rafts (ordered domains) containing an active form of the tyrosine kinase Lyn coalesced into larger rafts that contained cross linked receptor (FcεRI) (70). This model, supported by extensive amount of data collected over a period of several years provides a strong evidence that rafts can be clustered upon receptor activation, which is an important raft function. See figure 1.6B for a general idea of how rafts may help cluster or segregate proteins.

Another interesting example of how rafts may segregate some proteins away from others to prevent unwanted interactions is soluble NSF attachment protein receptor (SNARE) protein interaction (71). During membrane fusion, SNARE proteins present on both the donor and acceptor membrane interact with each other (trans-interaction) while the interaction between the SNARE proteins on the same membrane (cis-interaction) is prevented (71). The target SNARE protein syntaxin 1A is evenly distributed on the plasma membrane and yet membrane fusion takes place at only certain defined sites on the membrane suggesting that the segregation into domains may play a role in keeping some of these proteins in an 'off' or inactive mode (71).

Recently, an interesting study in a mouse model showed that a diet rich in saturated fatty acids increased the partitioning as well as activity of c-Src, a myristoylated protein (a saturated lipid anchored protein, normally found both within and outside rafts) into detergent resistant membranes extracted from the adipocytes. Increased levels of c-Src activated a Jun N-terminal kinase which, has been shown to be more active in obese mice and humans. In contrast, opposite results were obtained using unsaturated fatty acids (72). Thus there may seem to be a link between nutrition and lipid rafts.

Detecting ordered domains in model membranes:

Although the previous paragraphs describe growing evidence for raft (Lo domain) formation in cells, their direct, unambiguous detection in resting cells remains difficult. By contrast, in model membranes containing some lipid compositions, Lo domains can be unambiguously detected. Numerous examples are listed below.

1. Detecting ordered domains in model membranes derived from cells:

Giant plasma membrane vesicles, GPMV as the name suggests, are model membranes that are closest to the plasma membrane and are comparable to real cells in size and curvature. GPMVs are derived from cells in form of blebs by chemical induction or osmotic swelling. Large-scale phase segregation in GPMVs below room temperature has been imaged using dyes such as naphthopyrene and rhodamine-DOPE which partition into Lo and Ld phases respectively (73).

Similarly, plasma membrane spheres generated by osmotic swelling of cells show the appearance of raft domains at 37^{o}C upon cross linking of ganglioside GM1(74).

2. Detecting ordered domains in model membranes that are not derived from cells:

Cellular detergent resistant extracts are composed approximately of an equimolar ratio of glycerophospholipids (low Tm, unsaturated), sphingolipids (high Tm, mostly saturated) and cholesterol (19). For that reason, mixtures of unsaturated lipids such as POPC or DOPC, with saturated lipids such as SM or DPPC along with cholesterol make a simple model membrane system in which lipid phase behavior can be studied. Giant unilamellar vesicles (GUVs) are an example of such model membrane vesicles and are comparable to cells in size. GUVs may be prepared with desired combinations of phospholipids. Raft formation in GUV has been extensively studied using confocal microscopy and generalized polarization of laurdan. For example, in GUVs made up of the ternary lipid mixture DPPC, DOPC and cholesterol, Lo/Ld co-existence was observed by using probes that have a different partition preference for the Lo and Ld domains (75,76). Ordered regions in GUVs made from the intestinal brush border membrane lipids (rich in SM and cholesterol) or those containing ternary mixtures of lipids such as DOPC, SM and cholesterol were observed by measuring the generalized polarization of laurdan by fluorescence microscopy (35).

However, not all lipid mixtures form domains large enough to be visualized. For example, GUVs containing a lipid mixture that closely mimics the lipid composition of the outer leaflet of the plasma membrane i.e SM, POPC and cholesterol appear to be uniform when observed using fluorescence microscopy (15). This may reflect the fact that only domains larger than the wavelength of light used can be seen by microscopy (15). Evidently, domains on the order of tens of nanometers that cannot be resolved using light microscopy, can, under the same conditions, be detected by FRET and ESR (55,56,58). In fact, previous fluorescence quenching experiments in vesicles made up of high and low Tm lipid and cholesterol have shown domain formation on the scale of approximately 1nm in which the order of the ‘nearest neighboring lipid’ can be detected (14,77).

Size and temporal stability of ordered domains in model membranes and cells:

Measurement of raft stability or size in a resting cell is a desirable property. However, as emphasized above, the detailed characterization of Lo domains in cells is constrained mainly due to their proposed nanoscopic dimensions and possible short lived nature. One article based on fluorescence microscopy studies showed domains diffuse and join each other within one second upon collision (78). Another study measuring the diffusion of proteins, laser-trapped in a small area in living fibroblasts estimated protein-containing rafts of radius in between 10 to 50 nm that are stable and diffuse as one unit for 10 to 50 seconds (63). This seems a long time compared to the raft localization of proteins studied using single molecule FRET, which showed that GPI anchored proteins form transient rafts that remain stable for only 200 ms (79). Simulation studies carried out using models of high Tm and low Tm lipids with cholesterol, described a model of small lipid domains surrounding individual cholesterol molecules (80,81). Models for small rafts in cells, composed of only a few lipid molecules, relevant to the above examples, had been predicted/proposed many years ago (23).

An important factor that may be responsible for small domain size is cholesterol levels in the plasma membrane. The cholesterol content of plasma membranes is high. It makes up 30 to 40 mol percent of the total lipid present in the plasma membrane (82). Concentration of cholesterol was shown to have an effect on ordered domain size (83). Model membranes made up of high Tm lipid (DPPC), a low Tm lipid (DLPC) and cholesterol were studied using microscopy and FRET; In mixtures containing less than 16mol% cholesterol, large domains could be visualized in GUVs by microscopy; By contrast, at higher cholesterol levels, domains in GUVs could not be visualized at all (83). However, in the same mixtures, domains were detected using FRET (83). (FRET can detect small nanodomains of diameter greater only than the interaction distance of the FRET donor-acceptor pair ~2 to 7nm.) This study observed that high concentrations of cholesterol rendered domains too small to be observed by microscopy (83). This shows how small domains, that are outside the resolution limit of the detection method, can be sometimes misinterpreted as no domains.

How difference in bilayer width in between domains may affect domain size

1. Certain molecules may tend to decrease domain size:

AFM studies have shown that the Ld domains are thinner (shorter) than the Lo domains (28). The uneven heights of the Lo and Ld domains, which leads to the exposure of the hydrophobic lipid acyl chains to the aqueous environment, gives rise to line tension at the domain interface. One lipid that may reside at the interface of Lo and Ld domains is cholesterol. It is predicted that the rigid ring of cholesterol called the alpha side packs well and thus faces towards the Lo domain forming lipid; while, the protruding methyl groups on the beta side of cholesterol would face the Ld and as a result, reduce the line tension between the two phases. (80,84). Such a lipid is called a line active lipid since it resides at the edges of a domain and tends to reduce the line tension between the two domains. An earlier AFM study that supports this hypothesis showed that high levels of cholesterol reduce the difference in the height between Lo and Ld domains in supported lipid bilayers (39). Another example of a line active lipid is POPC (56), a mixed acyl chain-lipid that has Ld-like unsaturated acyl chain as well as an Lo-like saturated acyl chain. Its saturated acyl chain will prefer to pack with the Lo domain lipids and its unsaturated chain will prefer to face the fluid like Ld domain forming lipids. (Figures 1.1B and 1.9).

Consider a bilayer having Lo and Ld domains. When present, line active lipids will reside at the domain interface and reduce line tension. This will lead the equilibrium towards having more edges, and more edges means smaller domains. Accordingly, more cholesterol or POPC may cause less energy penalty at the edges by reducing the height difference between Lo and Ld and thus lead to more interfaces and smaller domains. This may be the reason why domains can be small and difficult to detect at high cholesterol concentrations. In a similar manner proteins that like to associate with raft edges may also reduce the size of domains by increasing the edge to interior ratio (85). Since both POPC and cholesterol are abundantly present in the plasma membrane, this may explain why domains in cells are so small (23).

2. Certain molecules may tend to increase domain size:

The relationship between line tension and domain size has been further explored by another study involving AFM and confocal microscopy that used unsaturated PC lipids differing in the acyl chain length (86). Lipids having lowest number of carbons in the acyl chains formed the thinnest Ld bilayer and mixtures of these lipids with saturated lipids (sphingomyelin) and cholesterol showed largest most circular Lo domains that were more stable as judged by the domain de-mixing temperatures (86). Since domains isolated by TX-100 are large and have a bilayer appearance (19), it has been hypothesized that TX-100 may, in a similar fashion, increase domain size by coalescing smaller domains together (23). AFM studies revealed that TX-100 addition decreased the height of both Ld and (to a smaller extent) Lo domains leading to an effective increase in the height difference between the two domains (34). It can be reasoned that TX-100 is more likely to enter the loosely spaced Ld lipid bilayer than the tightly packed Lo lipid bilayer and therefore may reduce the thickness of the Ld bilayer to a greater extent. A mismatch in bilayer width leads to exposure of the hydrophobic acyl chains to water resulting in unfavorable energy at the edges. The bilayer may try to minimize edge to interior ratio (number of edges) by coalescing similar domains and thus making them larger (23). (See Figure 1.10).

Effect of sterol structure on domain formation:

As mentioned above, the molecular basis of raft formation lies in the tight packing of sterols such as cholesterol that have flat rigid ring structures with sphingolipids and lipids having saturated acyl chains. Due to this tight packing interaction, sterols promote the formation of Lo and Ld domains in ternary mixtures. Effect of various physiologically relevant sterols, (and those having different abilities to promote tight packing) on domain formation has been studied extensively using fluorescence quenching along with detergent insolubility (87,88). Sterols that lack the structural ability to pack tightly in a bilayer do not support ordered domain formation and may sometimes inhibit domain formation. For example, a bend in the steroid ring of coprostanol, prevents it from tight packing in a bilayer. Therefore coprostanol inhibits domain formation in model membranes (88). (Figure 1.11). In contrast, sterols that have a double bond in the ring in between carbon atoms 7 and 8, for example ergosterol, lathosterol and 7-

dehydrocholesterol support domain formation to a greater extent than cholesterol which has a double bond between carbon atoms 5 and 6 (87). In addition, it was shown that the structure of the 3' hydroxyl group of cholesterol is also critical for domain formation and that a small change in the hydroxyl group such as conversion to a keto group or addition of a methyl or formate group can reduce the ordered domain forming ability of the DPPC/sterol mixture. On the other hand, the epimer of cholesterol (epicholesterol, which has an alpha hydroxyl group) was shown to form rafts to a similar extent as cholesterol (89).

The dependence of domains upon sterol structure, (similar to the pioneering work on sterol structure done in our lab (88,89)) was studied in GUVs using fluorescence microscopy. GUVs made up of high Tm lipid and low Tm lipid and ordered domain promoting sterols showed co-existing liquid ordered and disordered phases whereas those that contained domain inhibiting sterols showed gel and liquid co-existence. (78) A molecular dynamics study showed that the methyl groups in the steroid ring of cholesterol reduce the tilt of the cholesterol molecule in the plane of the bilayer and thus enhance lipid-sterol interactions (90).

Sterols that are naturally present in plants, such as sitosterol and those in fungi, such as ergosterol, mentioned above, also help to form ordered domains similar to cholesterol. Furthermore, there are also instances where domains were visualized in the absence of cholesterol (75,91). Interestingly, a model membrane study of bacterial and eukaryotic lipids showed an unexpected similarity in the membrane order, caused by lipid-transmembrane peptide interactions that were independent of sterol (92). This suggests that lipid segregation into domains need not be limited to eukaryotic cells (87).

Microdomains in prokaryotes:

The above discussion seems to be limited only to eukaryotic cell membranes since prokaryotes do not contain the promoter of ordered domains, namely, cholesterol. However, surprisingly, microdomains were recently discovered in a bacterium. Even though prokaryotes do not synthesize cholesterol, bacteria such as *Helicobacter*, *Mycoplasma* and *Borrelia* can incorporate cholesterol in their membrane from their host (93-96). The outer membrane of bacterium *Borrelia burgdorferi* the causative agent of Lyme disease (97) and relapsing fever (98), contains

along with PG and PC, high levels of free cholesterol and three glycolipids, two of which have covalently linked cholesterol. These glycolipids are mono-galactosyl diacyl glycerol (MGalD, having some molecules with mixed saturated and unsaturated and some with both saturated acyl chains), cholesteryl-6-O-acyl-galactopyranoside (ACGal, saturated acyl chain in half the molecules) and cholesteryl-β-D-galactopyranoside (CGal) (99) (Figure 1.12). The Borrelia outer membrane also contains lipid anchored outer surface protein B (OspB) (100). Building upon their important recent observation that, complement-independent antibodies such as CB2, made against OspB (that work by forming pores in the membrane leading to osmotic lysis of the cell), fail to lyse *E.coli* cells containing CB2, (100,101) the Benach group showed that both cholesterol and cholesterol glycolipids are required for the bactericidal action of CB2 (100). Furthermore, using gold labeled anti asialo GM1 antibodies against cholesterol glycolipids, electron microscopic and detergent resistant membrane analysis of outer membrane of *B.burgdorferi* cells showed the presence of membrane domains containing cholesterol and OspB (along with other outer membrane proteins). Our contributions to these studies are reported in this thesis.

Summary:

Whether rafts are small transient Lo domains in a membrane primarily composed of disordered lipids, or, are a continuous ordered phase, (64,102) is dependent upon experimental conditions, and the situation in cell membranes is not yet completely clear. Nevertheless, research as well as intuition points towards the idea of functional domains in cells being too small to be resolved by light microscopy. The idea of these small domains coalescing into larger ones by cross linking individual proteins is being widely accepted in the scientific community.

The goal of this work:

Detection of ordered domain formation in model membranes and cells.

As discussed above, lipid microdomains have been implicated in various biological processes. These lipid microdomains are commonly extracted from cells by detergent treatment. The goal of this work is to understand the effect of detergent TX-100 on the formation and stability of ordered domains and to devise new methods for unambiguous detection of very small nanodomains. Secondly in collaboration with the lab of Dr. Jorge Benach, cholesterol rich domains in *B. burgdorferi*, were investigated in detail to determine whether they represent true ordered domains. This work has implications for the use of the detergent extraction technique and for the existence of nanoscopic lipid rafts in the presence of physiological (high) levels of cholesterol. Proving rafts exist in living cells is important for the advancement of research on cell membrane structure and organization.

Table 1.1

Gel to Ld melting temperatures, Tm, of pure lipids decrease as the number of cis-double bonds in the acyl chains increases. The cis-double bonds give rise to kinks and inhibit tight packing of lipid acyl chains. Tm is a measure of the stability of the gel state of a lipid.

Lipid	Number of cis-double bonds	Melting temperature (Tm ^{o}C)
DPPC	0	41
SM	0	(approximately) 37
POPC	1	- 4
DOPC	2	- 20
DArPC	8	-70

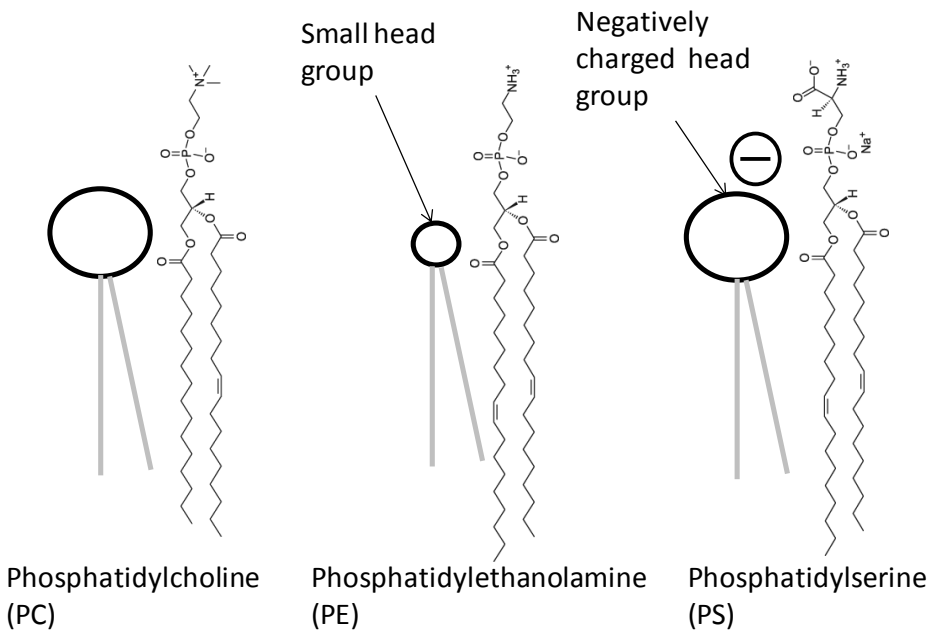

Figure 1.1A. Structural differences in lipid head groups: Plasma membrane lipids having different headgroup size are shown. For example, PE has a smaller headgroup than PC, lipids having zwitterionic and negatively charged head groups for example PC is zwitterionic whereas PS is negatively charged. Lipid structures taken from www.avantipolarlipids.com

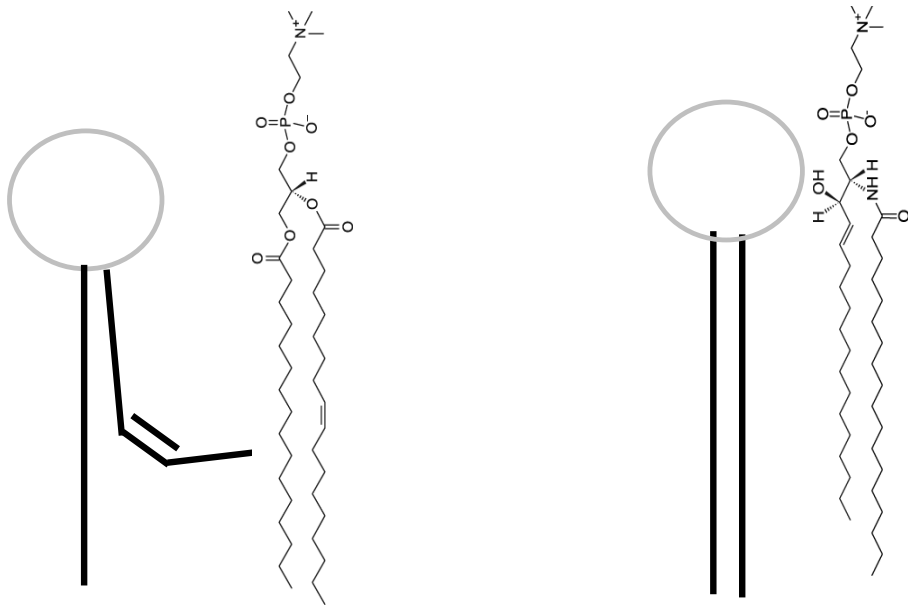

1-palmitoyl,2-oleoyl-PC
(POPC)

Sphingomyelin
(SM)

Figure 1.1B. Structural differences in lipid tails: Plasma membrane lipids differing in the saturation of their acyl chains. POPC has one saturated acyl chain and one unsaturated acyl chain with a cis double bond which forms a kink in the acyl chain. SM has a saturated acyl chain and the double bond on the other acyl chain is near the head group region and is a trans-double bond which may not interfere in its packing ability. Lipid chemical structures taken from www.avantipolarlipids.com

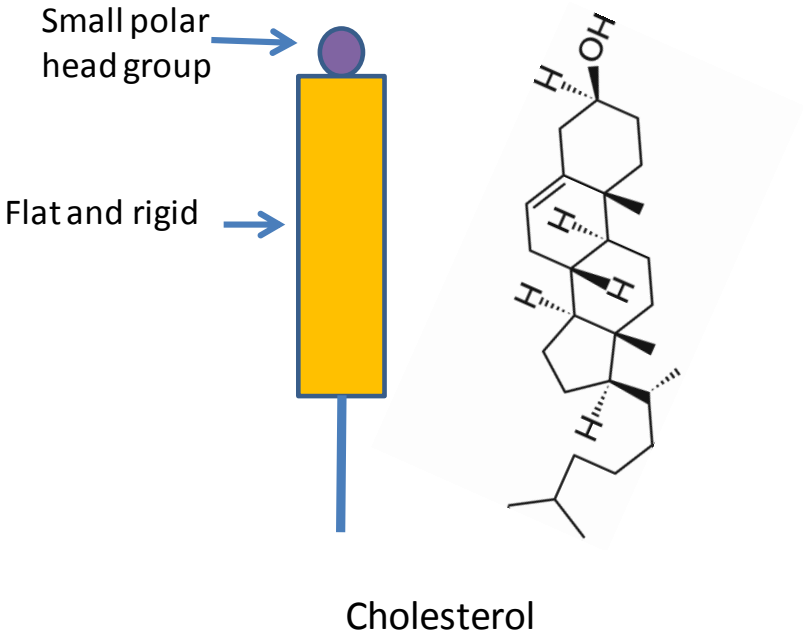

Figure 1.1C. Structure of cholesterol. Cholesterol is abundantly present in the plasma membrane. It is a flat, rigid molecule with a small polar head group. Structures taken from www.avantipolarlipids.com

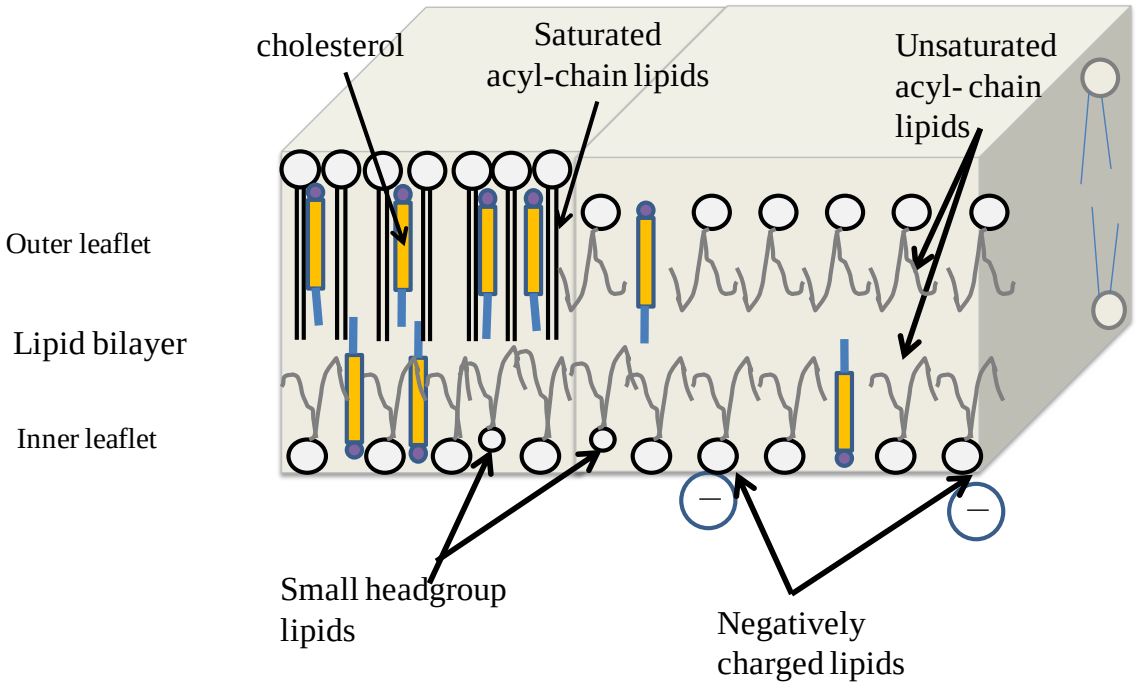

Figure 1.1D. Asymmetric distribution of plasma membrane lipids. Note that negatively charged lipids and those with a smaller head group such as PS and PE respectively are situated in the inner leaflet. Lipids with saturated acyl chains such as sphingolipids are more abundant in the outer leaflet. Cholesterol has a small polar head group and prefers to hide under the larger head groups of phospholipids in order to avoid contact with the surrounding water.

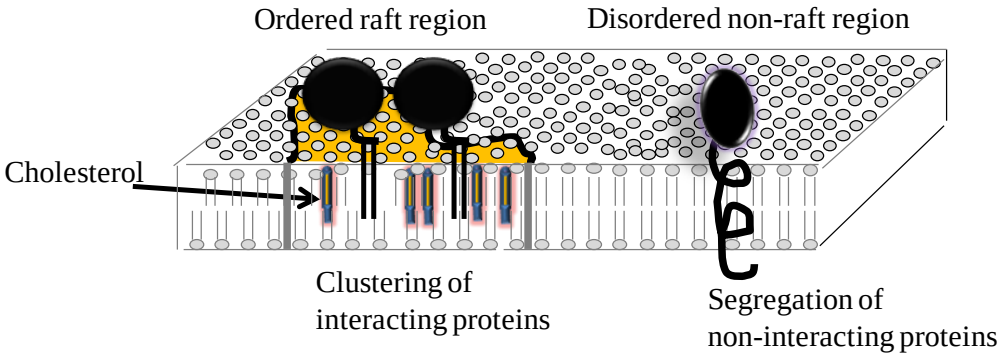

Figure 1.2A: The Raft Model. Figure shows ordered rafts in the plasma membrane segregated from the disordered non-raft region. Lipids and proteins are organized into domains.

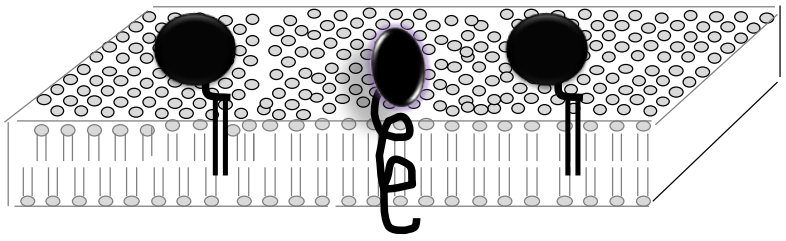

Randomly distributed proteins in a disordered lipid bilayer

Figure 1.2B: The Fluid Mosaic Model. Figure shows that lipids and proteins are randomly distributed in the membrane lipid bilayer.

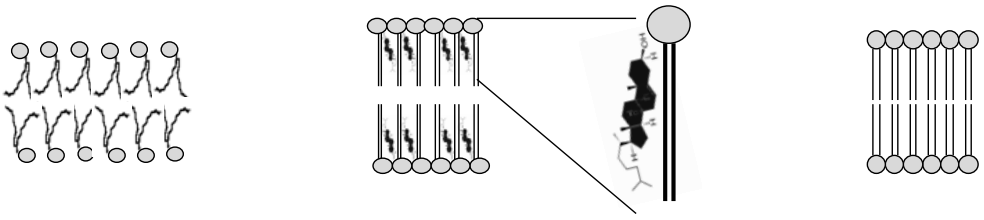

Ld	Lo	G
Liquid disordered	Liquid ordered	Gel
Fluid like, disordered	Intermediate ordered	Solid-like, ordered
Loosely packed acyl chains	Tightly packed acyl chains	Tightly packed acyl chains
Fast lateral diffusion	Fast lateral diffusion	Slow lateral diffusion
Thinner bilayer	Thicker bilayer	Thicker bilayer

Figure 1.3. Lipid phase behavior. Figure describes the three physical states of a lipid bilayer. The Lo state is formed when saturated lipids are mixed with flat rigid sterols like cholesterol.

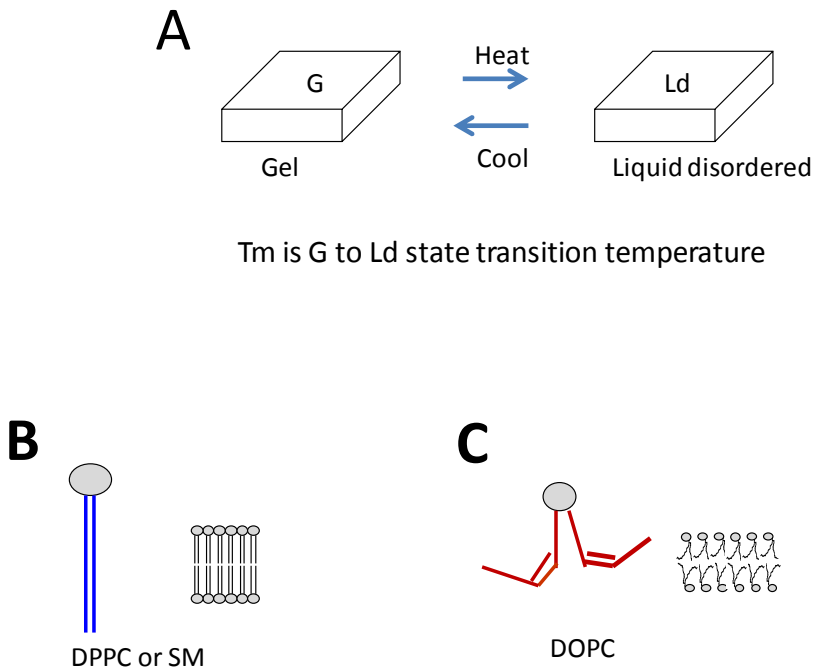

Figure 1.4: Lipid phase transition. A: Bilayers of lipids in the gel state reversibly transition into Ld state when heated above their melting temperature, Tm. Tm is the characteristic temperature of each lipid and is the measure of its thermal stability. B: Lipids having saturated acyl chains form bilayers that have a high gel to Ld transition temperature. These bilayers have lipids that are tightly packed and have extended acyl chains. Examples are SM and DPPC. C: Unsaturated lipids having at least one cis double bond have a kink in their acyl chains and thus do not pack well in a bilayer. They form bilayers that have a low gel to Ld transition temperature. Examples are DOPC and POPC.

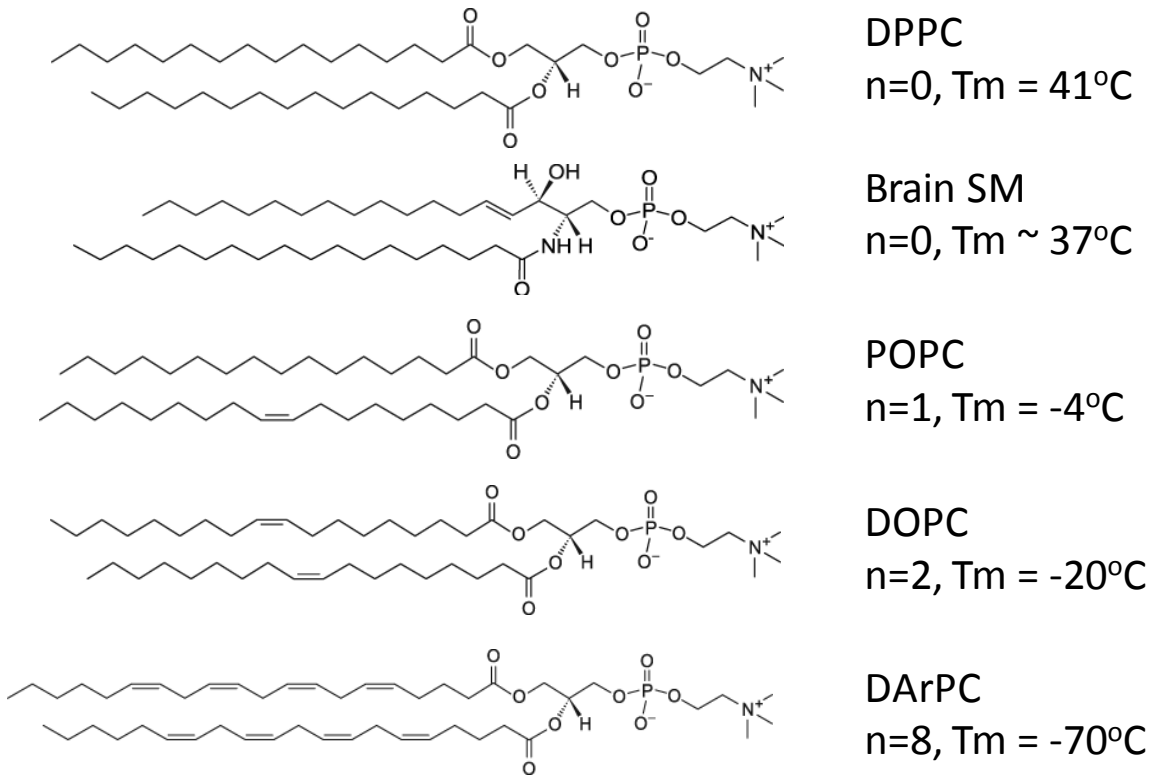

Figure 1.5 Lipid structure and phase transition temperature, Tm. Thermal stability of the gel state decreases with the increase in number of cis-double bonds in the lipid acyl chain. n= total number of cis-double bonds in the lipid molecule. Structures taken from www.avantipolarlipids.com

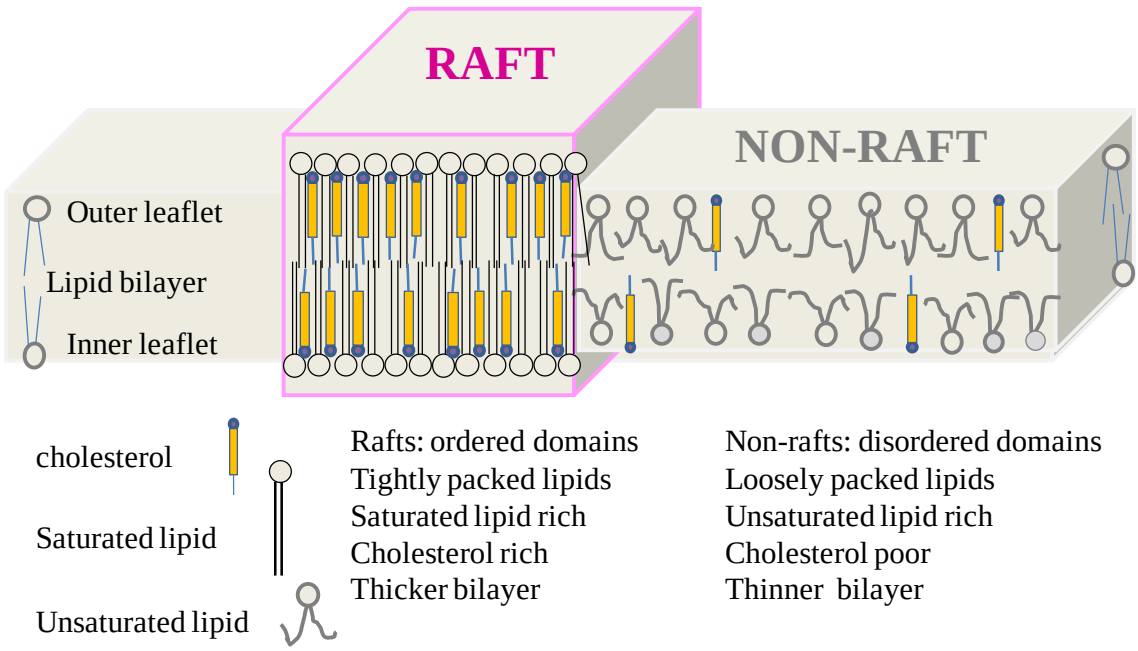

Figure 1.6A. Raft and non-raft i.e. ordered and disordered domain co-existence. Figure shows regions in a membrane lipid bilayer that are enriched in tightly packed cholesterol and saturated lipid. The extended acyl chains of saturated lipids packed with cholesterol makes the lipid bilayer wider and more ordered. The rest of the membrane is disordered and rich in unsaturated lipids having at least one cis double bond.

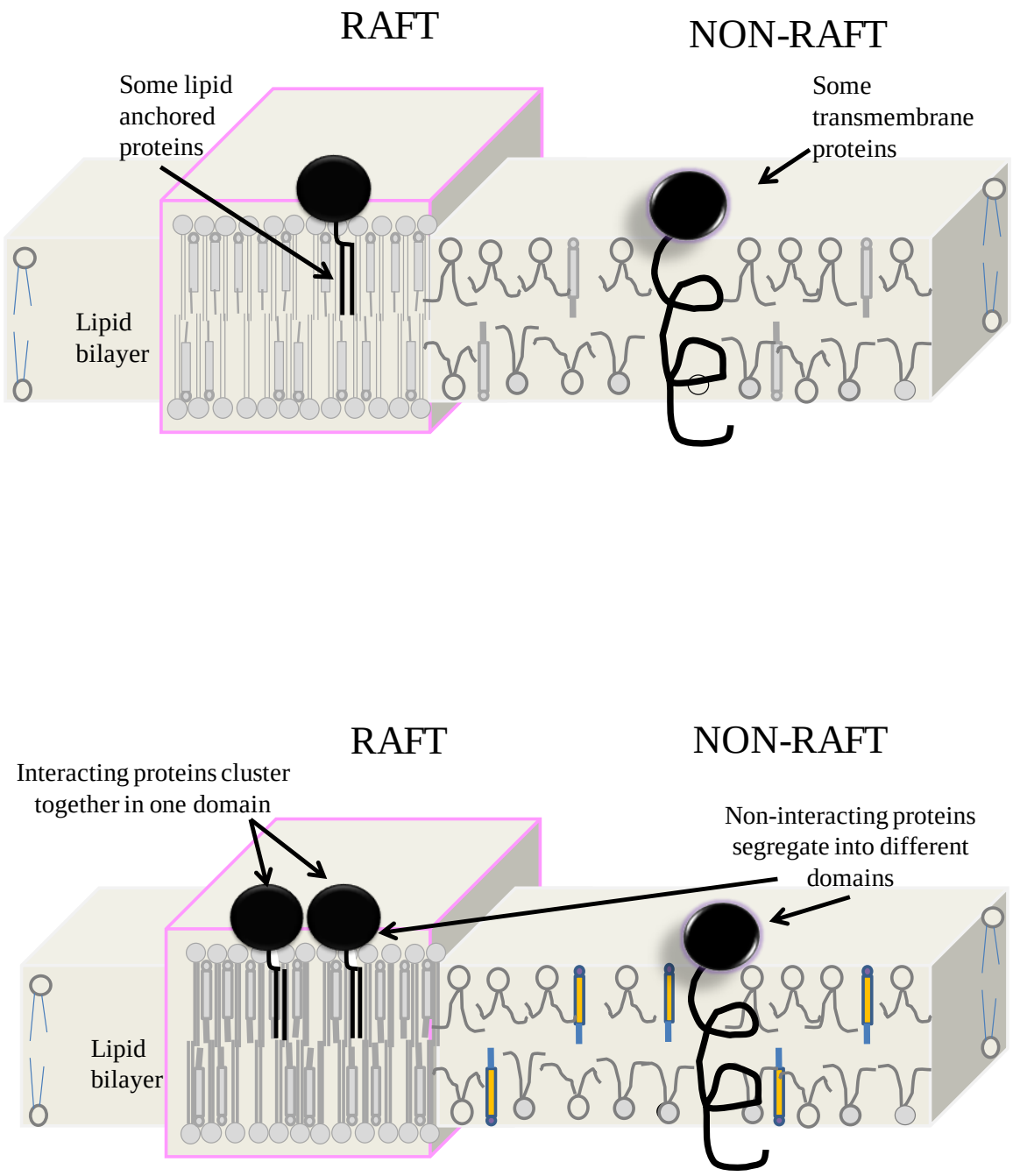

Figure 1.6B. Raft and non-raft i.e ordered and disordered domain co-existence help control protein-protein interactions. Top panel: Some lipid anchored proteins partition into ordered domains and some transmembrane proteins partition into disordered regions of the membrane. Bottom panel: Lipid segregation into raft and non-raft domains may help interacting proteins cluster together and segregate from the non-interacting proteins.

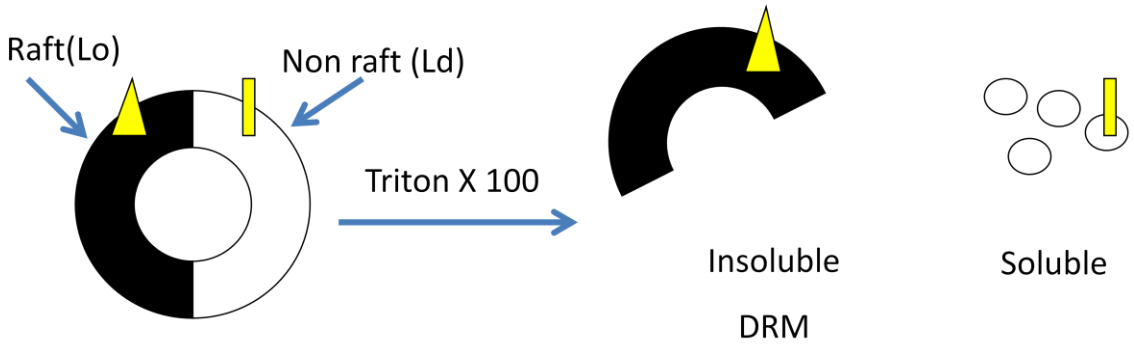

Figure 1.7 Formation of detergent resistant membrane. When added to a membrane containing co-existing raft (Lo) and non-raft (Ld) domains, TX-100 does not readily solubilize Lo domains but does readily solubilize Ld domains. The insoluble detergent resistant membrane is hypothesized to originate from the pre-existing Lo domains in cells. The detergent soluble membrane is hypothesized to originate from the Ld domains in cells, co-existing with the Lo domains.

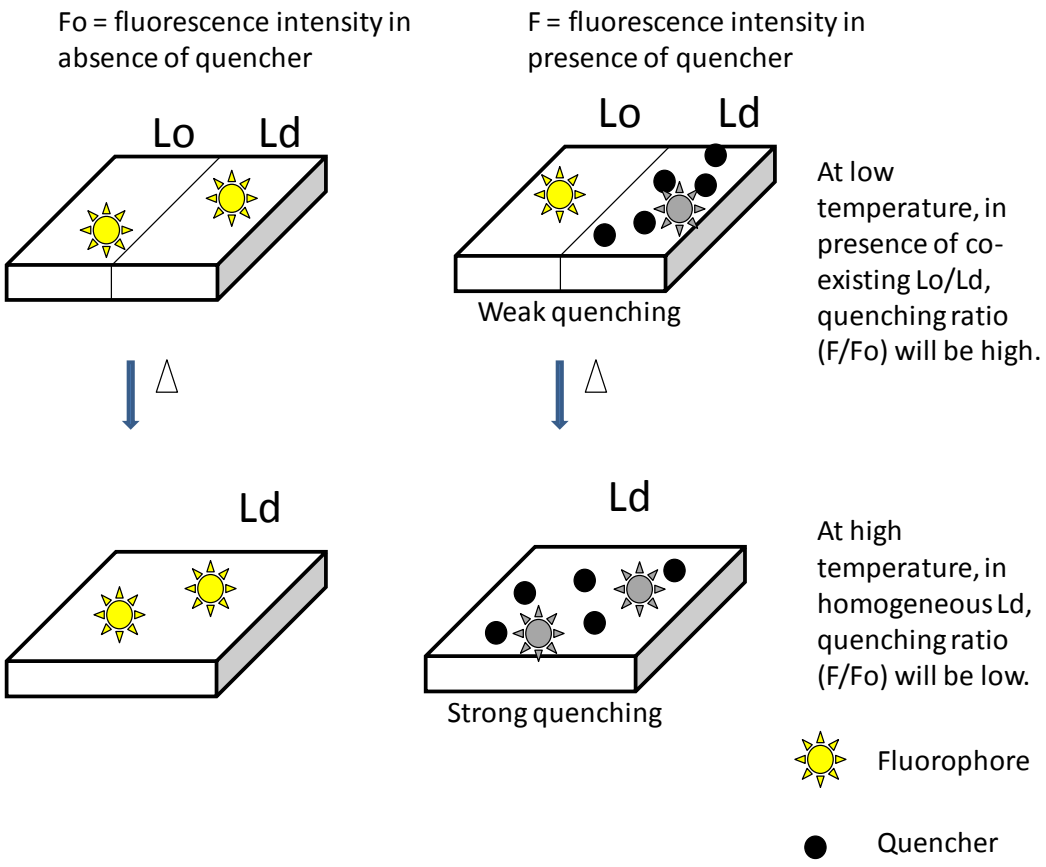

Figure 1.8: Detection of lipid segregation by Quenching or FRET assay. The quencher has a strong preference for Ld domains. The fluorophore has a moderate affinity for Lo domains. At low temperature, quencher is segregated from the fluorophore and quenching is weak. At high temperature, lipid segregation is lost due to Lo domain melting and quenching is strong. For FRET, fluorophore will be donor and quencher will be acceptor.

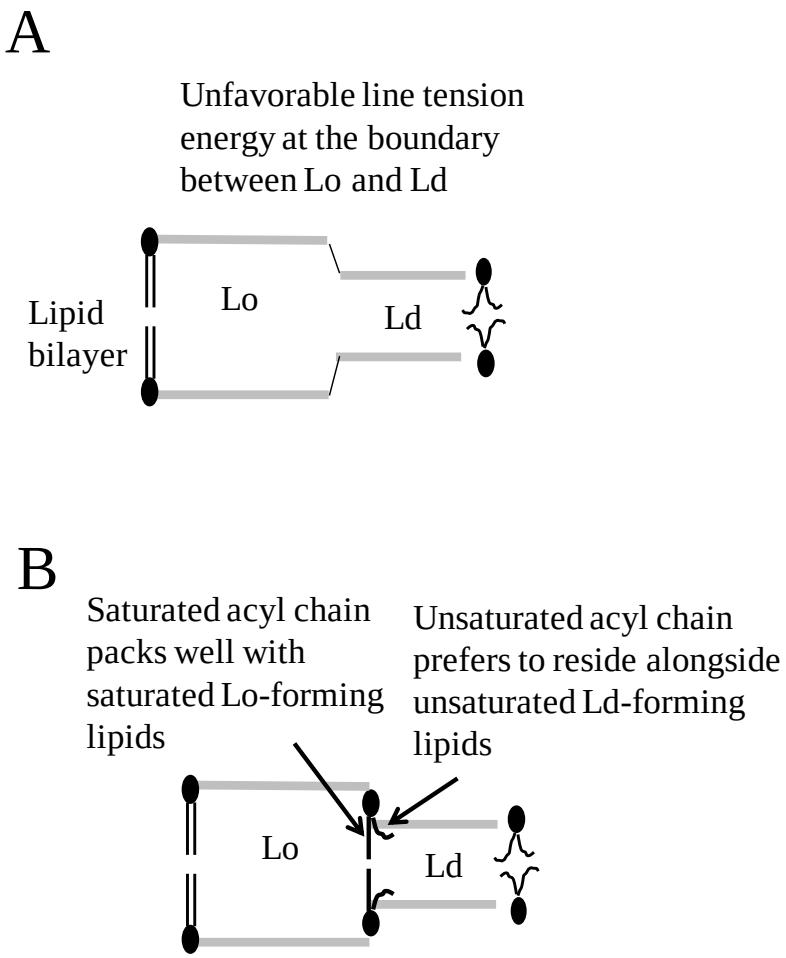

Figure 1.9: How certain molecules may decrease ordered domain size. A: Height difference between Lo and Ld domains exposes the hydrophobic acyl chains to the surrounding water and creates an unfavorable energy called line tension at the boundary of the two domains. B: Line active molecules like to reside on the boundary and reduce the height difference between the two domains and thus shift the equilibrium towards more edges and eventually smaller domains.

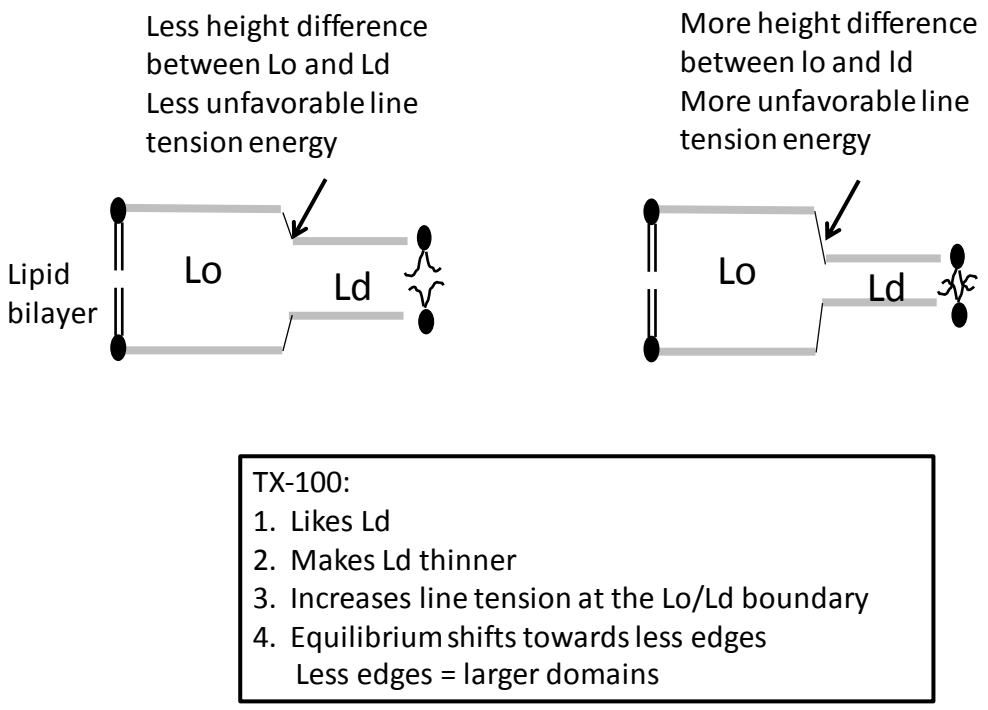

Figure 1.10: How certain molecules may increase ordered domain size. A: Height difference in between Lo and Ld domains in the absence of molecules such as TX-100. B: Molecules such as TX-100 may decrease the thickness of the Ld bilayer more than that of Lo since they prefer to partition in the Ld domains. This may increase the overall height difference in between the two domains leading to more unfavorable energy at the boundary, finally leading to the merger of small domains to minimize the unfavorable lipid-lipid interactions.

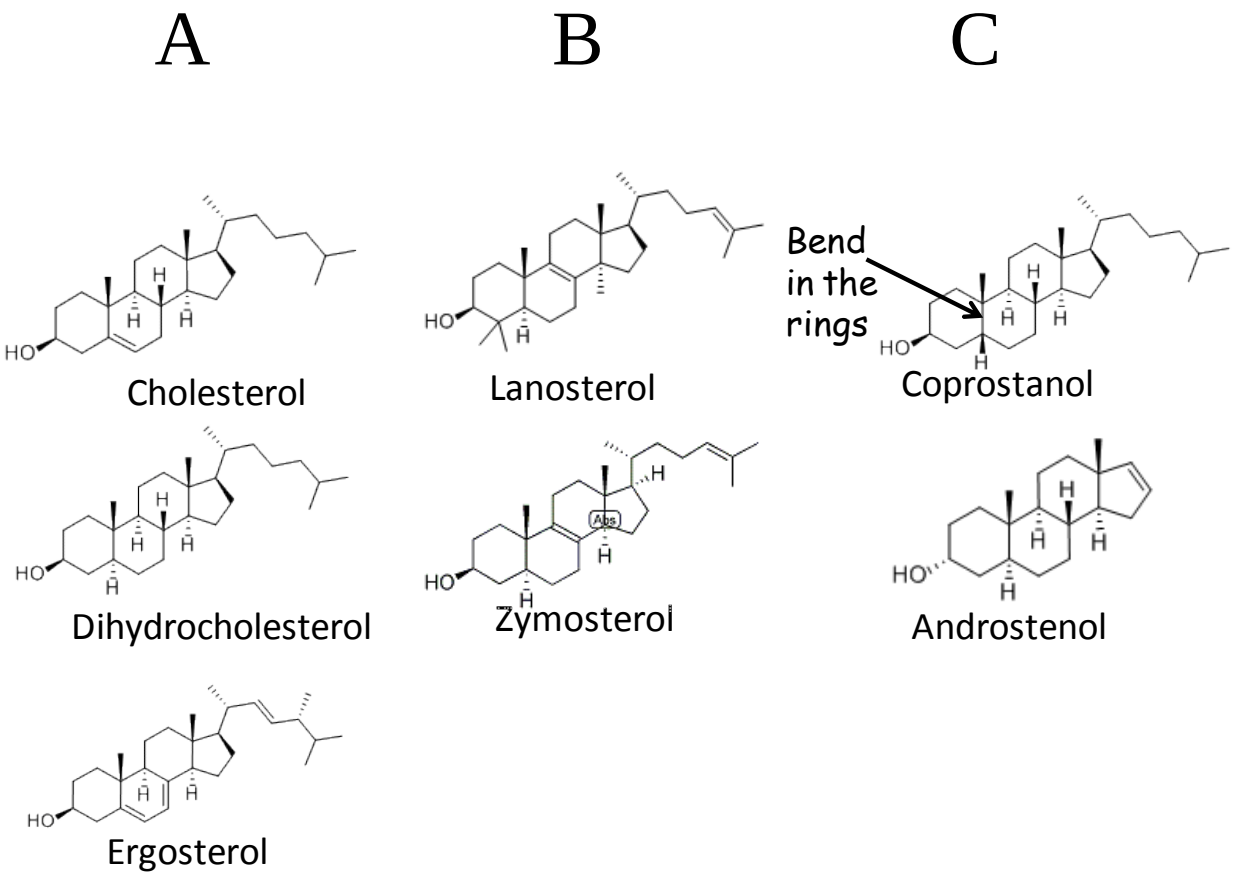

Figure 1.11. Structures of various raft supporting and inhibiting sterols. A. Sterols that strongly support Lo domain formation, B. Sterols that moderately support Lo domain formation and C. Sterols that inhibit Lo domain formation. Structures taken from www.steraloids.com

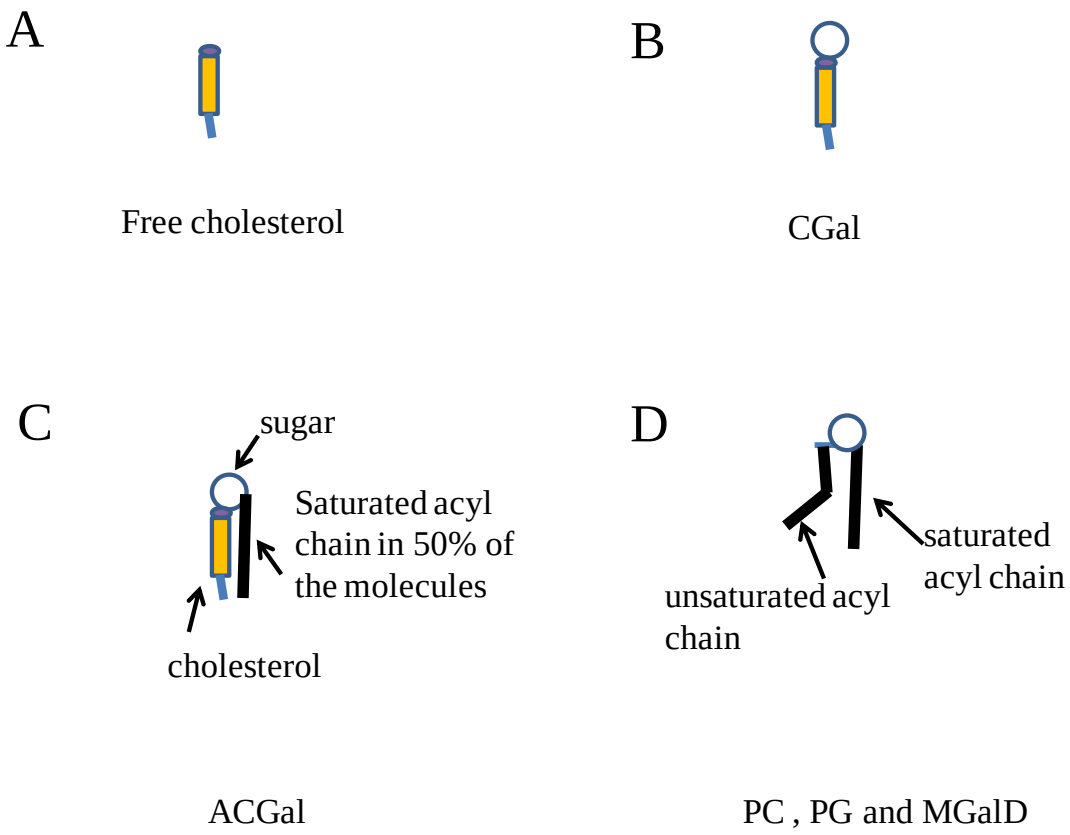

Figure 1.12 Schematic showing lipids that may be responsible for domain formation in *Borrelia burgdorferi*. *Borrelia burgdorferi* membrane contains A. host derived free cholesterol, B and C. cholesterol glycolipids namely, cholesteryl β-D-galactopyranoside (CGal) and cholesteryl-6-O-acyl-β-D-galactopyranoside (ACGal) in which the acyl chain is saturated in 50 % of the molecules. D. Commonly found lipids such as Phosphatidyl cholines, phosphatidyl glycerols and a glycolipid mono-galactosyl-diacylglycerol (MGalD) (99).

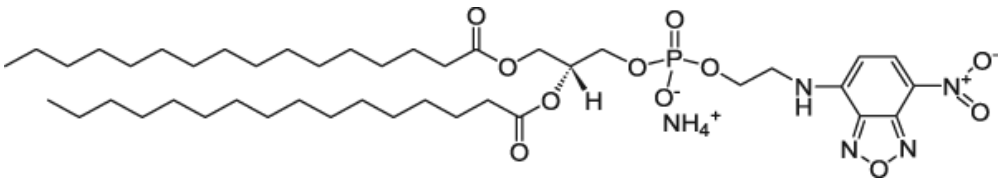

NBD-DPPE

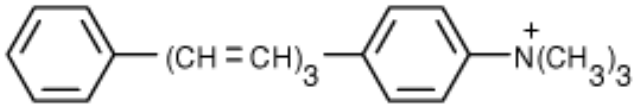

TMADPH

Figure 1.13A Structures of fluorescence donors used in this report. Structures taken from www.avantipolarlipids.com

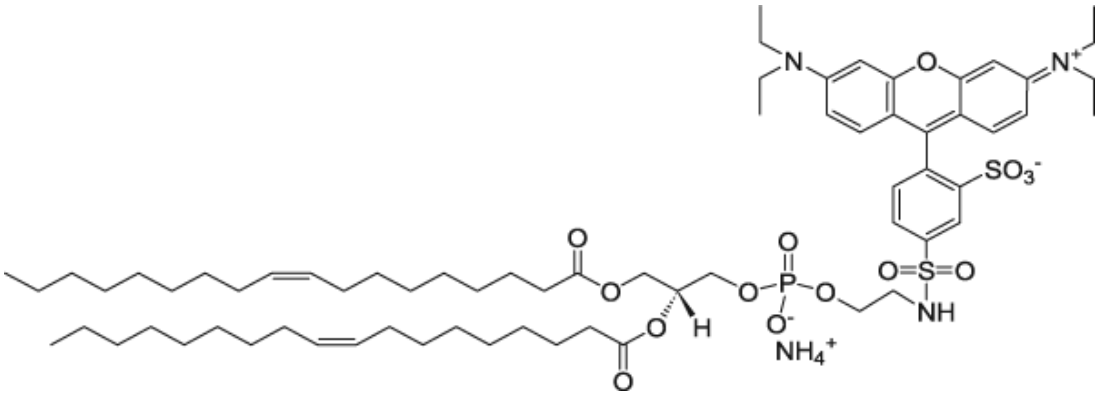

rhodamine-DOPE

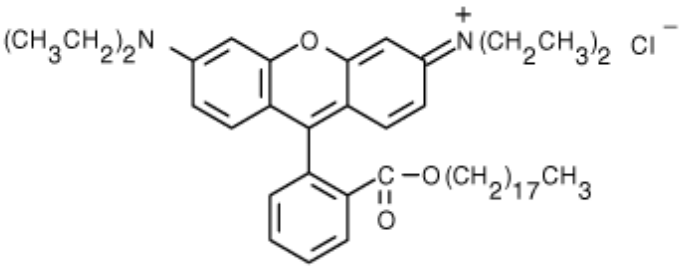

Octadecyl rhodamine B (ODRB)

Figure 1.13B Structures of fluorescence acceptors used in this report. Structures taken from www.avantipolarlipids.com

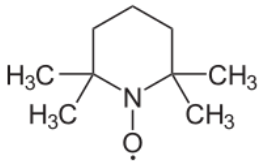

TEMPO

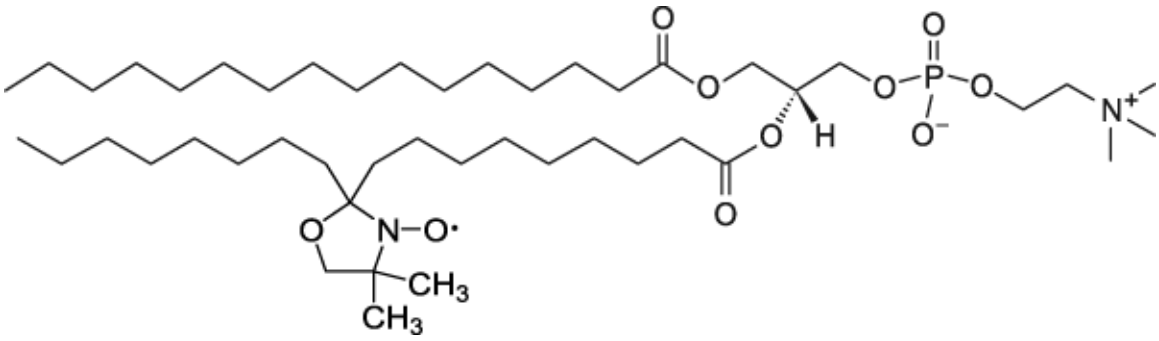

10 SLPC

Figure 1.13C Structures of fluorescence quenchers used in this report. Structures taken from www.avantipolarlipids.com

Chapter 2

MATERIALS AND METHODS

Materials:

Porcine brain sphingomyelin (bSM), chicken egg sphingomyelin , 1-palmitoyl-2-oleoyl-phosphatidylcholine (POPC), 1, 2- dipalmitoyl-sn-glycero-3-phosphatidylcholine (DPPC), 1, 2-dioleoyl-sn-glycero-3-phosphatidylcholine (DOPC), zymosterol, cholesterol and fluorescently labeled lipids 1,2-dipalmitoylphosphatidylethanolamine-N-(7-nitro-2-1,3-benzoxadiazol-4-yl) (NBD-DPPE), 1,2-dipalmitoylphosphatidylethanolamine-N-(1-pyrenesulfonyl) ammonium salt (pyrene-DPPE), 1,2-dioleoylphosphoethanolamine-N-(Lissamine Rhodamine B Sulfonyl) (rhod-DOPE) and quencher labeled lipid 1-palmitoyl-2-stearoyl-(10-doxyl)-phosphatidylcholine (10SLPC) were purchased from Avanti Polar Lipids (Alabaster, AL). Fluorescent probes 1-(4-trimethylammonium)-6-phenyl-1, 3, 5-hexatriene *p*- toluenesulfonate (TMADPH) and octadecyl rhodamine B (ODRB) were purchased from Molecular Probes division of Invitrogen, stored in ethanol, 1,6-diphenyl-1,3,5-hexatriene (DPH) and the stable free radical quencher TEMPO were purchased from Sigma-Aldrich (St. Louis, MO). Acetyl-$K_2W_2L_8AL_8W_2K_2$-amide (LW peptide) was purchased from Anaspec (San Jose, CA) and was used without further purification. TX-100 was purchased from Yorktown Research (Hackensack NJ). Other sterols were purchased from Steraloids Inc. (Newport, RI). Lipids and probes were dissolved in chloroform (with the exception of DPH, TMADPH, ODRB and TEMPO which were dissolved in ethanol). Ethanol was solvent for sterols used for substitution in cells whereas chloroform was solvent for sterols used for the model membrane experiments. Lipids and probes were stored at -20^{o}C. The concentrations of lipids were determined by dry weight and those of fluorescent molecules and transmembrane peptide were determined by absorbance using $\varepsilon_{\text{NBD-DPPE}}$ 21,000 $M^{-1}cm^{-1}$ at 460nm, $\varepsilon_{\text{pyrene-DPPE}}$ 35,000 $M^{-1}cm^{-1}$ at 350 nm, $\varepsilon_{\text{rhod-DOPE}}$ 88,000 $M^{-1}cm^{-1}$ at 560 nm, ε_{DPH} 84,800 $M^{-1}cm^{-1}$ at 352nm, and $\varepsilon_{\text{LW peptide}}$ 22,000 $M^{-1}cm^{-1}$ at 280nm, $\varepsilon_{\text{TMADPH}}$ 84,800 $M^{-1}cm^{-1}$ at 353 nm, $\varepsilon_{\text{ODRB}}$ 125,000 $M^{-1}cm^{-1}$ at 555 nm . High performance thin layer chromatography (HP-TLC) plates (Silica Gel 60) were purchased from VWR International (Batavia, IL). TLC analysis of 10 µg samples of sterols (reference to our protocol) showed at most minor impurities after long term storage except in the case of stigmasterol, and especially ergosterol. However, anisotropy measurements on ergosterol-substituted cells confirmed that ergosterol retained its ability to support a high degree of membrane order despite the presence of impurities.

Vesicle Preparation:

Multilamellar Vesicles (MLV) and ethanol dilution small unilamellar vesicles (SUV) were prepared similar to as described previously (30). For SUV, lipids and fluorophores were pipeted in glass tubes, dried under nitrogen, re-dissolved in 25µL ethanol and dispersed in 975µL phosphate buffered saline (PBS: 1mM KH_2PO_4, 10mM Na_2HPO_4, 137mM NaCl and 2.7mM KCl, pH 7.4). For preparing MLV, the dried lipid was re-dissolved in 20µL chloroform, re-dried under nitrogen followed by drying under high vacuum for 2h and dispersal in 70^{o}C PBS pH 7.4. Final samples contained 500µM lipid. When present, TX-100 and LW peptide were pipetted along with lipids. Background samples lacking fluorescent probe were also prepared. Large unilamellar vesicles (LUV) were prepared by subjecting MLVs to 5 cycles of freeze/thaw, alternately placing the sample in a dry ice/acetone bath and room temperature water bath. The vesicles were then passed (11 cycles) through a mini-extruder (Avanti Polar Lipids Alabaster, AL) to obtain LUV. For FRET measurements, LUV were prepared only by extrusion (without freeze/thawing, which was found to segregate FRET probes into different vesicles). All samples were incubated at room temperature for 1h before fluorescence measurements were made.

Fluorescence and Absorbance Measurements:

Fluorescence was measured on SPEX Fluorolog 3 spectrofluorimeter (Jobin-Yvon, Edison, NJ) using quartz semi-micro cuvettes (excitation path length 10mm and emission path length 4mm). DPH fluorescence was measured at an excitation wavelength of 358nm and emission wavelength of 430nm. NBD fluorescence was measured at an excitation wavelength of 460nm and an emission wavelength of 534nm. Pyrene fluorescence was measured at an excitation wavelength of 350nm and an emission wavelength of 379nm. TX-100 fluorescence was measured at an excitation wavelength of 260nm and emission wavelength of 310nm. Slit-width bandwidths for fluorescence intensity measurements were set to 4nm (2mm physical size) for excitation and emission. The reported values were corrected for background fluorescence except for DPH fluorescence, where background values were less than 0.02% of the sample values. Absorbance was measured with a Beckman 640 spectrophotometer (Beckman Instruments, Fullerton, CA) using quartz cuvettes.

Measurement of TX-100 Binding to MLV

The amount of vesicle-bound TX-100 was calculated as follows. 2mL aliquots of MLV samples containing 500µM bSM/POPC/chol (1:1:1) and various concentrations of TX-100 (150, 300 and 500µM) were prepared as described above, and then incubated at room temperature for 1 h. 1 mL aliquots were centrifuged at 14000 rpm (11,000 x g) for 20min. in an Eppendorf 5415C tabletop centrifuge; the supernatant was separated from the pellet and the pellet was re-suspended in 1mL PBS pH 7.4. Then 250 µL aliquots each of MLV prior to centrifugation, supernatant and resuspended pellet were diluted to 1mL with 750µL PBS pH 7.4, and fluorescence measured. Controls showed no loss of TX-100 during vesicle preparation (e.g. due to sublimation during the high vacuum step). The intensity of TX-100 fluorescence per unit concentration was found to be insensitive to whether TX-100 concentration was above or below its critical micelle concentration or whether the TX-100 was bound to lipid or not (not shown).

Determination of Lipid Composition after TX-100 Solubilization by High Performance-TLC

Lipids were analyzed by TLC essentially as previously described (103). Details are given below. MLV samples containing SM/POPC/Chol (1:1:1) and various concentrations of Triton X100 (0, 150, 300 and 500 µM) were prepared as described above, and were incubated at room temperature for 1 hr. Samples were centrifuged at **(11,000 x g)** 14000 rpm for 20 minutes in an Ependorf 5415C tabletop centrifuge; supernatant was separated from the pellet; 500µL supernatant was dried under Nitrogen to evaporate the PBS. The pellet was dispersed in 1mL PBS and vortexed. A 500µL aliquot of the dispersed pellet was dried under Nitrogen. The dried lipid was then dissolved in choloroform: methanol (1:1) (v:v) and a 5µL aliquot was applied drop by drop with a 1mL syringe to the HP-TLC plates that had been pre-heated at 100^{o}C for 30min and then cooled to room temperature. The plates were chromatographed using a sequential solvent system. The first solvent (50:38:4:8) (v:v) (chloroform: methanol: acetic acid: water) was allowed to migrate half way up the plate. The plate was then air dried for 10 min, introduced into a second chamber containing the solvent system 22:1 hexane: ethyl acetate (v:v) until the solvent migrated to near the top of the plate. (For each solvent, chambers were equilibrated with solvents

4 h before chromatography.) The plate was then air dried for 15 minutes and evenly sprayed with 3% (w/v) cupric acetate dissolved in 8% (v/v) phosphoric acid in water and air dried for 45 min. To detect the lipids, plates were charred at 180^{o}C for 2 to 5 minutes until the bands were clearly visible. After the plate was cooled, it was scanned as an image (CanonScan N124OU). Spot intensity was analyzed using the NIH/Scion Image Software (Scion Corp., Frederick, MD). Unknown lipid and sterol amounts were quantified by comparing band intensity to that of lipid standards (which were made in the same fashion as the experimental samples) fit to an exponential intensity *versus* concentration curve (Slide Write Plus software).

Measurement of the Temperature Dependence of DPH Fluorescence Quenching by TEMPO:

The temperature dependence of TEMPO quenching was carried out as described in (30). SUVs and MLVs with 500µM lipid and 0.1mol% DPH were prepared as described above. A 6.2µL aliquot of a 322mM stock solution of TEMPO dissolved in ethanol was added to the samples (defined as F samples) to obtain a final concentration of 2mM unless otherwise stated. The same volume of ethanol was added to the samples that did not contain quencher (Fo samples). The samples were incubated at room temperature for 10min, after which they were cooled to 16^{o}C and the fluorescence measurements were initiated. The cuvette temperature was measured with a probe thermometer placed in the cuvette before each measurement (Fisher brand traceable digital thermometer with a YSI microprobe, Fisher Scientific). The cuvette temperature was increased at a rate of ~0.5^{o}C per minute and readings were taken every 4^{o}C. The ratio of the average fluorescence intensity in the presence of quencher to its absence (F/Fo) was calculated. Background fluorescent measurements were taken at 16 and 60^{o}C. The backgrounds were not subtracted because they were less than 0.02% of the DPH fluorescence signal. The "melting" midpoint temperature (T_{mid}) was calculated for each curve. T_{mid} was defined as a point of maximum slope of a sigmoidal fit of F/Fo data. (Slide Write Plus software, Advanced Graphics Software Inc., Encinitas, CA).

Measurement of the Temperature Dependence of Fluorescence Anisotropy:

DPH fluorescence anisotropy measurements were made using a SPEX automated Glan-Thompson polarizer accessory with slit-width band-widths set to 4.2nm (excitation) and 8.4nm (emission). Anisotropy values were calculated as described previously (30). Anisotropy as a function of temperature was measured for MLV samples containing 0.1mol% DPH and 500μM lipid, prepared as described above. The samples were incubated at room temperature for 1h and then cooled to 16^{o}C. Samples were then heated in steps of 4^{o}C and anisotropy was measured at each step once the temperature stabilized.

Measurement of the Temperature Dependence of FRET:

Förster (Fluorescence) Resonance Energy Transfer, FRET, using donor acceptor pairs having different Förster radii (Ro) was measured in MLV prepared as described above. Unless otherwise noted vesicles contained 0.1mol% (for NBD-DPPE and DPH) or 0.05mol% (for pyrene-DPPE) donor and 2 mol% acceptor (rhod-DOPE) in F samples. Fo samples contained only donor. Background samples for Fo (containing only lipid and lacking donor) and for F (containing lipid plus acceptor) were also prepared. Samples were prepared at 70^{o}C and then incubated at room temperature for 1h, after which they were cooled to 16^{o}C and the fluorescence measurements initiated. The cuvette temperature was measured with a probe thermometer placed in the cuvette before each measurement (Fisher brand traceable digital thermometer with a YSI microprobe, Fisher Scientific). The cuvette temperature was increased at a rate of ~0.5^{o}C per minute and readings were taken every 4^{o}C. In addition, background fluorescence at 16 and 64^{o}C was measured, averaged for the two temperatures (as backgrounds were found to be independent of temperature), and then subtracted from the FRET sample values. The ratio of fluorescence intensity in the presence of acceptor to its absence (F/Fo) was calculated. The domain detection midpoint temperature (T_{mid}) was calculated for each curve. T_{mid} was defined as a point of maximum slope of a sigmoidal fit of F/Fo data. The maximum temperature at which there is facile detection of Lo domains by FRET (T_{upper}) was calculated from the intersection of a line fit to T_{mid}, and the 2 points closest above and 2 below T_{mid} and the line F/Fo = F/Fo value at the upper limit of the sigmoidal fit to F/Fo vs. temperature. (Due to their temperature dependence in the Ld state, T_{upper} could not be calculated for TEMPO quenching and anisotropy.)

Estimating the effect of domain size upon the ability to detect domains by FRET or quenching.

Calculating exact nanodomain size is very difficult as FRET depends upon acceptor concentration, partition of donor and acceptor between ordered and disordered domains, domain shape, and whether domains in the opposing leaflets are or are not in register. However, it is possible to estimate how FRET and quenching will be affected by domain size for some simple geometries (Fig. 3.18A) under some conditions. Consider the case in which quenching can be approximated by an all-or-none distance dependence, such that quenching is complete when fluorophore and quencher are within a critical distance (Rc) of each other. Next, consider the condition in which quencher/acceptor concentration outside of domains is high, so that any fluorescent molecule within distance Rc from the edge of a domain will be quenched. In this case, the interior area for a circular domain (the area within which there is no quenching by quenchers outside of the domains) will be given by the equation:

$$A_{interior}/A_{total} = \pi(R_{domain} - R_c)^2/\pi R_{domain}^2 = (R_{domain} - R_c)^2/R_{domain}^2 = 1 - 2(R_c/R_{domain}) + (R_c/R_{domain})^2$$

Where $A_{interior}$ is the area within the domain too far from the edge of the domain for a fluorescent molecule within the interior to be quenched by a quencher outside the domain, A_{total} is the total area of a domain, and R_{domain} is the radius of the domain. We can define $F/F_{maximum}$ as the fluorescence of molecules within small domains relative to that of a large domain for which $R_{domain} >> R_c$, i.e. $A_{interior} \sim A_{total}$, and which has an area equal to that of the sum of the areas of the small domains. In that case:

$$F/F_{maximum} = A_{interior}/A_{total} = 1 - 2\,R_c/R_{domain} + (R_c/R_{domain})^2$$

Fig. 3.18B shows $F/F_{maximum}$ vs. R_c/R_{domain}. Notice that $F/F_{maximum}$ equal ½ $F_{maximum}$ at when $R_{domain}/R_c \sim 3.5$.

Bacteria and Growth Conditions

High-passage *Borrelia burgdorferi* strain B31 was used for all studies. The bacteria were grown in Barbour-Stoenner-Kelly-H (BSK-H) medium (Sigma) under microaerophillic conditions at 33^{o}C.

Sterol substitutions

To substitute different sterols for cholesterol in live *B. burgdorferi* for various studies the following procedure was used. Cultures of 50 ml with spirochetes grown to about 1 x 10^{8}cells/ml were pelleted from the BSK-H culture medium by centrifugation at 5000 X g for 10 min on a Sorvall RC-5B centrifuge (DuPont instruments) at room temperature. The supernatant was discarded and the pellet was resuspended in 50 mL Hank's Balanced Salt Solution (HBSS). The pellet was repelleted to wash off any remaining culture medium. After discarding the supernatant, the pellet was resuspended in 1mL of HBSS and mixed well by pipeting up and down, followed by additional 47.5 mL of HBSS. Then 2.5mL of 200 mM MβCD (dissolved in PBS (Invitrogen) was added to the cells in HBSS to obtain a final concentration of 10 mM MβCD, the cells mixed gently, and incubated for 30 min at 33^{o}C. The samples were again centrifuged at 5000 x g for 10 min and supernatant was decanted in order to remove the MβCD and bound cholesterol lipids (cholesterol plus cholesteryl glycolipids). These MβCD treatment conditions result in the depletion of ~ 50% total cholesterol (including cholesterol glycolipids) from *B. burgdorferi* (100) (Tim LaRocca 2010). Spirochetes were then centrifuged and MβCD-bound cholesterol lipids and MβCD were removed by decanting the supernatant. *B. burgdorferi* cell numbers were determined by microscopy and the cells resuspended in HBSS to different concentrations depending on experiment. For FRET analysis of live *B. burgdorferi*, the cell concentration was 4 X 10^{8} spirochetes/mL. Once spirochetes were resuspended in HBSS, sterols (stored in 100% ethanol at 2 mg/ml) were warmed to room temperature and added to the bacteria at a final concentration of 10 μg/ml and allowed to incubate at 33^{o}C for 10–30 min. For studies where osmotic lysis of *B. burgdorferi* was investigated, spirochetes were treated in the same manner with the exception of the osmoprotectant, dextran T500 (6% w/v, Pharmacia), being present in the HBSS.

FRET measurement in B.burgdorferi cells and model membranes:

Spirochetes at a concentration of $4x10^8$ cells/mL in HBSS were used for the FRET measurements. An aliquot of 5.2 µL (from a 73 µM ethanolic stock solution) of FRET donor TMADPH was added to 4mL of cells, mixed well by stirring and incubated at room temperature for 10 min. The cells were divided into four 900 µL aliquots, placed in quartz cuvettes and heated to 35^{o}C. Donor fluorescence intensity of all four samples was measured before adding acceptor. Two samples out of the four were defined as F samples, and to them 5.2µL (out of a 322 µM ethanolic stock solution) of the acceptor, octadecyl rhodamine B (ODRB), was added, followed by incubation at 35 ^{o}C for 15 min. FRET measurements were then initiated on the F samples and Fo samples (the two samples containing donor but not acceptor). Fluorescence in background samples lacking donor and ones lacking donor but containing acceptor was also measured. The temperature of the samples was measured using a probe thermometer placed in a cuvette. (Fisher brand traceable digital thermometer with an YSI microprobe, Fisher Scientific). The cuvette temperature was slowly decreased from 35^{o}C to 15^{o}C in steps of 5 ^{o}C and the cells were incubated at each temperature for 7 min once the temperature stabilized. Donor fluorescence intensity of Fo and F samples was measured at each temperature and the ratio of TMADPH fluorescence intensity in the presence of acceptor to its absence (F/Fo) was calculated and plotted as a function of temperature. Background fluorescence was measured at 35 and 15 ^{o}C and averaged for the two temperatures because they were found to be independent of temperature. The backgrounds were $\leq$ 2% of the TMADPH fluorescence signal and were subtracted from the FRET sample values.

FRET measurement in model membranes was carried out similarly to that in cells with the following changes. FRET donor, 0.1 µM TMADPH was added to SUV prepared by ethanol dilution containing 100 µM lipid and was allowed to incubate at 50^{o}C for 10 min. FRET acceptor, 3 µM ODRB, was added to the F samples and further incubated for 10 min after which the cuvettes were cooled to 45^{o}C and fluorescence measurements were initiated. Cuvettes were further cooled slowly to 15^{o}C in steps of 5^{o}C increments and the fluorescence measured once the temperature stabilized.

Chapter 3:

Measurement of Lipid Nanodomain formation and Size in Sphingomyelin/POPC/cholesterol vesicles and effect of TX-100 and transmembrane helices on domain size

This work has been published. Please refer to page xvii of this dissertation for a reference.

Introduction

The subject of the formation of membrane lipid domains (rafts) in cells has received much attention because of its implications for membrane-associated processes, including bacterial and viral infection, signal transduction, and sorting. Early studies speculated that sphingolipid microdomains played a role in sorting (9), and the observation that detergent resistant membranes (DRM) rich in sphingolipids (and cholesterol) could be isolated from cell membranes upon addition of Triton X-100 (TX-100) suggested that these DRM might correspond to cellular sphingolipid microdomains (19). The observation that sphingolipid and cholesterol -rich DRM could be isolated from model membranes when liquid ordered (Lo) domains are present, and that insolubility appeared only under conditions in which spectroscopic methods showed that ordered domains formed, led to the hypothesis that DRM might arise from cellular Lo domains that co-exist with disordered Ld domains enriched in unsaturated phospholipids (1,14).

Because addition of detergent to membrane-containing samples is a perturbation, there is concern that TX-100 could alter domain formation (5,29). However, in addition to the studies above, many subsequent studies have confirmed that when Lo and Ld domains co-exist, the DRM arise from the Lo region of the membrane (34-36,104,105). On the other hand, it has been reported by one group that Lo domains in the mixture 1:1:1 SM/POPC/chol can be stabilized by TX-100, such that they form at higher temperatures only in the presence of TX-100 (106,107), and this has been frequently cited as evidence that DRM may be a detergent artifact.

In this study we have used spectroscopic methods to detect the presence and size of ordered domains as a function of temperature for SM/POPC/chol. This mixture was found to form nanodomains whose size decreased as temperature increased. The presence of TX-100 (or transmembrane helices) increased domain size, without increasing the amount of the bilayer in an ordered state. These results have important implications for the organization of lipid domains in cells, as well as for the reliability of TX-100 insolubility as a method to detect ordered domain formation.

Results

Stability of ordered state in 1:1:1 bSM/POPC/chol vesicles: Neither TX-100 nor a transmembrane peptide stabilize ordered state formation

First, quenching of DPH fluorescence by TEMPO was measured (30). TEMPO is a nitroxide-bearing molecule that binds to disordered (Ld) domains more strongly than to ordered (Lo) domains (30,108), so in bilayers partly or wholly in an ordered state quenching of DPH, which partitions evenly between ordered and disordered domains (14,109), by TEMPO is weak, but when a bilayer is fully in the Ld state, quenching is strong (30). By measuring the temperature dependence of quenching the midpoint melting temperature (T_{mid}) of Lo domains can be determined (30). The T_{mid} value, given by the inflection point in the quenching curve, represents the point at which the slope of the curve, and thus the decrease in membrane order as a function of temperature, is a maximum. (It is not necessarily the point at which the membrane is 50% in the Lo state.) The higher the T_{mid} value, the greater the stability of ordered domains (30). Fig. 3.1A (circles) shows the temperature dependence of TEMPO quenching in multilamellar vesicles (MLV) composed of a 1:1:1 (mol:mol) mixture of bSM/POPC/chol. There is a sigmoidal dependence of normalized DPH fluorescence (=F/Fo, the fraction of unquenched fluorescence) upon temperature, with quenching levels in good agreement with recent studies on similar mixtures (30). The T_{mid} value occurs at about 45^{o}C (Table 3.1). Controls in which TEMPO concentration was varied show that TEMPO binding to vesicles did not alter T_{mid} values up to 2mM (Figure 3.6).

A similar DPH quenching curve, with perhaps a small decrease in T_{mid} was observed in 1:1:1 bSM/POPC/chol when lipids were mixed with TX-100 prior to vesicle formation (final TX-100 concentration 150μM) (Table 3.1 and Fig. 3.1A, filled triangles). There was very little if any additional dependence of T_{mid} upon increasing TX-100 concentration up to several-fold above the critical micelle concentration (cmc) of TX-100 (~200-300μM (110)) (Figure 3.7 and Table 3.1). The presence in the vesicles of 0.45 mol% of LW peptide, a Leu-rich transmembrane-type peptide that partitions strongly into Ld domains (85) also had little, if any, effect upon T_{mid} (Table 3.1 and Fig. 3.1A, open triangles).

Other experiments showed that the temperature-dependent change in quenching was reversible (Fig. 3.8A), and that similar T_{mid} values with and without TX-100 were observed using large unilamellar vesicles (LUV) or small unilamellar vesicles (SUV) in place of MLV (Table 3.3).

To confirm results obtained from TEMPO quenching, the thermal stability of ordered state formed by 1:1:1 bSM/POPC/chol was measured using steady state DPH fluorescence anisotropy (Fig. 3.1B). The anisotropy of DPH fluorescence is high when it is in the Lo state, and decreases in the Ld state (30,111). Anisotropy in 1:1:1 bSM/POPC/chol at low temperature (filled circles) was equal to those previously observed for a mixture of Lo and Ld states, while the values at high temperature corresponded to those in an Ld state (30). As in the case of TEMPO quenching, there was a sigmoidal dependence upon temperature, with estimated T_{mid} values very similar to that measured with TEMPO quenching (Table 3.1). Samples containing 1:1:1 bSM/POPC/chol plus TX-100 (Fig. 3.1B, filled triangles) also exhibited a slight decrease in T_{mid} value similar to that determined by TEMPO quenching (Fig. 3.1B and Table 3.1). As in the case of TEMPO quenching higher TX-100 concentrations did not greatly affect T_{mid} (Fig. 3.9 and Table 3.1). Samples containing membrane-inserted LW peptide (Fig. 3.1B and Table 3.1, open triangles) showed a slight decrease in T_{mid}.

Membrane composition in the presence of TX-100

To evaluate the effect (or lack of effect) of TX-100 on T_{mid}, it was important to determine how much TX-100 was bound to membranes. Both the amount of TX-100 bound to vesicles and the degree to which it solublized vesicular lipids could influence T_{mid}. As shown in Table 3.2, the amount of bound TX-100 varied from about 4 mol% of the lipid at 150µM TX-100 to about 10 mol% of total lipid in 500µM TX-100. Lipid solubilization at different TX-100 concentrations was also measured. As shown in Table 3.2, most of the lipid was not solubilized by TX-100 at any of the concentrations tested. However, a significant amount of POPC was solubilized at 300µM and especially at 500µM TX-100. This lipid selectivity is expected because TX-100 selectively dissolves the lipids that are within Ld domains, which should be predominantly composed of POPC.

Segregation-detected nanodomain formation and size

The methods used above measure membrane order. To more directly probe lipid segregation into separate domains, methods dependent on lipid segregation were used. First, domain formation was detected by nitroxide-quenching using DPH as the fluorophore and the phospholipid 10SLPC which contains a nitroxide-bearing doxyl ring in the middle of one fatty acyl chain, as quencher. Unlike TEMPO quenching, which is strongly dependent upon TEMPO binding to membranes, and thus lipid packing, quenching by a nitroxide-labeled lipid directly detects lipid segregation (14). The doxyl group imparts a strong tendency to form and incorporate into Ld domains (14,85,112). As noted above, the effective quenching range for nitroxides (Rc) is generally close to 12Å (113). T_{mid} detected by 10SLPC quenching was similar to that obtained by TEMPO quenching (Fig.3.2 and Table 3.1). In general, TX-100 and LW peptide slightly decreased T_{mid}, similar to what was measured by TEMPO quenching and anisotropy (Table 3.1).

Another method commonly used to detect domain formation is FRET. When a membrane has co-existing ordered and disordered domains, the segregation of donor and acceptor with different affinities for ordered and disordered domains results in a decrease in FRET, which is detected as an increase in normalized donor fluorescence (F/Fo). For measuring FRET, the acceptor used was rhod-DOPE, which partitions strongly into Ld domains (114). Donors with a significant affinity for ordered domains, NBD-DPPE, DPH, and pyrene-DPPE were used. Their FRET to rhod-DOPE has an effective Ro of 49Å, 36Å, and 26Å, respectively, as determined from experimental measurements in homogeneous bilayers (Table 3.4).

The dependence of FRET upon temperature showed patterns very different from those measured by nitroxide quenching. Fig. 3.3A (circles) shows that in bSM/POPC/chol vesicles when the donor was NBD-DPPE, FRET was strong throughout the range 10-60^{o}C. Domains were only barely detected at low temperature, as shown by the weaker FRET (higher F/Fo) below 30^{o}C. For FRET, T_{mid} is the temperature at which the change in FRET vs. temperature is at a maximum. A crude T_{mid} value for domain detection is 9^{o}C. In POPC/chol vesicles, which lack SM and form homogeneous bilayers FRET is very strong at all temperatures (Fig. 3.3B). FRET curves were similar for 1:1:1 bSM/POPC/chol LUV samples, showing that the FRET and its temperature dependence were not greatly influenced by inter-bilayer FRET in MLV (Fig. 3.10

and Table 3.5). In contrast to samples lacking TX-100, domains could be easily detected for 1:1:1 bSM/POPC/chol vesicles in the presence of 150μM TX-100 (in which TX-100 is mixed with the lipids prior to vesicle formation), which exhibited dramatically decreased FRET at lower temperatures (Fig. 3.3A, filled triangles). The domains detected had an apparent T_{mid} ~25^{o}C. The effect of TX-100 on FRET increased in a TX-100 dose-dependent fashion (Fig. 3.11).

A decrease in FRET and increase in T_{mid} (to 23^{o}C) was also observed in vesicles containing 0.45 mol% LW peptide (Fig. 3.3A, open triangles). Samples containing both 0.45 mol% LW peptide and 150μM TX-100 gave curves very similar to those with TX-100 alone (Fig 3.3A). POPC/chol vesicles showed no effect of TX-100 or LW peptide on FRET (Fig. 3.3B).

Using NBD-DPPE to rhod-DOPE FRET samples containing 1:1:1 egg SM/POPC/chol gave similar FRET results to those with brain SM, although domain formation in the absence of TX-100 was more easily detected at lower temperatures (Fig. 3.12).

At first glance, the observation that T_{mid} measured by FRET is lower than that measured by nitroxide quenching and anisotropy, and that there is a lack of FRET-detected domain formation in bSM/POPC/chol at temperatures at which they can be detected in the presence of TX-100 or LW peptide might seem to contradict conclusions of the nitroxide quenching and anisotropy results. How can FRET change so strongly in a temperature range in which the amount of ordered domains does not change? The likely explanation is that the domains formed in bSM/POPC/chol are too small to detect using the NBD-DPPE/rhod-DOPE FRET-pair under some conditions, and that TX-100 and LW peptide influence domain size. Nitroxide-induced quenching (which has a range of 12Å (113) and anisotropy are both very short range processes that measure behavior of the lipid in which the probes are in direct contact, while NBD-to-rhod FRET is a longer range interaction, and requires that domain radius be greater than the interaction distance (i.e. Ro) in order to allow facile domain detection (see Discussion).

To test the hypothesis that T_{mid} measured by FRET reflects domain size, and that domain size is altered by TX-100, FRET experiments were repeated with the DPH/rhod-DOPE (Fig. 3.4A and 3.4B) and pyrene-DPPE/rhod-DOPE FRET pairs (Fig. 3.4C and 3.4D), FRET pairs with smaller Ro values than the NBD-DPPE/rhod-DOPE pair. As predicted, without TX-100 domain

formation (weakened FRET) could now be detected more easily in bSM/POPC/chol at lower temperatures, and the smaller the Ro, the higher the apparent T_{mid} for loss of Lo domain detection (Table 3.1). We also estimated the temperature (T_{upper}) that represents the upper limit of facile Lo domain detection (see Methods). A similar pattern was observed, in which the T_{upper} increased as Ro decreased. This progressive and Ro-dependent loss of domain detection as temperature increases indicates that domain size gradually decreases as temperature increases (see below). Also, as in the case for T_{mid}, T_{upper} increased in the presence of TX-100 and LW peptide (Table 3.1).

In addition, the increase in apparent T_{mid} values in the presence of TX-100 or LW peptide when pyrene-DPPE and DPH were donors were smaller than when NBD-DPPE was the donor (Table 3.1). This is as expected if TX-100 and LW peptide only induce an increase in domain size, because for smaller Ro values FRET is less sensitive to domain size. [Also, notice that at low temperatures the difference between FRET levels with and without TX-100 is largest when NBD-DPPE is donor, smaller when DPH is donor and smallest when pyrene-DPPE is donor.] Notice that even for these smaller Ro pairs, no evidence of domain formation was observed in POPC/chol vesicles which form more homogeneous bilayers.

Using the DPH/rhod-DOPE pair, we also confirmed that thermal changes in FRET were reversible both in the presence and absence of TX-100 (Fig. 3.8B).

It is unlikely that the results above reflect probe-induced perturbation of the lipid bilayers. For the FRET studies, a large perturbation of lipid melting due to donor is unlikely because the donors were used in very small amounts (1/2000 lipids for pyrene-DPPE and 1/1000 lipids for NBD-DPPE and DPH), and the same acceptor, rhod-DOPE and acceptor concentration was used. Thus, perturbation cannot explain the apparent differences in domain properties observed for different FRET pairs. A different issue is whether samples with the acceptor (2% rhod-DOPE), have different physical behavior than samples without acceptor. Controls also show that this is unlikely. First, similar FRET results were obtained at 1 mol% rhod-DOPE (Fig. 3.13 and Table 3.5). Second, when DPH-10SLPC quenching experiments were carried out both in the absence and presence of 2mol% DOPE, no difference in quenching or its temperature dependence was observed (Fig. 3.14 and Table 3.5).

NBD-DOPE to rhod-DOPE FRET, and the effect of TX-100 upon FRET with this donor acceptor pair, were very similar in samples containing 4.7mol% 10SLPC and those lacking 10SLPC (Fig. 3.15 and Table 3.5). This indicates that 10SLPC did not greatly perturb domain formation or size. The conclusion that 10SLPC did not perturb domain formation is further supported by the similarity of T_{mid} detected by 10SLPC quenching to the T_{mid} values determined by TEMPO quenching and anisotropy (Table 3.1).

Combining FRET and 10SLPC quenching results, it appears that TX-100, and LW peptide do not induce nanodomain formation, but do increase domain size. This means that in the presence of TX-100 and LW peptide there are larger Lo domains, but since the amount of the bilayer in the Lo state has not increased (as shown by TEMPO quenching, anisotropy and 10SLPC quenching) there must also be also fewer of them.

Effect of cholesterol concentration upon FRET-detected nanodomain formation in the absence and presence of TX-100 or transmembrane peptide

In additional studies, the effect of chol concentration upon domain segregation in bSM/POPC/chol, both in the absence and presence of TX-100 and LW peptide, was studied. As shown in Fig. 3.5, at room temperature for both the NBD-DPPE/rhod-DOPE FRET pair (Fig. 3.5A) and the pyrene-DPPE/rhod-DOPE FRET pair (Fig. 3.5B) domains could be detected by FRET at both medium and very high concentrations of chol. This is consistent with previous FRET studies showing that domain formation can occur at very high chol concentrations in a very similar mixture, SM/SOPC/chol (58).

There was a maximum degree of FRET-detected segregation near 25-35mol% chol in both the absence and presence of TX-100. This suggests domain formation is either most stable, or domains are largest, at this chol concentration. In contrast, the effect of LW peptide upon FRET-detected segregation increased monotonically as chol concentration increased. These results indicate that the effects of TX-100 and a transmembrane helix upon domain properties are not restricted to values around 33mol% chol, and that at high chol concentrations transmembrane helices have a stronger effect upon domain properties than TX-100. Even at very high chol (45

mol%), with TX-100 or LW peptide present FRET showed segregation persisted to above 37^{o}C (Fig. 3.16).

Estimating nanodomain size

As noted in Chapter 2, calculating exact nanodomain size from FRET is difficult as FRET also depends upon acceptor concentration, partition of donor and acceptor between ordered and disordered domains, domain shape, and whether domains in the opposing leaflets are or are not in register. However, using multiple FRET/quencher pairs makes it possible to roughly estimate nanodomain size (Fig. 3.18). Processes such as FRET and nitroxide quenching have a distance-dependence such that quenching is very strong only when fluorophore and quencher are within a critical distance (Rc) (Fig.3.18A). Strong protection of a donor inside a domain from quenchers outside the domain requires an Lo domain radius greater than Rc. Crudely speaking, Rc~Ro (113).

As shown in Fig. 3.18B, FRET basically cannot detect domains when domain radius is <Ro. Thus, T_{upper}, the estimated maximum temperature for facile domain detection is the temperature at which domain radius is close to Ro. If the amount of ordered domains is nearly constant over a temperature range, but domain size decreases as temperature increases, Fig. 3.18B shows that the T_{mid} value, the midpoint for loss of domain detection, should be close to 3Ro.

Based on this, we can use T_{mid} and T_{upper} values for different FRET donors, to estimate domain sizes. As shown in Fig. 3.18C, it can be estimated that in 1:1:1 bSM/POPC/chol nanodomain radius gradually decreases from ~150Å near 10^{o}C to 80-100Å at 23^{o}C to as small as ~ 36Å before melting at 45^{o}C. Assuming a lipid cross-sectional area of about 70Å^{2}, this gives the number of lipids in a domain decreasing from about 1000 lipids in one leaflet at 10^{o}C to about 360 lipids at 23^{o}C and about 60 lipids at 45^{o}C. Fig. 3.18C also shows the estimated increase in domain size induced by the presence of TX-100. There is a several-fold increase in size. The size increase in the presence of LW peptide was somewhat smaller (not shown).

It must be noted that these domain radii values are only estimates. If domains are irregular they will have a larger circumference to area ratio than circular domains, and many more molecules near domain edges, leading to an underestimate of domain size. In addition, for the actual acceptor concentrations we used, which are not sufficient to totally quench fluorescence, calculations (not shown) suggest the domain radii may be overestimates by up to a factor of almost two.

Discussion

Nanodomain size and the effect of TX-100 and transmembrane helices on domain formation and size.

This study shows that nanodomain size in bSM/POPC/chol is strongly temperature dependent, decreasing as temperature increases. A temperature-dependent decrease in domain size is also predicted by the critical fluctuation model for nanodomains (115), and that similar nanodomain sizes have been proposed for other lipid mixtures (56). FRET data also shows that in the presence of TX-100 or LW peptide domain size in bSM/POPC/chol vesicles increases significantly. Given the apparent T_{mid} for FRET for the NBD-rhodamine pair at 23^{o}C when there is 4 mol% TX-100 in the membrane (samples with 150μM total TX-100), domain radius must increase to 150Å near room temperature based on the analysis above. An important question is how this size increase relates to prior work on the effect of TX-100 in SM/POPC/chol. It has been proposed that TX-100 binding to vesicles induces domain formation by reducing the miscibility of SM with molecules (unsaturated lipids and TX-100) concentrated within the Ld state (106,107). The analysis of the calorimetric studies on which this was based predicted that the temperature at which domain separation occurs in 1:1:1 SM/POPC/chol exhibits an increase from 20^{o}C to about 35^{o}C when the membranes contain 3mol% TX-100 (107), and raw calorimetric data showed that a transition at 23^{o}C was accompanied by an additional peak near 45^{o}C as TX-100 concentration was increased from 0 to 3 or 7.7 mol% in these mixtures (106). This is the same range of TX-100 concentrations in the membrane that we investigated. (We also find that at a very high TX-100 concentration (1% v/v), solubilization vs. temperature had a midpoint (50% solubilization) that was also close to 35^{o}C (not shown).)

However, in contrast to conclusions from calorimetry, our studies find that the interaction of TX-100 with membranes does not increase the thermal stability of ordered domains, i.e. methods that can detect small nanodomains, such as nitroxide quenching show there are no temperatures at which the total fraction of the membrane in the form of ordered domains increases in the presence of TX-100. Instead, we find that TX-100 increases the size of individual domains. This may not be inconsistent with calorimetric data. The melting of the small nanodomains

might not be sufficiently cooperative in temperature, or might not involve a high enough enthalpy change, to have been detected by calorimetry. In fact, the statement that TX-100 induces phase separation may be formally correct if large domains can be considered phases while small nanodomains cannot. Nevertheless, the key point is that the formation of nanodomains is not dependent upon TX-100. Since nanodomains are similar to the type of domains thought to form in plasma membranes, they are likely to be the most physiologically-relevant species. In fact, experimentally the tendency of TX-100 to increase domain size may be a desirable property that allows the physical isolation of merged nanodomains as detergent-resistant membranes (DRM), even if the merger of small domains into large ones is an artifact.

The lack of domain formation by TX-100 is consistent with the overwhelming evidence that when there is *pre-existing* domain formation, TX-100 solubilization reflects underlying domain behavior. In particular, it has been observed many times that when membranes have co-existing Lo and Ld domains prior to TX-100 addition, the Ld domains dissolve while the Lo domains are resistant to TX-100 solubilization (14,34-36,104,105). Studies also show that there is no expansion of preexisting Lo domains in supported bilayers (in which individual ordered domains cannot migrate and merge, and so individual domain size cannot increase) upon TX-100 addition (34,36,105), although such an expansion might be predicted if TX-100 reduced the miscibility of SM in the disordered domains. In fact, there is often partial solubilization of the Lo domains (34,36,105), consistent with the concept that the addition of TX-100 would lead to an *under*estimation of Lo domain formation (29). Furthermore, low concentrations of TX-100 tend to induce budding and fission of vesicles containing Lo domains from vesicles containing co-existing Lo and Ld domains (116), further enhancing the similarity between DRM and the Lo domains from which they arise. Nevertheless, we are not arguing that DRM are identical to pre-existing rafts, and the isolation of DRM from a cellular membrane, especially at 4^{o}C, cannot be *proof* of the existence of pre-existing rafts.

It is also interesting that the presence of a modest amount of transmembrane helices may be more effective than TX-100 at increasing domain size at cholesterol concentrations likely to exist in plasma membranes. This increases the probability of domain formation in natural membranes and suggests that the effect of TX-100 in a protein-containing membrane is less than in a simple lipid bilayer.

An important question is why TX-100 increases domain size. One possibility comes from the molecular dynamics studies P. Butler and colleagues (Penn State U.) showing that TX-100 decreases bilayer width (personal communication). TX-100 in Ld domains would increase the mismatch in width between Ld and Lo domains, and thus increase line tension. An increase in domain size would minimize the amount of lipid at Lo/Ld boundaries and thus the unfavorable line tension energy.

Table 3.1: Ordered domain melting temperatures under different conditions. MLV samples were composed of 500µM 1:1:1 (mol:mol) bSM:POPC:chol. T_{mid} for anisotropy and short range quenching is the point at which %melting/^{o}C is a maximum. T_{mid} for FRET is the temperature at which the change in F/Fo vs. temperature is a maximum. T_{upper} is the maximum temperature at which there is facile detection of Lo domains. Calculation of T_{mid} and T_{upper} is described in Methods. Average T_{mid} and T_{upper} values in the presence and absence of TX-100 or transmembrane peptide are shown. Sample number is shown in parenthesis. Samples with 10SLPC also contained 2mol% DOPE. Error bars are S.D. when n ≥3, and range if n=2. nd = not determined.

		T_{mid} [T_{upper}, estimated] (^{o}C)			
Method Donor/ Fluorophore	Acceptor/ Quencher	Lipid Alone	+TX-100 (150 µM)	+TX-100 (500 µM)	+LW peptide (0.45mol%)
Quenching DPH	TEMPO	46.9 ± 3.4 (6)	41.6 ± 1.4 (3)	43.3 ± 0.5 (6)	46.1 ± 3.7 (2)
Anisotropy DPH		46.3 ± 1.9 (6)	41.0 ± 4.4 (4)	39.0 ± 3.6 (3)	40.9 ± 2.8 (4)
Quenching DPH	10SLPC	47.1 ± 6.4 (4) [~69]	34.4 ± 2.7 (4) [~56]	nd	34.1 ± 2.4 (4) [~62]
FRET NBD-DPPE	rhod-DOPE	9.3 ± 0.3 (4) [~29]	25.7 ± 0.3 (4) [~40]	nd	23.4 ± 0.6 (4) [~37]
FRET DPH	rhod-DOPE	21.4 ± 0.1 (2) [~34]	33.1 ± 0.4 (2) [~52]	nd	30.8 ± 0.2 (2) [~49]
FRET pyrene-DPPE	rhod-DOPE	25.4 ± 0.5 (6) [~36]	35.3 ± 3.5 (4) [~56]	nd	31.4 ± 0.4 (4) [~46]

Table 3.2: Lipid and TX-100 composition of vesicles at different TX-100 concentrations. The total lipid concentration was 500μM of 1:1:1 bSM:POPC:chol prior to solubilization. Error bars are S.D. (Triton X-100 fluorescence intensity was not affected by binding to vesicles (not shown).)

Triton X-100 (μM)	% Triton Fluorescence in Pellet	Triton Bound	% SM in Pellet	% Chol in Pellet	% POPC in Pellet
0	0	0	95.8	92.9	95.2
150	13.7 ± 0.6 (4)	21 μM	96.4	91.9	96.4
300	17.7 ± 0.4 (5)	53 μM	87.6	89.3	77.5
500	11.6 ± 0.5 (5)	58 μM	86.1	91.1	56.2

Table 3.3. Effect of TX-100 on stability of ordered domains in different vesicle types. Melting midpoint temperatures,Tm, in presence and absence of TX-100 is shown. The samples were composed of 500 µM 1:1:1 (mol:mol) bSM:POPC:chol with or without 500µM TX-100. Tm was defined as the point of maximum slope of a sigmoidal fit of F/Fo data (Slidewrite Program, Advanced Graphics Software, Encinitas, CA). Average Tm values and S.D is shown. For this and following tables, error bars are S.D. when n is ≥3, and range if n = 2. Sample number (n) is shown in parenthesis.

Vesicle Type	Tm ^{o}C	
	Without Triton	500µM Triton
SUV	41.2 ± 3.2 (4)	39.3 ± 0.6 (4)
LUV	42.3 ± 0.7 (3)	42.1 ± 0.9 (3)
MLV	46.9 ± 3.4 (6)	43.3 ± 0.5 (6)

Table 3.4 Experimentally calculated values of effective Ro (Å). Samples were composed of ethanol dilution SUV containing100µM POPC. Fo samples contained only FRET donor and F samples contained both FRET donor and acceptor at concentrations shown (1 mol% = 1.4×10^{-4} molecules/Å^2). Effective Förster radii (Ro) were calculated as follows. Ethanol dilution SUV composed of 100µM POPC were prepared containing 0.1mol% NBD-DPPE and 0.33mol% rhod-DOPE, 0.1mol% DPH and 0.5mol% rhod-DOPE or 0.1mol% pyrene-DPPE and 1mol% rhod-DOPE. Donor fluorescence in the absence (117) and presence (F) of acceptor was measured and Ro was calculated using the following equation (113) $F/Fo = \exp(-(1.1Ro)^2 \pi C$ where C is the number of acceptors per 70Å^2. The calculated effective Ro values were 49Å for NBD-DPPE and rhod-DOPE, 36Å for DPH and rhod-DOPE, and 26Å for pyrene-DPPE and rhod-DOPE. These are only effective Ro values because they do not take into account possible orientation factor effects or FRET between donors in one leaflet and acceptors in the opposite leaflet. Average values and range for duplicate samples is shown.

FRET donor	Rhodamine DOPE concentration C (molecules/Å^2)	F/Fo	Ro effective (Å)
Pyrene-DPPE	1.4×10^{-4}	0.482 ± 0.014	26 ± 0.5 (2)
DPH	7×10^{-5}	0.497 ± 0.010	36 ± 0.5 (2)
NBD-DPPE	4.7×10^{-5}	0.423 ± 0.003	49 ± 0.2 (2)

Table 3.5. Effect of acceptor concentration, vesicle type, or presence of 10SLPC upon FRET and omitting 2mol% DOPE in 10SLPC quenching experiments on Tm. nd = not determined

Lipid composition and Detection method	Donor/ Fluorophore	Acceptor/ Quencher	Tm (^{o}C)		
			Lipid	+TX-100 150 µM	+LW peptide 0.45mol%
1:1:1 bSM/POPC/Chol MLV FRET	NBD-DPPE	rhod-DOPE (1mol%)	11.6 ± 0.1 (2)	26.4 ± 0.3 (3)	22.6 ± 0.3 (2)
1:1:1 bSM/POPC/Chol LUV FRET	NBD-DPPE	rhod-DOPE	11.9 ± 0.1 (2)	26.4 ± 0.2 (3)	25.5 ± 0.4 (2)
7:6:1:7 bSM/POPC/10SLPC/Chol MLV FRET	NBD-DPPE	rhod-DOPE	13.8 ± 2.7 (2)	31.6 (1)	nd
7:6:1:7 bSM/POPC/10SLPC/Chol, MLV,(no 2mol%DOPE) Quenching	DPH	10SLPC	47.4 (1)	35.7 (1)	nd

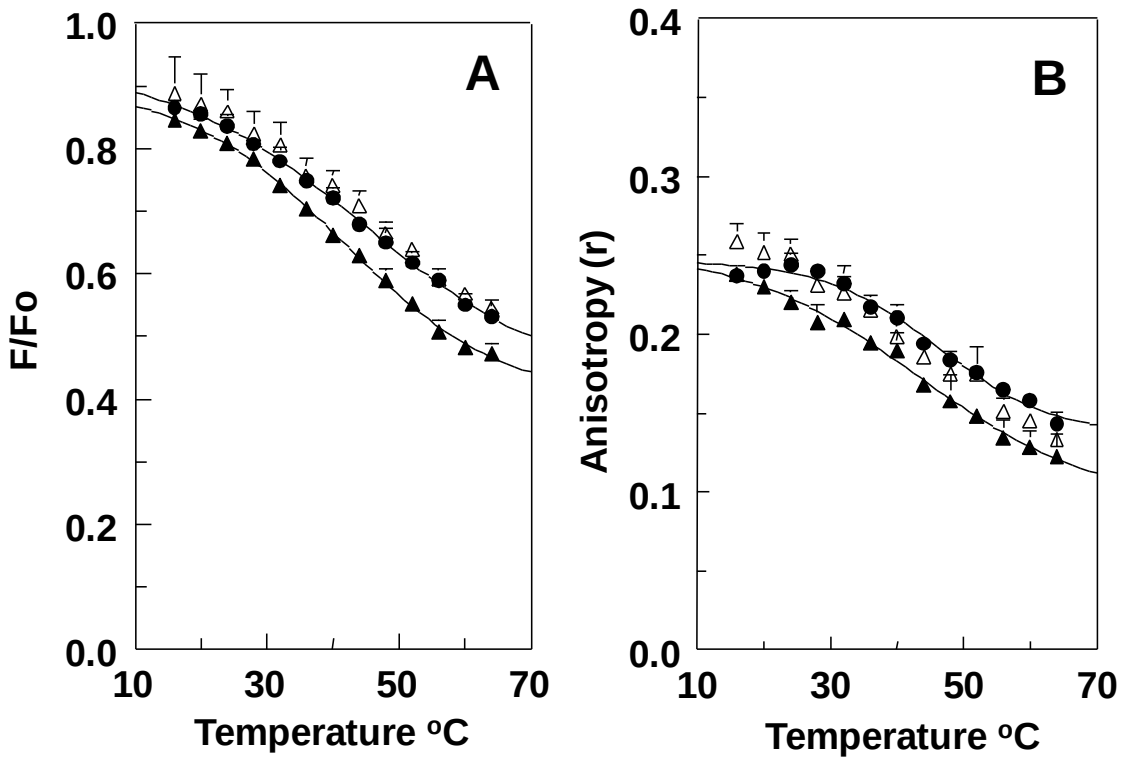

Figure 3.1. Ordered domain thermal stability in lipid vesicles and how it is affected by TX-100 and transmembrane peptide as measured by: A. quenching of DPH fluorescence by TEMPO and B. DPH fluorescence anisotropy. In A. MLV were composed of 0.1mol% DPH and 500µM 1:1:1 (mol:mol) bSM/POPC/chol. Samples contained lipid only (filled circles, average of 6), lipid plus 150µM TX-100 (filled triangles, average of 3), or lipid plus 0.45mol% (2.25µM) LW peptide (open triangles, average of duplicates). In addition, F samples contained 2mM TEMPO. F/Fo is the ratio of fluorescence in the presence of TEMPO to that in the absence of TEMPO. B. MLV were composed of 0.1mol% DPH and 1:1:1 (mol:mol) bSM/POPC/chol. Samples contained: lipid alone (filled circles, average of 6), lipid plus 150µM TX-100 (filled triangles, average of 4), or lipid plus 0.45mol% LW peptide (open triangles, average of 4). The error bars in this and the following figures are standard deviations (S.D.), or if n=2 range. Where error bars are not shown, they were too small to be displayed.

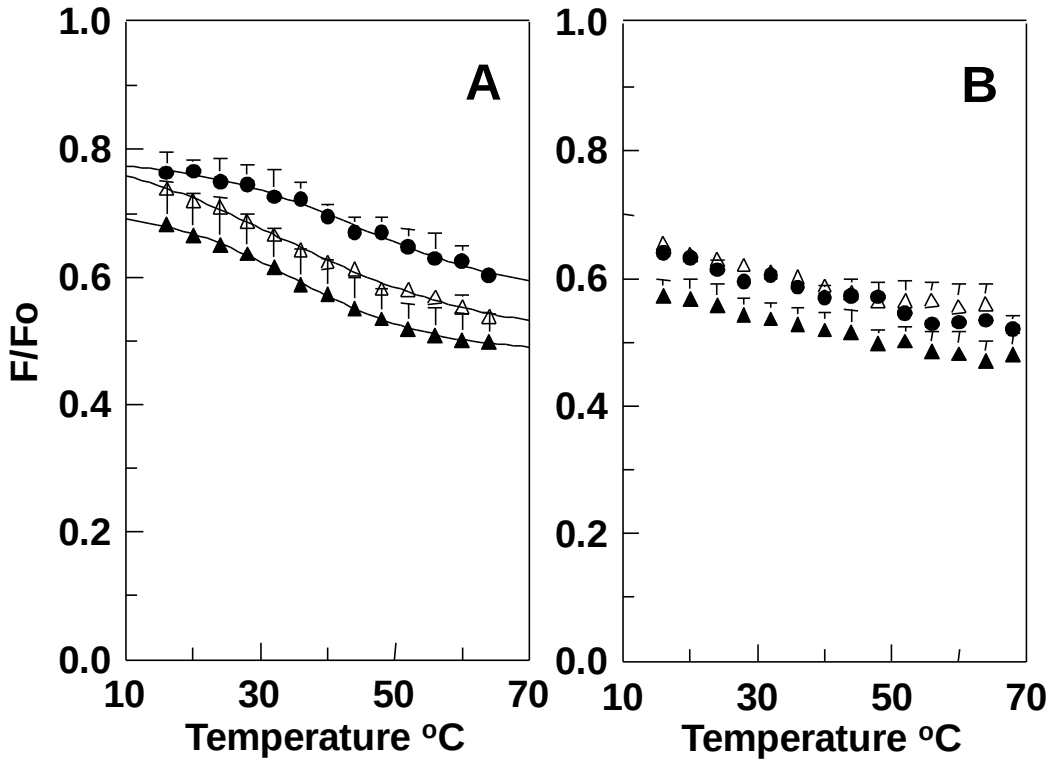

Figure 3.2. Effect of TX-100 and transmembrane peptide on detection of ordered domains assayed by quenching of DPH fluorescence by 10SLPC. Samples were composed of MLV containing 0.1mol% DPH and 500 μM lipid. A. Fo samples contained 1:1:1 bSM/POPC/chol and F samples contained 7:(6:1):7 of bSM/(POPC/10SLPC)/chol (= 4.8mol% 10SLPC). B. Samples lacking SM. Fo samples contained 2:1 POPC/chol and F samples contained (POPC/10SLPC)/chol in the ratio (6:1):3.5 (= 4.8mol% 10SLPC). All samples also contained 2 mol% DOPE. Samples contained: lipid only (circles), lipid plus 150μM TX-100 (filled triangles), or lipid plus 0.45mol% LW peptide (open triangles).

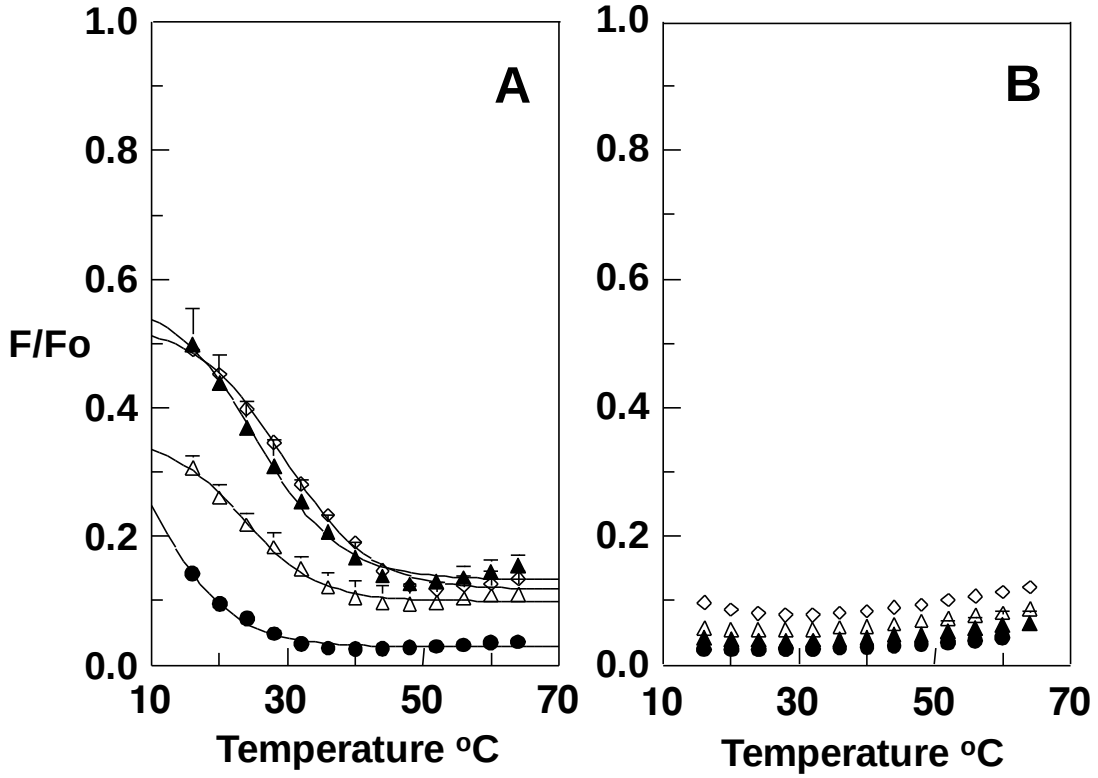

Figure 3.3. Detection of ordered domains by FRET and the effect of TX-100 and transmembrane peptide on domain detection. Samples were composed of MLV containing 500 µM: A. 1:1:1 bSM/POPC/chol, or B. 2:1 POPC/chol. F samples contained also FRET donor (0.1mol% NBD-DPPE) and FRET acceptor (2mol% rhod-DOPE). Fo samples also contained only FRET donor (0.1mol% NBD-DPPE). Samples contained: lipid only (circles, average of 4), lipid plus 150µM TX-100 (filled triangles, average of 4), lipid plus 0.45mol% LW peptide (open triangles, average of 4), or lipid plus both 150µM TX-100 and 0.45mol% LW peptide (diamonds, average of 3). The ratio of donor fluorescence in the presence of acceptor to that in its absence (F/Fo) is graphed.

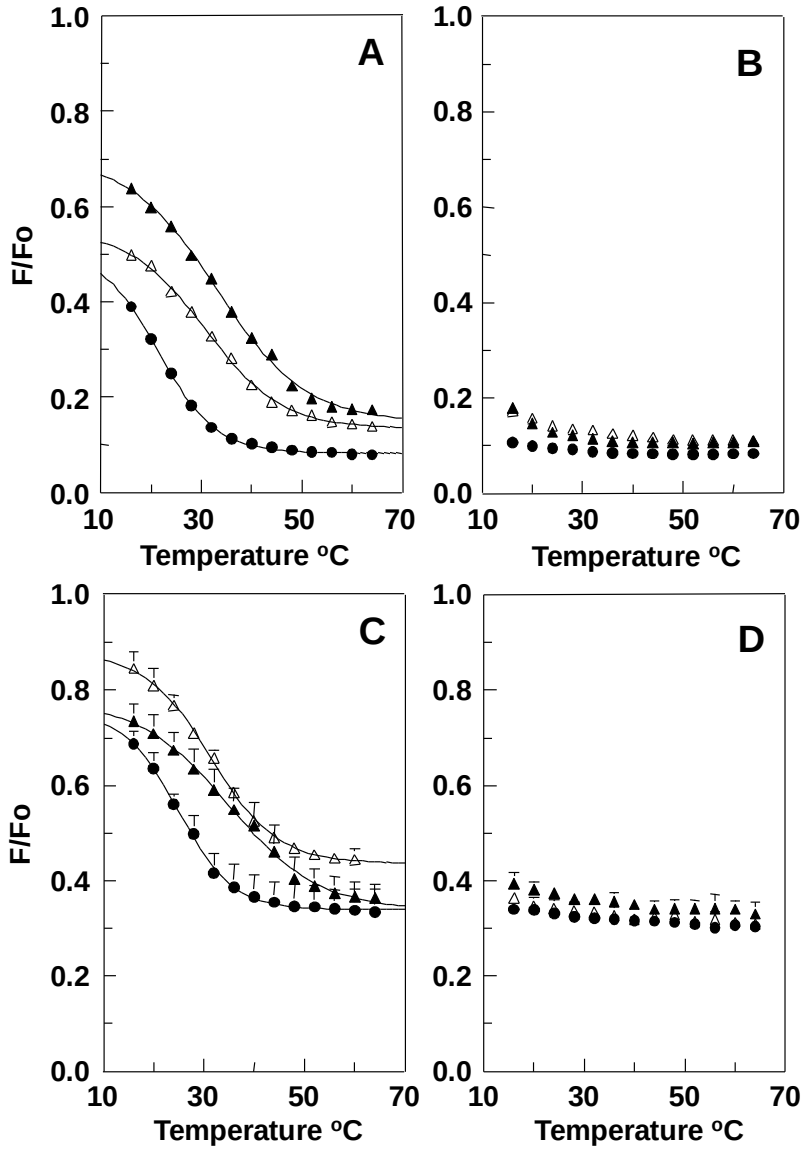

Figure 3.4. Effect of TX-100 and transmembrane peptide on ordered domain detection assayed by FRET pairs with shorter Ro than the NBD-rhodamine pair. Samples were composed of MLV containing 500 μM: (A and C) 1:1:1 bSM/POPC/chol or (B and D) 2:1 POPC/chol. In A. and B. F samples also contained 0.1mol% DPH as the FRET donor and 2mol% rhod-DOPE as FRET acceptor. Fo samples also contained only 0.1mol% DPH. Samples contained: lipid only (circles, average of duplicates), lipid plus 150μM TX-100 (filled triangles, average of duplicates), or lipid plus 0.45mol% LW peptide (open triangles, average of duplicates). In C. and D. F samples contained as the FRET donor 0.05mol% pyrene-DPPE and as the FRET acceptor 2mol% rhod-DOPE. Fo samples contained only 0.05mol% pyrene-DPPE. Samples contained lipid only (circles, average of 6), lipid plus 150 μM TX-100 (filled triangles, average of 4), or lipid plus 0.45 mol% LW peptide (open triangles, average of 4).The ratio of donor fluorescence in the presence of acceptor to that in its absence (F/Fo) is graphed.

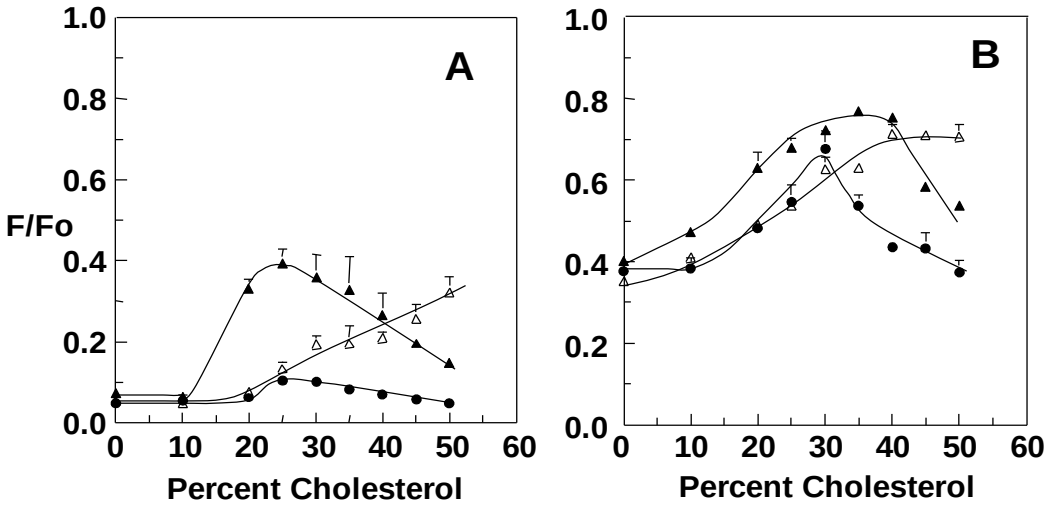

Figure 3.5. Effect of TX-100 and transmembrane peptide on FRET-detection of domain formation as a function of chol concentration at room temperature. In: A. Donor: 0.1mol% NBD-DPPE, acceptor: 2mol% rhod-DOPE. B. Donor: 0.05mol% pyrene-DPPE, acceptor: 2mol% rhod-DOPE. Samples were composed of MLV containing 500µM 1:1:x bSM/POPC/chol. F samples also contained both FRET donor and acceptor. Fo samples also contained only FRET donor. The ratio of donor fluorescence in the presence of acceptor to that in its absence (F/Fo) is plotted *versus* chol concentration. A. Samples contained: lipid (circles), lipid plus 150µM TX-100 (filled triangles, average of 3), or lipid plus 0.45mol% LW peptide (open triangles, average of 4). B. Samples contained lipid (circles, average of duplicates), lipid plus 150µM TX-100 (filled triangles, average of duplicates), or lipid plus 0.45mol% LW peptide (open triangles, average of duplicates).

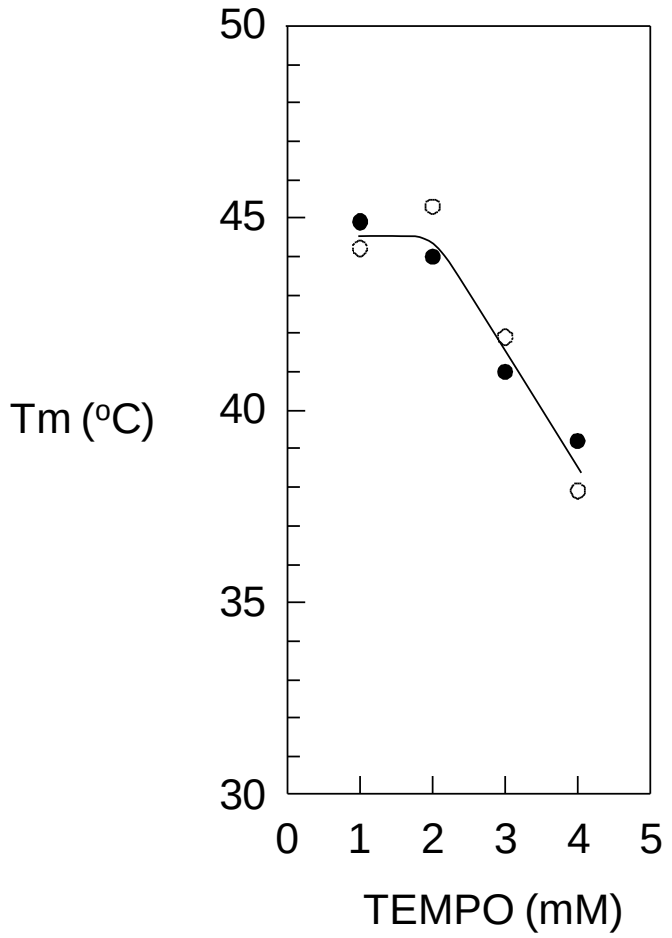

Figure 3.6. Effect of TEMPO concentration upon Tm. MLV samples contained 0.1mol% DPH and 500μM of 1:1:1 (mol:mol) bSM/POPC/chol. F samples also contained various concentrations of TEMPO. Average of duplicate samples is shown for 1, 3 and 4mM TEMPO concentrations and average of six samples is shown for 2mM TEMPO.

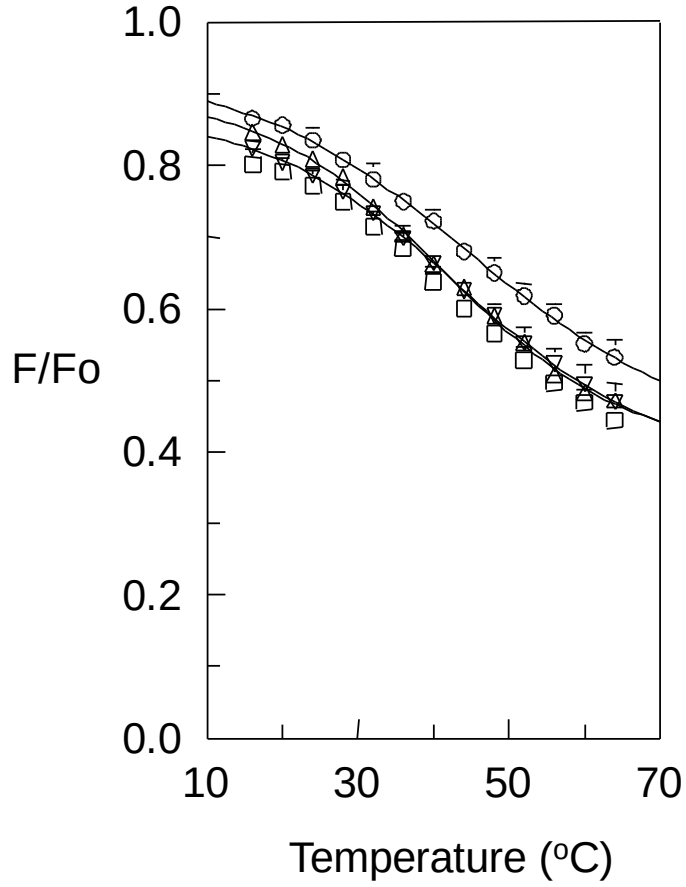

Figure 3.7. Effect of TX-100 concentration on Tm detected by quenching of DPH fluorescence by TEMPO. Vesicles were composed of 0.1mol% DPH and 500 µM 1:1:1 (mol:mol) bSM/POPC/chol and contained various amounts of TX-100: 0µM (circles, average of 6), 150µM (triangles, average of 3), 500µM (inverted triangles [=vertex down], average of 6) and 750µM (squares, average of duplicates). Data is summarized in Table 1. The error bars in this and the following figures are standard deviations or, if n=2, range. In the cases in which error bars are not shown, they were too small to be displayed relative to the symbols.

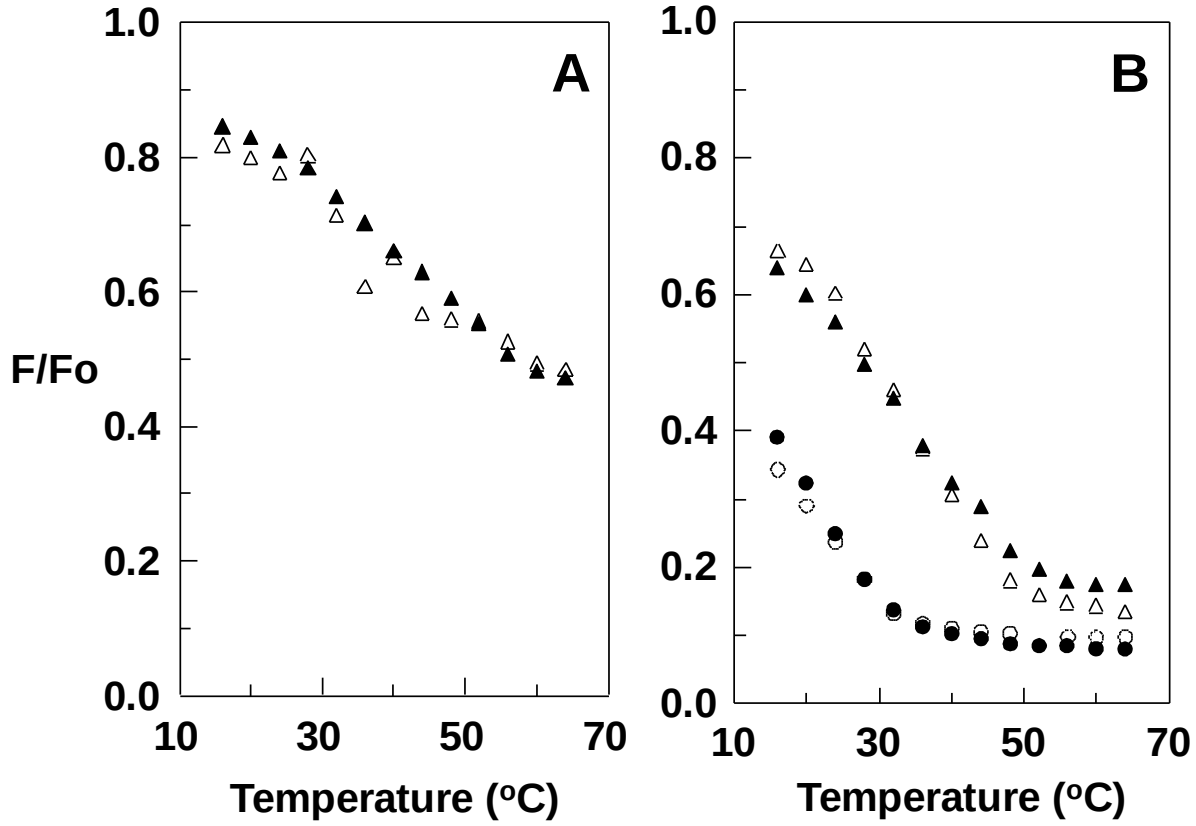

Figure 3.8. Thermal reversibility of changes in fluorescence. A. TEMPO-induced quenching of DPH fluorescence. B. FRET between DPH and rhod-DOPE. MLV samples contained 0.1mol% DPH and 500µM of 1:1:1 (mol:mol) bSM/POPC/chol, and where indicated contained 150µM TX-100. F samples also contained: A. 2mM TEMPO or B. 2mol% rhod-DOPE. Samples were slowly heated from 16 to 64°C or slowly cooled from 64 to 16°C and the ratio of DPH fluorescence in the presence and absence of quencher or acceptor (F/Fo) was measured. In A. symbols denote lipid plus TX-100 heating cycle (filled triangles) or lipid plus TX-100 cooling cycle (open triangles). In B symbols denote lipid only heating cycle (filled circles), lipid only cooling cycle (open circles), lipid plus TX-100 heating cycle (filled triangles), lipid plus TX-100 cooling cycle (open triangles). In A. single samples were used, B. shows average of duplicates.

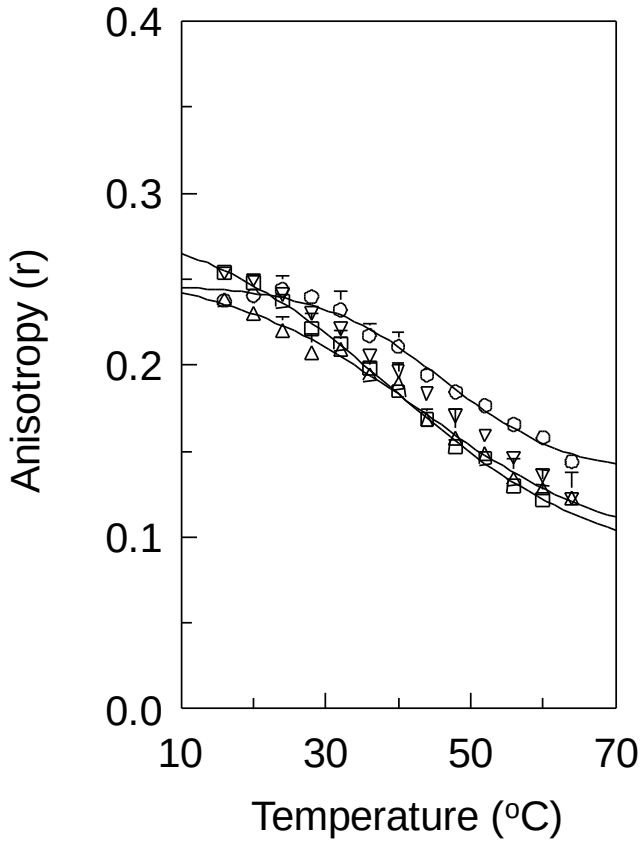

Figure 3.9 Effect of TX-100 concentration on domain thermal stability measured by DPH anisotropy. Samples were composed of MLV containing 0.1mol% DPH and 1:1:1 (mol:mol) bSM/POPC/chol plus various amounts of TX-100: 0μM (circles, average of 6), 150μM (triangles, average of 4), 500μM (inverted triangles, average of 3) or 750μM (squares, average of 3). Data is summarized in Table 1.

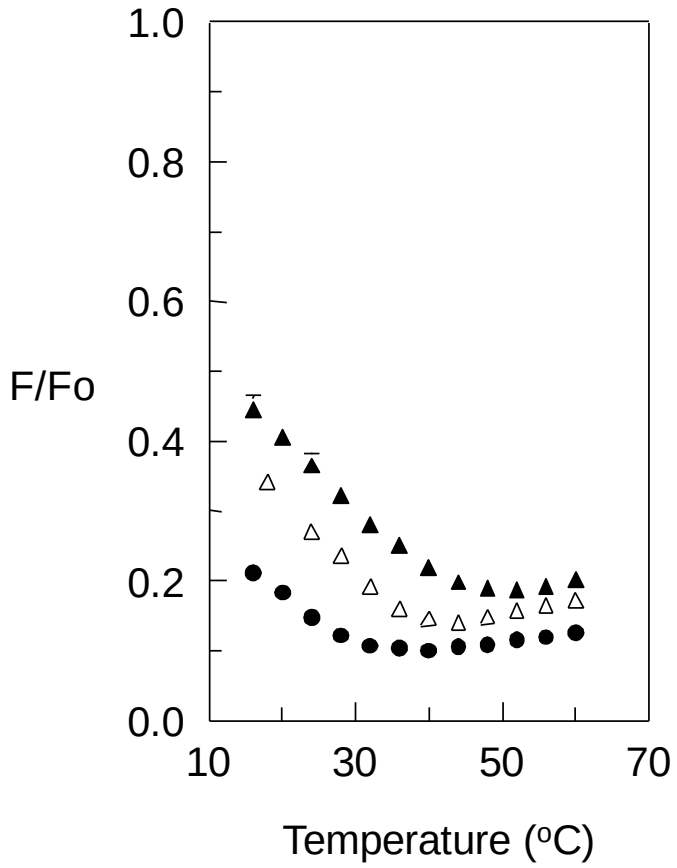

Figure 3.10. Detection of ordered domains by NBD-DPPE to rhod-DOPE FRET in LUV. Samples were composed of LUV containing 500µM 1:1:1 bSM/POPC/chol. F samples also contained FRET donor (0.1mol% NBD-DPPE) and FRET acceptor (2mol% rhod-DOPE). Fo samples also contained only FRET donor (0.1mol% NBD-DPPE). Samples contained lipid only, (circles, average of duplicates), lipid plus 150µM TX-100 (filled triangles, average of 3), or lipid plus 0.45 mol% LW peptide (open triangles, average of duplicates). The ratio of donor fluorescence in the presence of acceptor to that in its absence (F/Fo) is plotted *versus* temperature.

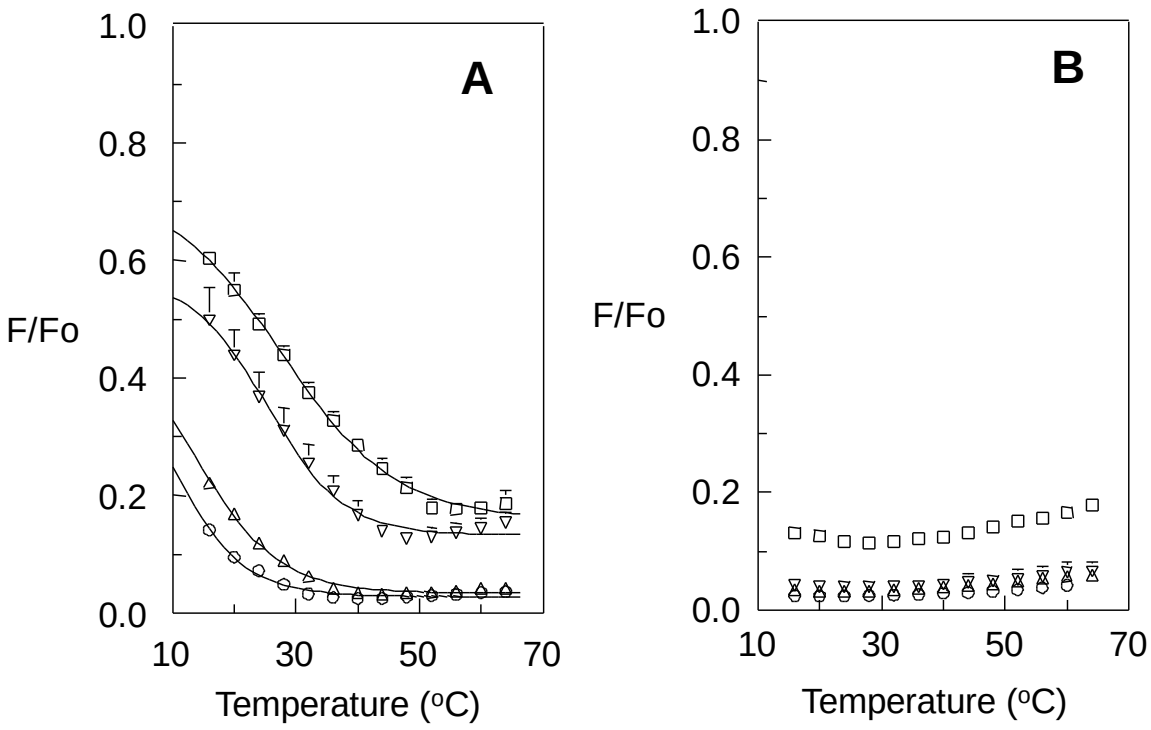

Figure 3.11. Effect of TX-100 concentration on ordered domain formation assayed by FRET. MLV samples contained 500µM lipid composed of: A. 1:1:1 (mol:mol) bSM/POPC/chol or B. 2:1 (mol:mol) POPC/chol. Samples contained various amounts of TX-100: 0µM (circles, average of 4), 75µM (triangles, average of 3), 150µM (inverted triangles, average of 4) and 300µM (squares, average of duplicates). F samples also contained FRET donor (0.1mol% NBD-DPPE) and FRET acceptor (2mol% rhod-DOPE). Fo samples also contained only FRET donor (0.1mol% NBD-DPPE). The ratio of donor fluorescence in the presence of acceptor to that in its absence (F/Fo) is plotted *versus* temperature.

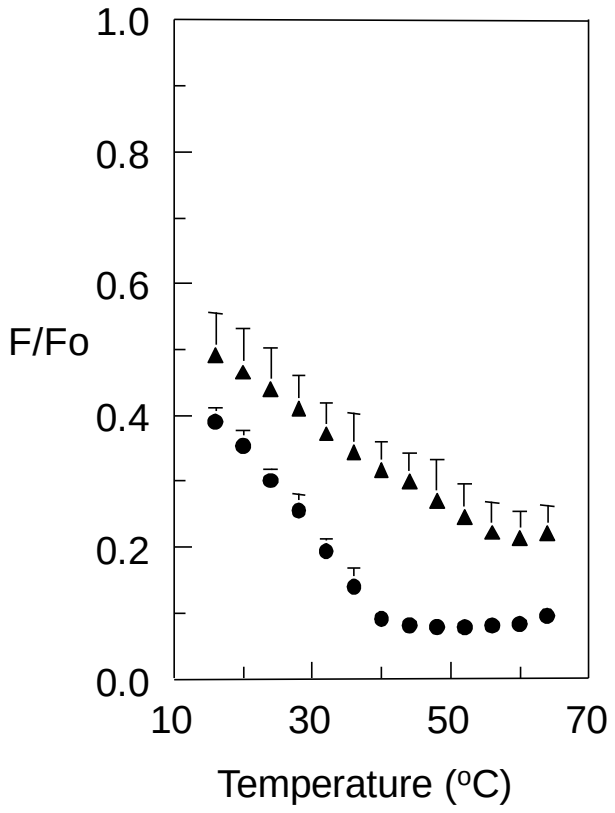

Figure 3.12. Thermal stability of ordered domains containing egg SM in the presence and absence of TX-100 measured by NBD-DPPE to rhod-DOPE FRET. Samples were composed of MLV containing 500μM 1:1:1 (mol:mol) egg SM/POPC/chol. F samples also contained FRET donor (0.1mol% NBD-DPPE) and FRET acceptor (2 mol% rhod-DOPE). Fo samples also contained only FRET donor (0.1mol% NBD-DPPE). Lipid only (circles), lipid plus 150μM TX-100 (filled triangles). The ratio of donor fluorescence in the presence of acceptor to that in its absence (F/Fo) is plotted *versus* temperature. Average of triplicates is shown.

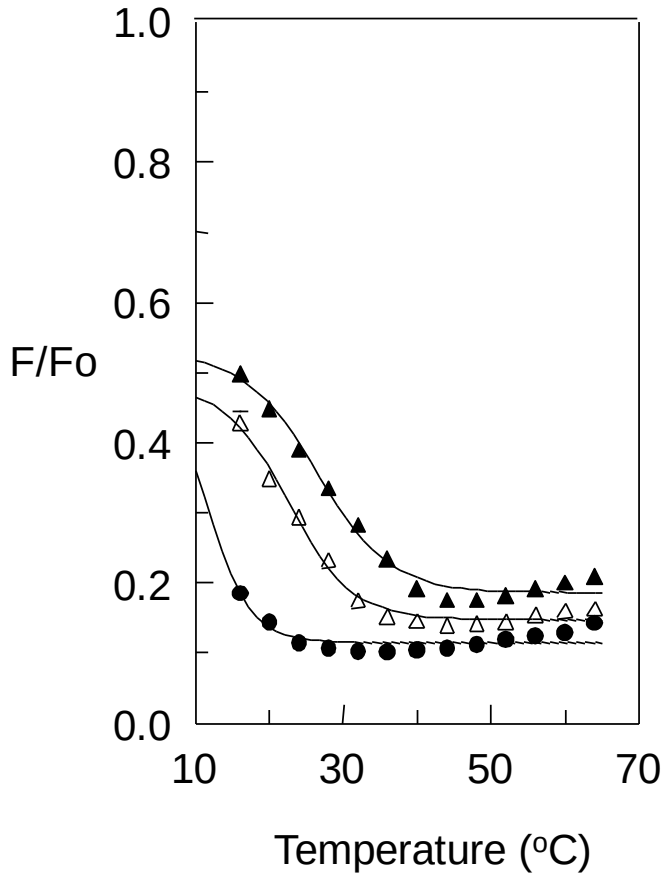

Figure 3.13. Effect of using 1mol% rhod-DOPE on FRET detection of ordered domains. Samples were composed of MLV containing 500µM 1:1:1 bSM/POPC/chol. F samples also contained FRET donor (0.1mol% NBD-DPPE) and FRET acceptor (1mol% rhod-DOPE). Fo samples also contained only FRET donor (0.1mol% NBD-DPPE). Samples contained lipid only (circles), lipid plus 150µM TX-100 (filled triangles), or lipid plus 0.45mol% LW peptide (open triangles). The ratio of donor fluorescence in the presence of acceptor to that in its absence (F/Fo) is plotted *versus* temperature. Average of duplicates is shown.

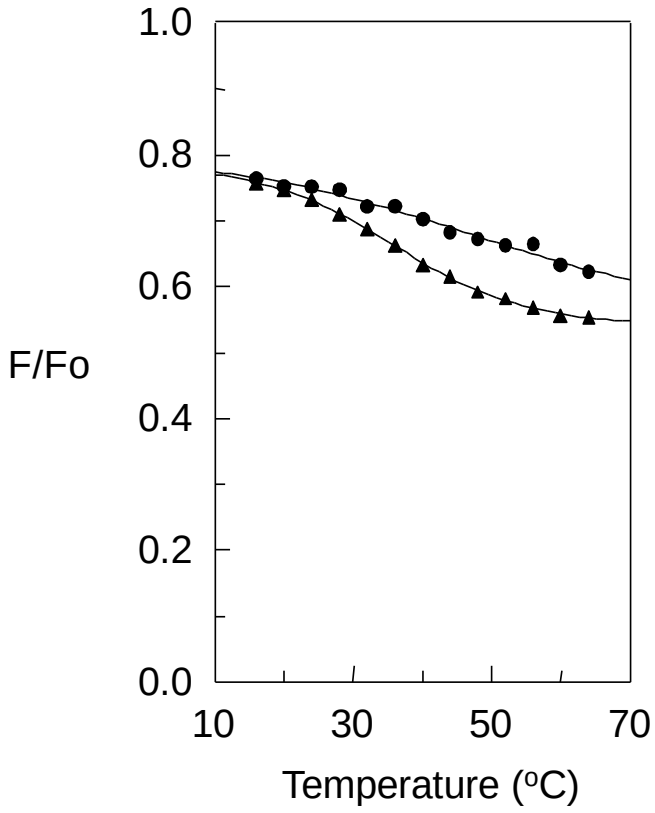

Figure 3.14. Quenching of DPH by 10SLPC in the absence of DOPE. Vesicles were composed of MLV containing 0.1mol% DPH and 500 μM lipid. Fo samples contained 1:1:1 bSM/POPC/chol and F samples contained 7:(6:1):7 of bSM/(POPC/10SLPC)/chol (= 4.8mol% 10SLPC). Lipid only (filled circles), lipid plus 150μM TX-100 (filled triangles). The ratio of DPH fluorescence in the presence of 10SLPC to that in its absence (F/Fo) for single samples is plotted *versus* temperature.

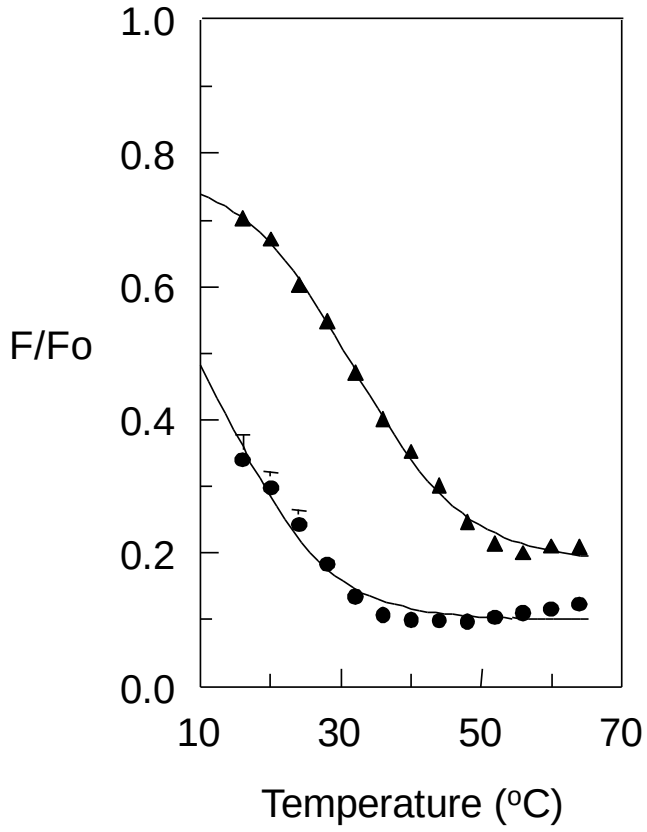

Figure 3.15. Detection of ordered domains by NBD-DPPE to rhod-DOPE FRET in the presence of 10SLPC. MLV samples contained 500 μM lipid composed of: 7:(6:1):7 bSM/(POPC/10SLPC)/chol (= 4.8mol% 10SLPC). F samples also contained FRET donor (0.1mol% NBD-DPPE) and FRET acceptor (2 mol% rhod-DOPE). Fo samples also contained only FRET donor: (0.1mol% NBD-DPPE). Samples contained lipid only (circles, average of duplicates), or lipid plus 150μM TX-100 (filled triangles). The ratio of donor fluorescence in the presence of acceptor to that in its absence (F/Fo) is plotted *versus* temperature.

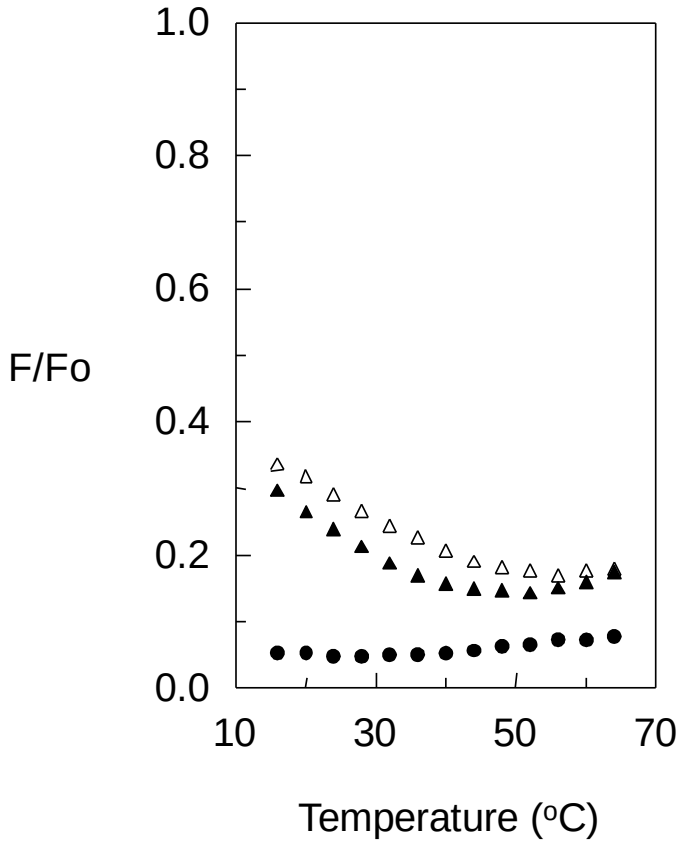

Figure 3.16. FRET detection of ordered domains at 45mol% chol vs. temperature in the presence and absence of TX-100 or LW peptide. Samples were composed of MLV containing 500µM 1:1:1.64 bSM/POPC/chol. F samples also contained FRET donor (0.1mol% NBD-DPPE) and FRET acceptor (2mol% rhod-DOPE). Fo samples also contained only FRET donor (0.1 mol% NBD-DPPE). Samples contained lipid only (filled circles), lipid plus 150µM TX-100 (filled triangles), or lipid plus 0.45 mol% LW peptide (open triangles). The ratio of donor fluorescence in the presence of acceptor to that in its absence (F/Fo) is plotted *versus* temperature. Results shown are from single samples (except the average of duplicates in the presence of LW peptide).

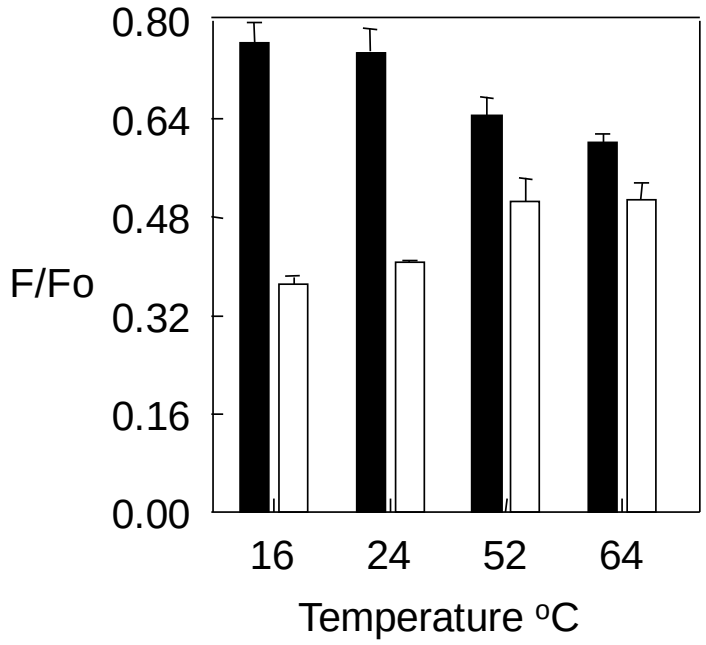

Figure 3.17: Comparison of 10SLPC quenching for fluorophores having different affinities for ordered domains. Samples were composed of MLV containing 500μM lipid. Fo samples contained 1:1:1 bSM/POPC/chol and F samples contained 7:(6:1):7 of bSM/(POPC/10SLPC)/chol. Shaded bars represent quenching of (0.1mol%) DPH and unshaded bars represent quenching of (0.1mol%) oleoyl tryptophan (Sigma-Aldrich) by 10SLPC. Fraction of unquenched fluorescence is plotted at various temperatures. DPH has a significant affinity for ordered domains while oleoyl tryptophan strongly prefers to locate in Ld domains. Notice the opposite direction of the temperature dependence of quenching for DPH and oleoyl tryptophan, which confirms that the temperature dependence of quenching reflects either low temperature segregation (in the case of DPH) or co-segregation (in the case of oleoyl tryptophan) of fluorophore and quencher.

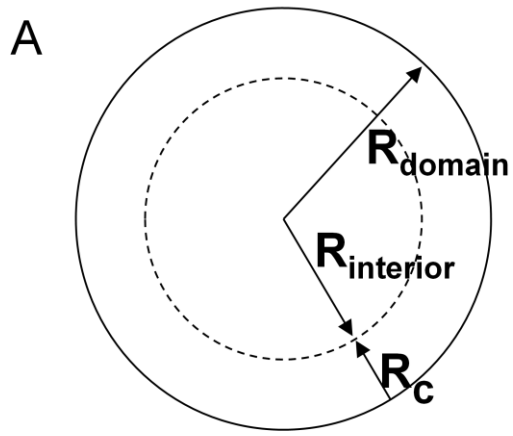

Figure 3.18. Schematic figure showing how FRET and quenching are affected by domain size.

Figure 3.18A. Illustration of interior zone in a circular domain. Rc, is the critical interaction distance (~Ro). R interior is the radius of the region in the domain largely protected from interaction with acceptors outside the domain.

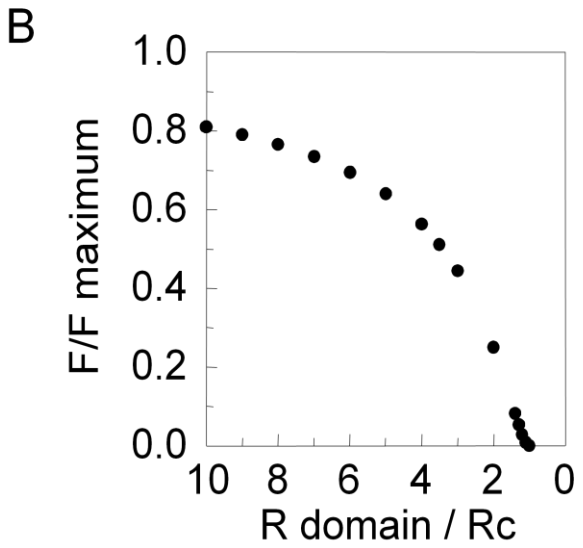

Figure 3.18B. The dependence of protection of a fluorescent group from quenchers outside of a domain upon domain radius. Protection is calculated for high enough quencher concentration to quench all fluorescence outside of domains and within Rc of the domain boundary. [(F/Fo)/(F maximum/ Fo)] = F/ F maximum = interior area of domains/ total area = ratio of fluorescence arising within domains to that in domains approaching "infinite" size, at a constant fraction of membrane area within domains, i.e. when individual domain area decreases, domain number increases such that the fraction of bilayer area within domains is constant. The change of F/F maximum vs. R domain/Rc would be more gradual than shown for a quenching with a gradual distance dependence.

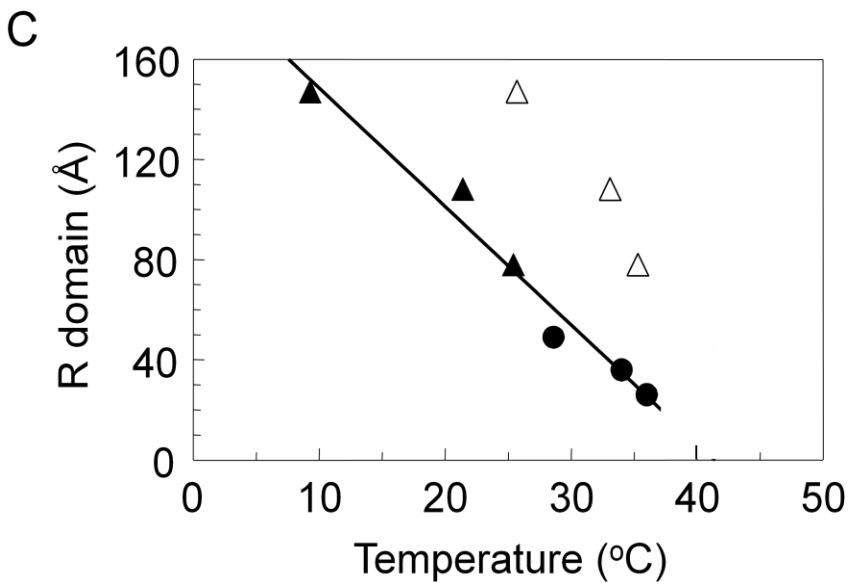

Figure 3.18C. Lo domain size (Å) estimated using T_{mid} and T_{upper} values for different FRET pairs. Filled symbols, lipids alone, open symbols, lipids plus 150 μM TX-100. Triangles and circles show estimated radii of Lo domains at T_{mid} and T_{upper}, respectively. T_{upper} values ≥40°C were not included because above 35°C, FRET changes will reflect domain melting to a greater degree than changes in domain size. The linear fit shown is only to guide the eye.

Chapter 4:

Detection of Ordered Domains in Living Borrelia burgdorferi Cells:

Important Note: This dissertation only includes the data from experiments performed by Pathak P. It does not include data from experiments performed by other authors. Therefore, Chapter 4 may seem incomplete to the readers. Readers are kindly referred to the above publications for a complete manuscript

Introduction

The spirochete *Borrelia burgdorferi* is the causative agent of Lyme disease (97,118), a tick-borne illness that can have manifestations in the skin, heart, joints, and nervous system of mammals (98). *B. burgdorferi* has outer and inner membranes, and the periplasmic space between these membranes contains the flagellar bundles. The periplasmic flagella contribute to the spiral morphology of *B. burgdorferi* cells (119), and are not exposed to the extracellular environment unless the outer membrane has been damaged (98,120).

The membranes of *B. burgdorferi* contain phosphatidylcholine and phosphatidylglycerol and lipoproteins (121-123). They also contain free cholesterol, two cholesterol glycolipids (acylated cholesteryl galactoside (ACGal) and cholesteryl galactoside (CGal)), and the glycolipid, monogalactosyl diacylglycerol (MGalD) (99,124,125)**.** Cholesterol is not a common constituent of prokaryotic cells, with only a few bacteria known to incorporate it into their membranes (93-96,126).

In eukaryotic cells, sterols (together with sphingolipids having saturated acyl chains) are believed to participate in the formation of ordered membrane domains called rafts, which co-exist with disordered membrane domains, and to play an important role in many membrane functions (1,2,5,9,14,127).

In model membranes, ordered sterol-rich domains are readily detected (4). However, it has been difficult to characterize rafts in eukaryotic cells due to their small size and dynamic properties, and their formation and properties remain controversial, although important advances have been made, especially in immune cells (73,128-130).

We previously presented evidence that lipid microdomains containing cholesterol glycolipids exist in *B. burgdorferi* membranes (100). In this study we demonstrate that these domains are ordered lipid domains with the properties that define lipid rafts, and that the domains are present in living *B. burgdorferi* cells. We investigated whether ordered and disordered lipid domains co-exist in living *B. burgdorferi* cells using a novel FRET approach. Next, a sterol substitution strategy was developed using sterols with varying abilities to form or

disrupt ordered lipid domains (87-89,131) to determine if sterols with raft-forming properties are necessary and sufficient for the formation of *B. burgdorferi* membrane domains. From the results, we conclude that lipid rafts form in the membranes of live *B. burgdorferi cells*. These studies may lead to approaches to identify rafts in other types of cells.

Results

Sterols with the ability to form ordered membrane domains are necessary and sufficient to form membrane domains detected by FRET in live B. burgdorferi

The hypothesis that *B. burgdorferi* domains are lipid rafts predicts that their formation should require lipids having the ability to form tightly packed domains. In previous studies we demonstrated that different sterols have a structure-dependent range of abilities to support formation of ordered raft lipid domains in model membrane vesicles (87-89,131). Therefore, sterol substitution experiments were carried out in *B. burgdorferi* using sterols (Table 1.1) ranging from those that are strongly ordered domain forming to those that are ordered domain inhibiting (87-89)**.**

Free cholesterol and cholesterol glycolipids from *B. burgdorferi* can be substantially removed from cells with methyl-β-cyclodextrin (MβCD) while phospholipids and MGalD are unaffected (100). When depletion is followed by incubation of the spirochetes with a diverse set of sterols, sterol substitution was confirmed by a strong correlation between the ability of a sterol to support ordered domain formation in model membranes (87-89) and membrane order in *B. burgdorferi* membranes (in intact cells), as measured by the anisotropy of trimethylaminodiphenylhexatriene (TMADPH) fluorescence subsequent to sterol substitution (Table 4.1 and Fig.4.6).

A fluorescence resonance energy transfer, FRET method was developed to detect domains in living cells. In this method, weak FRET is observed when co-existing ordered and disordered lipid domains are present because the donor used, trimethylaminodiphenylhexatriene (TMADPH) partitions moderately into ordered domains and so partially segregates from the acceptor, octadecylrhodamine B (ODRB) which partitions preferentially into disordered lipid domains (132,133). The FRET method was calibrated in model membranes (Fig. 4.4A). At low temperatures, there was higher TMADPH fluorescence (higher F/Fo = weaker FRET) in vesicles having a composition (dipalmitoylphosphatidylcholine (DPPC)/ dioleoylphosphatidylcholine (DOPC)/cholesterol) in which segregation into DPPC-rich ordered and DOPC-rich disordered domains occurs (134) than in vesicles (DOPC/cholesterol or palmitoyloleoylphosphatidylcholine (POPC)/cholesterol) forming a homogeneous bilayer. At higher temperatures, in

DPPC/DOPC/cholesterol samples lipid segregation is lost due to melting of the ordered domains, and FRET levels come close to that in homogeneous vesicles, which exhibit temperature-independent FRET.

When TMADPH and ODRB were added to living *B. burgdorferi* cells, weak FRET which increases at higher temperatures is observed (Fig. 4.4B and Fig. 4.5). This indicates that there is formation of co-existing ordered and disordered domains (at least up to ~35-40^{o}C). The FRET experiments were repeated after sterol substitutions (Fig 4.4B). Weak FRET which increased at higher temperatures was observed with sterols that strongly or moderately support ordered domain formation. In contrast, strong, temperature-independent FRET was observed after androstenol and coprostanol substitutions, sterols that do not support ordered domain formation. Similar dependence was obtained by TEM (data from Benach lab not shown). Partial depletion of cholesterol lipids with MβCD without subsequent sterol substitution did not totally abolish domain formation at lower temperatures, but did decrease their thermal stability, as shown by the transition from weak to strong FRET occurring at a lower temperature (Fig. 4.4B). This indicates that there are residual cholesterol lipids remaining after extraction that are sufficient to form ordered microdomains.

Discussion:

B. burgdorferi membrane domains are true lipid rafts

The studies in this report show that the domains present in *B. burgdorferi* are true lipid rafts using several independent approaches. Having raft-forming properties was both *necessary* and *sufficient* for sterols to support the formation of *B. burgdorferi* membrane domains as judged by FRET. Furthermore, sterols with intermediate raft-forming abilities tended to show intermediate domain forming behavior. The observation of ordered domain formation by FRET is especially important as it indicated that domains formed in live *B. burgdorferi*. Thus, the domains of *B. burgdorferi* membranes have the key properties of true lipid rafts. We believe that the combination of internally consistent experiments provides the most convincing evidence for the existence of lipid rafts in living cells to date. The use of complementary domain detection techniques involving different principles and conditions greatly reduces the possibility that experimental artifacts can explain these results. These studies do not resolve the controversy concerning the formation of lipid rafts in eukaryotic cells. However, the methods used here should be adaptable to eukaryotic cells, and so may point the way to further progress in the characterization of eukaryotic lipid rafts.

Physical origin of B. burgdorferi raft formation

The correlation between ordered domain properties previously characterized in sphingolipid and sterol containing model membranes and those of *B. burgdorferi* domains is very close. Yet *B. burgdorferi* has no sphingolipids. ACGal, which has been identified as being enriched in both DRM from *B. burgdorferi* and DRM from plant cells (135), is likely to play a role that combines that of sphingolipids and sterols in eukaryotes. However, we cannot rule out some role for proteins in *B. burgdorferi* raft formation. It is also uncertain whether the sterol-glycolipids that appear after sterol substitution incorporate the new sterols added, or instead reflect incorporation into glycolipids of residual cholesterol remaining after partial MβCD extraction.

Using FRET to detect ordered domains in B. burgdorferi.

The FRET approach used for detecting lipid domain segregation in this study may be useful in other systems. TMADPH and ODRB are charged hydrophobic probes that can readily be added externally to cells. In this assay, decreased FRET (increased F/Fo) is indicative of segregation into co-existing ordered and disordered domains. Domains larger than Ro (~23 Å) for the TMADPH/ODRB pair when calculated as described previously, and assuming all ODRB is membrane bound (136) (data not shown) can be detected by this approach (136). It is very unlikely that the fluorescent probes used altered domain formation to a significant degree. In addition to the consistency of FRET results with those obtained with other methods, FRET results in untreated cells after halving ODRB concentration showed a temperature dependence of FRET similar to that observed at higher ODRB concentrations. Other controls showed that the fluorescent probes used did not alter domain formation detected by TEM, cell morphology, or cell viability as judged by cell growth (not shown).

That domain-forming sterols, and thus lipid rafts, are necessary to maintain membrane integrity and viability of *B. burgdorferi* is not surprising from an evolutionary standpoint. The life cycle of *Borrelia* involves infection of a tick vector or mammalian host, they are never free-living (98)**.** The cells of mammals and many species of ticks contain cholesterol (137) so it is logical to assume that *B. burgdorferi* has evolved a preference for domain-forming sterols, like cholesterol, as these would be the main sterols available during the spirochete life cycle.

Table 4.1. Sterols used for sterol-substitution experiments in *B. burgdorferi* and their ability to form lipid raft domains in model membranes are shown.

Sterol	Ability to support ordered domain formation in model membranes
Ergosterol	Strong
Cholesterol	Strong
Dihydrocholesterol	Strong
Lanosterol	Moderate
Zymosterol	Moderate
Androsterol	Inhibits ordered domain formation
Coprostanol	Inhibits ordered domain formation

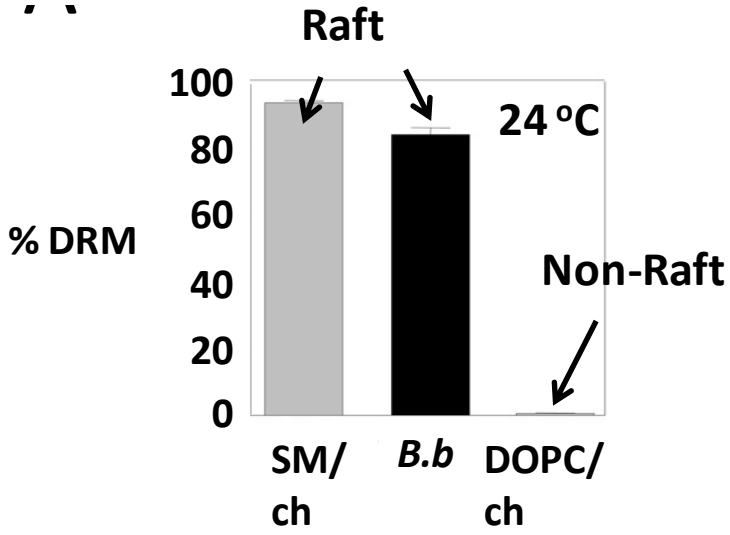

Figure 4.1. *B.burgdoreri* lipids form detergent resistant membranes. MLV made up of total extract of *B.burgdorferi* lipids display resistance to solubilization by TX-100. 2:1 mol:mol SM/cholesterol forms bilayers in the Lo phase and 2:1 mol:mol DOPC/cholesterol forms bilayers in the Ld phase. ch=cholesterol

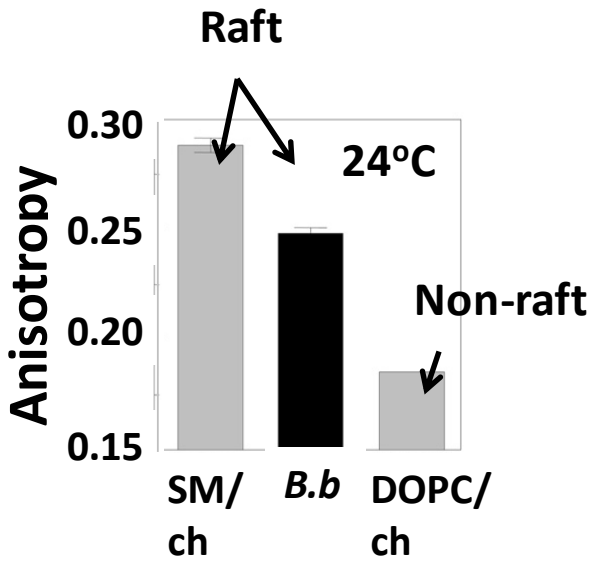

Figure 4.2. *B.burgdorferi* lipids display high anisotropy in model membranes Fluorescence anisotropy of DPH demonstrates a high degree of order among lipids in *B.burgdorferi* MLVs. 2:1 mol:mol SM/cholesterol forms bilayers in the Lo phase and 2:1 mol:mol DOPC/cholesterol forms bilayers in the Ld phase.

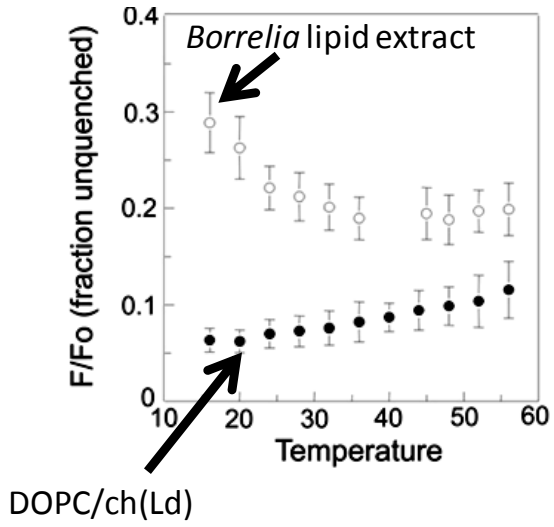

Figure 4.3: *B.burgdorferi* lipids display segregation detected domain formation in model membranes. FRET as a function of temperature for Borrelia lipids in model membranes demonstrates the coexistence of Lo (raft) and Ld domains (high F/Fo values). MLVs contained Borrelia lipid extract (open circles) or DOPC/cholesterol 2:1 (filled circles). F/Fo is the ratio of fluorescence in samples containing donor (NBD-DPPE) and acceptor (rhodamine-DOPE) to that in samples containing donor. Average of triplicate experiments.

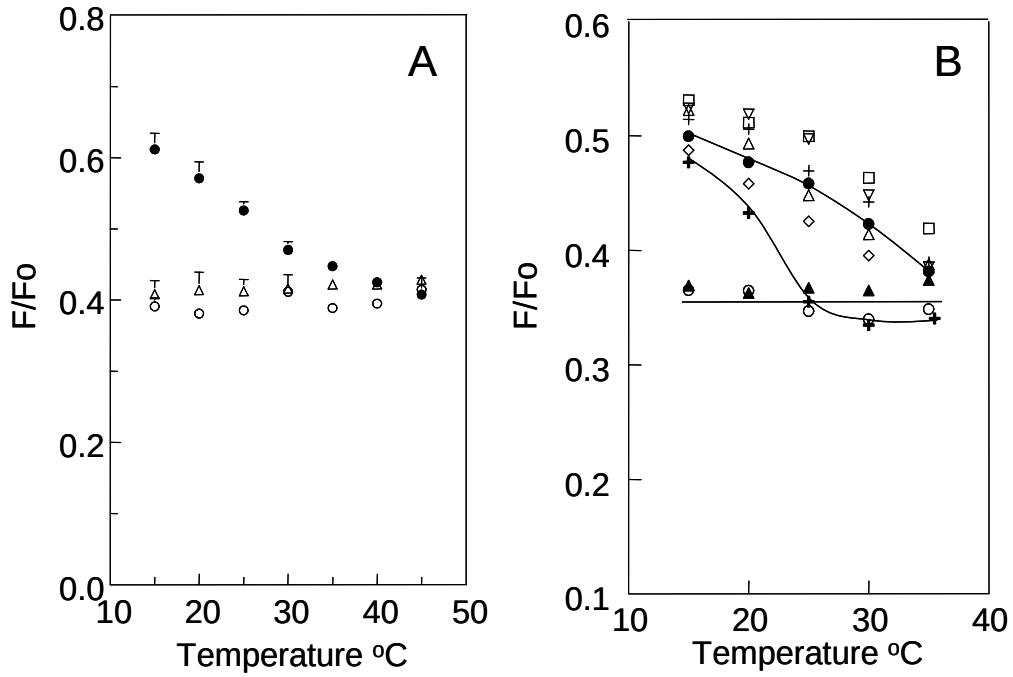

Figure 4.4. FRET detection of ordered domain formation as a function of temperature in *B. burgdorferi*. A. Demonstration of FRET assay performance in model membranes. Samples of small unilamellar vesicles containing 100 µM lipid and (in Fo samples) TMADPH or (in F samples) both TMADPH and ODRB. Vesicles were composed of 2:1 (mol:mol) POPC/chol (open circles), 2:1 DOPC/chol (open triangles), or 1:1:1 DPPC/DOPC/chol (filled circles). F/Fo is the fraction of donor fluorescence unquenched by FRET. Average of duplicates and range are shown. B. Detection of ordered domain formation in *B.burgdorferi* by FRET. F and Fo samples contained *B.burgdorferi* (4 x10^8 cells/ml) with TMADPH (Fo samples) or both TMADPH and ODRB (F samples). Symbols: untreated cells , cholesterol depleted cells (bold plus sign), or cells substituted with cholesterol (filled circles), dihydrocholesterol (open triangles), ergosterol (inverted triangles), lanosterol (plus sign), zymosterol (squares), coprostanol (filled triangles) or androstenol (open circles). Mean F/Fo values from four samples, or two in the case of untreated cells and lanosterol, are shown. For clarity, error bars are omitted in B. (Summary FRET data with error bars is shown in Figure 4.6.) chol=cholesterol

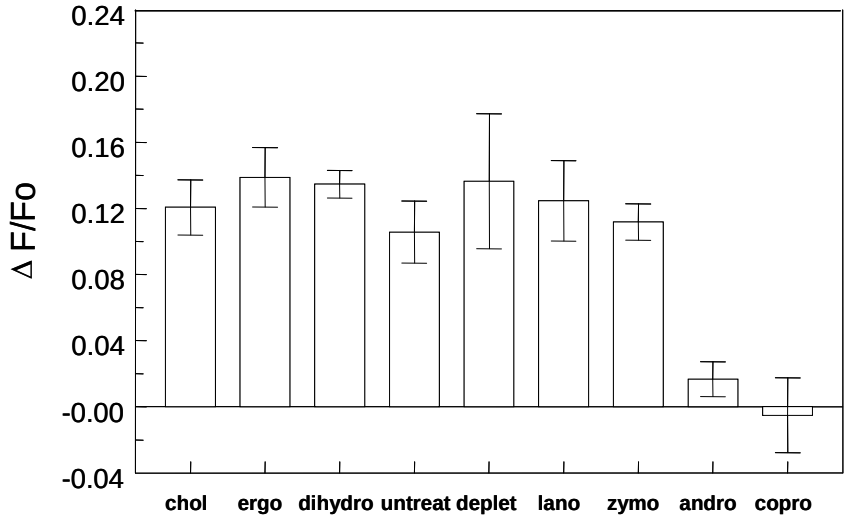

Figure 4.5. Dependence of FRET-detected domain formation in *B. burgdorferi* upon sterol composition. Samples are those from Figure 2. F/Fo is the ratio of TMADPH fluorescence in the presence of ODRB to that in its absence. ΔF/Fo is the difference between F/Fo at 35^{o}C and that at 15^{o}C. Temperature dependent domain formation is detected by a positive Δ F/Fo value. The experimental conditions are: chol = cholesterol substituted cells, ergo = ergosterol substituted cells, dihydro = dihydrocholesterol substituted cells, untreat = untreated cells, deplet = cholesterol lipid depleted cells, lano = lanosterol substituted cells, zymo = zymosterol substituted cells, andro = androstenol substituted cells, copro = coprostanol substituted cells. Mean and standard deviation from four samples is shown, except for the untreated and lanosterol samples for which the average and range of duplicates is shown.

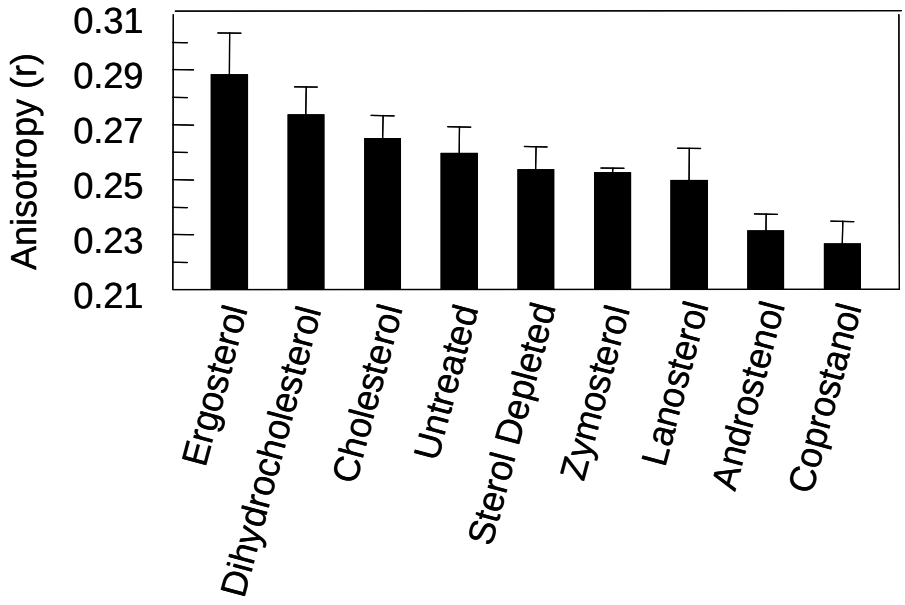

Figure 4.6. Dependence of anisotropy detected membrane order in *B. burgdorferi* upon sterol composition. DPH fluorescence anisotropy was used to measure membrane order at 24^{o}C. The mean and standard deviation for four experiments is shown. Notice that the order (anisotropy) is strongly correlated with sterol raft-forming ability (Table 4.1).

Chapter 5:

Summary and Future directions

Detection of ordered nanodomains in model membranes

Over the course of this thesis project, we studied ordered domain formation in model membranes and cells. Initially we measured the stability of the liquid ordered state in vesicles composed of an equimolar mixture of sphingomyelin, 1-palmitoyl-2-oleoyl phosphatidylcholine and cholesterol. The reason for choosing this lipid mixture was the reported lack of ordered domain formation by calorimetry in the absence of TX-100, and their formation once TX-100 was added. This was a concern since SM/POPC/chol closely represents the lipid composition of the outer leaflet of the mammalian cell plasma membrane. Another concern was that calorimetry, which detects melting of domains, may not detect the not-so-co-operative melting of small domains. Therefore, to test whether membranes made up of SM/POPC/chol are ordered, and to determine the effect TX-100 on their formation and stability, we used methods that can detect the formation of very small domains. Since fluorescence quenching is strong only when the fluorophore and quencher are placed within the critical distance co-incidentally comparable to the diameter of a lipid, quenching can, in theory detect order in a range as close as the circle of lipids surrounding the donor lipid molecule. We used quenching by TEMPO, which binds to Ld domains than to ordered domains. In addition, anisotropy is a measure of local order in the membrane. We found that SM/POPC/chol was ordered and thermally transitioned into a disordered membrane at a mid-point melting temperature centered at 46^{o}C. Importantly, neither TX-100 nor a transmembrane peptide had any effect on the amount of ordered domains as judged by the un-perturbed thermal transition.

However, we were ultimately interested in determining whether the membrane was segregated into Lo and Ld domains. Therefore, we used methods that were dependent on lipid segregation such as FRET. We chose donors and acceptors that had different affinities for Lo and Ld domains. So when domains were present, the donor and acceptor were segregated from each other resulting in weak FRET. At higher temperature, Lo transitioned into Ld and the segregation was lost resulting in strong FRET. Compared to quenching, the thermal stability of SM/POPC/chol by FRET between NBD-DPPE and rhodamine-DOPE showed a striking decrease in the T_{mid} value from 46 to 9 ^{o}C. FRET could not detect domains at the temperatures where both quenching and anisotropy could. In contrast, in the presence of TX-100 or a

transmembrane peptide, the domains could be easily detected by FRET at temperatures comparable to those detected by quenching and anisotropy.

Why were FRET and quenching measuring a different T_{mid} for SM/POPC/chol under the same experimental conditions? And why, in the presence of TX-100 and transmembrane peptide would FRET detected domain segregation increase so dramatically when the overall membrane order remained the same? These puzzling observations led us to a new hypothesis. Since in comparison to quenching, FRET between NBD and rhodamine was a longer range process, one having an interaction distance upto four times that of quenching, domains in SM/POPC/chol may be too small to be detected by the NBD-rhodamine FRET pair. In order to test this hypothesis, we needed a short range detection method that was based on lipid segregation and that could detect even smaller but separate Lo and Ld domains. Therefore we used a method that was previously developed by our lab: quenching by a nitroxide labeled phospholipid 10SLPC, which prefers to reside within the Ld domains in a bilayer containing Lo and Ld domains. The advantage of using a quencher labeled lipid over TEMPO was that 10SLPC is a lipid that would insert into the bilayers and quenching would depend on lipid segregation rather than quencher binding to membranes. Quenching by 10SLPC showed that domains were present at temperatures similar to those observed by the other short range methods, thus supporting our hypothesis that domain size gradually decreases with temperature. Long range FRET interactions could not detect small domains since domain radius was required to be greater than the FRET interaction distance in order to be detected. To further confirm this hypothesis, we used FRET pairs having a range of interaction distances that were in between that of long range NBD-rhodamine pair and the short range quenching pair. We observed that domains could be more easily detected at higher temperatures as a FRET pair with a smaller interaction distance was used.

Since the difference between T_{mid} in the absence and presence of TX-100 was lower when FRET probes with smaller Ro were used, it was concluded that the TX-100 as well as the transmembrane peptide increased domain size.

Cell membranes contain large amounts of transmembrane peptides, which are portions of transmembrane proteins. We found that at cholesterol levels close to physiological,

transmembrane peptide increased domain size even more than TX-100. This finding supports the hypothesis of lipid segregation in natural membranes where cholesterol concentration is high.

Proving rafts exist in living cells:

Still, proving that a model membrane vesicle contains segregated Lo and Ld domains does not prove their existence in living cells. We got an opportunity to modify and apply our FRET method of detecting lipid segregation to directly probe domain formation in living cells in collaboration with the laboratory of Dr. Benach. Their lab had recently discovered cholesterol-lipid rich domains in the outer membranes of *Borrelia burgdorferi*, a bacterium that causes Lyme disease. Together, we investigated whether these domains had all the characteristics of ordered domains by three different methods. My part of the project involved determining whether ordered domains formed in living cells using a novel FRET method that detected lipid segregation. Donor TMADPH and acceptor ODRB were chosen due to their different partition preferences in the Lo and Ld domains. We found that in living *B.burgdorferi* cells FRET was strong at high temperatures and became weaker at low temperatures. This clearly showed Lo and Ld domain segregation in the *B.burgdorferi* membrane.

Previously our lab had characterized sterols that have different abilities to form ordered domains. Our lab had shown that certain sterols such as ergosterol, 7-dehydrocholesterol and dihydrocholesterol have a strong tendency to support ordered domain formation. Other sterols such as lanosterol and zymosterol have intermediate tendency to support Lo domain formation. Sterols such as coprostanol and androsterol behave in the opposite direction and strongly destabilize ordered domain formation. In this report we tested the ability of a sterol to form domains in living *B.burgdorferi* cells. To determine whether formation of ordered domains was correlated with the raft forming ability of a sterol, we developed a sterol substitution strategy. We partially extracted cholesterol and cholesterol glycolipids (cholesterol-lipid) from the outer membrane and substituted with various domain promoting and domain inhibiting sterols. We found that in the outer membranes of *B.burgdorferi* the Lo domains were detected by FRET when Lo domain-promoting sterols were substituted for cholesterol lipid whereas Lo domains could not be detected when cholesterol-lipid was substituted with the domain-inhibiting sterols.

This clearly and unambiguously showed that domains rich in cholesterol and cholesterol glycolipids present in the *B.burgdorferi* outer membrane are indeed ordered domains.

These studies provide a novel FRET assay using probes that could be added externally to model membrane liposomes and cells. Since the effective Ro of the FRET pair used was found to be 23 Å, domains having radii just greater than just a couple of nanometers can be detected. Thus ordered domain formation based on lipid segregation in eukaryotic membranes (which are believed to form very small nanoscopic domains) may be studied using this approach.

Future Directions:

Effect of lipid composition on ordered domain stability and size:

Since the lipid mixture that mimics the composition of the outer leaflet of mammalian cell plasma membranes, namely SM/POPC/cholesterol, forms very small nanodomains at physiological temperature, it would be interesting to study how lipid composition affects the size of ordered domains . It would also be interesting to investigate the effect of TX-100 and transmembrane peptides on the size of ordered domains formed by the various lipid mixtures. If domains present without TX-100 are already large, we would not expect TX-100 to further significantly increase domain size.

We think the reason why TX-100 increases the domain size is that it increases the height mismatch between the Lo and Ld domains. Height mismatch between Lo formed by SM/chol and Ld formed by POPC may differ from other Lo and Ld forming molecules. For that reason, it would be interesting to use a lipid mixture that contains Lo and Ld forming lipids of different lengths. By making combinations of long and short Lo and Ld forming acyl chain lipids, we could investigate the effect of acyl chain length and domain thickness on domain size and the effect TX-100 and transmembrane peptide have on this domain size. It would be interesting to measure the heights of the domains by AFM and co-relate the height mismatch between the domains to the effect of TX-100 on the size of the Lo domains.

For example, since POPC is a line active lipid, it should induce formation of small domains by SM/chol as well as with DPPC/chol. See Figure 2. If domains formed by DPPC/chol with DOPC as the low Tm lipid are for some reason larger than those formed by SM/chol/DOPC and thus easily detectable, those domains will become a little smaller with POPC but will still remain detectable at temperatures where domains in SM/chol/POPC cannot be detected. This will answer the question whether TX-100 has an effect only when POPC is present or does it have an effect only when SM is the Lo forming lipid.

Transmembrane peptides of different lengths may have an effect on the domain size. Longer peptides may either tilt, or if vertical, may extend the lipids to reduce the mis- match between the width of the lipid bilayer and the length of the peptide. And since, by extending Ld lipids, the

height difference in between Lo and Ld will be reduced, these peptides may not make the domains larger.

Domain formation in bacteria:

Identifying ordered domain forming molecules in *B.burgdorferi*: We know that total lipid extracts from *B.burgdorferi* form co-existing Lo and Ld domains. The next step would be to focus on what lipids in the outer membrane of *B.burgdorferi* play a role in the formation of ordered domains. This can be done by isolating the lipids and re-constituting them in model membrane liposomes.

Apart from *B.burgdorferi,* a few other bacteria incorporate host derived cholesterol in their membranes and it is yet not known whether their membranes are organized into domains. It will be interesting to survey membrane structure and function of other sterol containing bacteria.

Chapter 6

References:

1. Schroeder, R., London, E., and Brown, D. (1994) *Proc Natl Acad Sci U S A* Interactions between saturated acyl chains confer detergent resistance on lipids and glycosylphosphatidylinositol (GPI)-anchored proteins: GPI-anchored proteins in liposomes and cells show similar behavior **91**, 12130-12134
2. Simons, K., and Ikonen, E. (1997) *Nature* Functional rafts in cell membranes **387**, 569-572
3. Brown, D. A., and London, E. (1998) *Annu Rev Cell Dev Biol* Functions of lipid rafts in biological membranes **14**, 111-136
4. London, E. (2005) *Biochim Biophys Acta* How principles of domain formation in model membranes may explain ambiguities concerning lipid raft formation in cells **1746**, 203-220
5. Brown, D. A., and London, E. (2000) *J Biol Chem* Structure and function of sphingolipid- and cholesterol-rich membrane rafts **275**, 17221-17224
6. Takeda, M., Leser, G. P., Russell, C. J., and Lamb, R. A. (2003) *Proc Natl Acad Sci U S A* Influenza virus hemagglutinin concentrates in lipid raft microdomains for efficient viral fusion **100**, 14610-14617
7. Field, K. A., Holowka, D., and Baird, B. (1995) *Proc Natl Acad Sci U S A* Fc epsilon RI-mediated recruitment of p53/56lyn to detergent-resistant membrane domains accompanies cellular signaling **92**, 9201-9205
8. Manes, S., del Real, G., and Martinez, A. C. (2003) *Nat Rev Immunol* Pathogens: raft hijackers **3**, 557-568
9. Simons, K., and van Meer, G. (1988) *Biochemistry* Lipid sorting in epithelial cells **27**, 6197-6202
10. Scolari, S., Engel, S., Krebs, N., Plazzo, A. P., De Almeida, R. F., Prieto, M., Veit, M., and Herrmann, A. (2009) *J Biol Chem* Lateral distribution of the transmembrane domain of influenza virus hemagglutinin revealed by time-resolved fluorescence imaging **284**, 15708-15716
11. Leslie, M. (2011) *Science* Mysteries of the cell. Do lipid rafts exist? **334**, 1046-1047
12. Singer, S. J., and Nicolson, G. L. (1972) *Science* The fluid mosaic model of the structure of cell membranes **175**, 720-731
13. Frye, L. D., and Edidin, M. (1970) *J Cell Sci* The rapid intermixing of cell surface antigens after formation of mouse-human heterokaryons **7**, 319-335
14. Ahmed, S. N., Brown, D. A., and London, E. (1997) *Biochemistry* On the origin of sphingolipid/cholesterol-rich detergent-insoluble cell membranes: physiological concentrations of cholesterol and sphingolipid induce formation of a detergent-insoluble, liquid-ordered lipid phase in model membranes **36**, 10944-10953
15. Feigenson, G. W. (2009) *Biochim Biophys Acta* Phase diagrams and lipid domains in multicomponent lipid bilayer mixtures **1788**, 47-52
16. Yu, J., Fischman, D. A., and Steck, T. L. (1973) *J Supramol Struct* Selective solubilization of proteins and phospholipids from red blood cell membranes by nonionic detergents **1**, 233-248
17. Thompson, T. E., and Tillack, T. W. (1985) *Annu Rev Biophys Biophys Chem* Organization of glycosphingolipids in bilayers and plasma membranes of mammalian cells **14**, 361-386
18. Brown, D. A., Crise, B., and Rose, J. K. (1989) *Science* Mechanism of membrane anchoring affects polarized expression of two proteins in MDCK cells **245**, 1499-1501
19. Brown, D. A., and Rose, J. K. (1992) *Cell* Sorting of GPI-anchored proteins to glycolipid-enriched membrane subdomains during transport to the apical cell surface **68**, 533-544
20. van Meer, G., Stelzer, E. H., Wijnaendts-van-Resandt, R. W., and Simons, K. (1987) *J Cell Biol* Sorting of sphingolipids in epithelial (Madin-Darby canine kidney) cells **105**, 1623-1635
21. van Meer, G., Gumbiner, B., and Simons, K. (1986) *Nature* The tight junction does not allow lipid molecules to diffuse from one epithelial cell to the next **322**, 639-641

22. Skibbens, J. E., Roth, M. G., and Matlin, K. S. (1989) *J Cell Biol* Differential extractability of influenza virus hemagglutinin during intracellular transport in polarized epithelial cells and nonpolar fibroblasts **108**, 821-832
23. Brown, D. A., and London, E. (1998) *J Membr Biol* Structure and origin of ordered lipid domains in biological membranes **164**, 103-114
24. Ostermeyer, A. G., Beckrich, B. T., Ivarson, K. A., Grove, K. E., and Brown, D. A. (1999) *J Biol Chem* Glycosphingolipids are not essential for formation of detergent-resistant membrane rafts in melanoma cells. methyl-beta-cyclodextrin does not affect cell surface transport of a GPI-anchored protein **274**, 34459-34466
25. Lawrence, J. C., Saslowsky, D. E., Edwardson, J. M., and Henderson, R. M. (2003) *Biophys J* Real-time analysis of the effects of cholesterol on lipid raft behavior using atomic force microscopy **84**, 1827-1832
26. Ipsen, J. H., Karlstrom, G., Mouritsen, O. G., Wennerstrom, H., and Zuckermann, M. J. (1987) *Biochim Biophys Acta* Phase equilibria in the phosphatidylcholine-cholesterol system **905**, 162-172
27. Almeida, P. F., Vaz, W. L., and Thompson, T. E. (1992) *Biochemistry* Lateral diffusion in the liquid phases of dimyristoylphosphatidylcholine/cholesterol lipid bilayers: a free volume analysis **31**, 6739-6747
28. Gandhavadi, M., Allende, D., Vidal, A., Simon, S. A., and McIntosh, T. J. (2002) *Biophys J* Structure, composition, and peptide binding properties of detergent soluble bilayers and detergent resistant rafts **82**, 1469-1482
29. London, E., and Brown, D. A. (2000) *Biochim Biophys Acta* Insolubility of lipids in triton X-100: physical origin and relationship to sphingolipid/cholesterol membrane domains (rafts) **1508**, 182-195
30. Bakht, O., and London, E. (2007) *Methods Mol Biol* Detecting ordered domain formation (lipid rafts) in model membranes using Tempo **398**, 29-40
31. Koynova, R., and Caffrey, M. (1995) *Biochim Biophys Acta* Phases and phase transitions of the sphingolipids **1255**, 213-236
32. Baumgart, T., Hess, S. T., and Webb, W. W. (2003) *Nature* Imaging coexisting fluid domains in biomembrane models coupling curvature and line tension **425**, 821-824
33. Brown, D. A. (2007) *Methods Mol Biol* Analysis of raft affinity of membrane proteins by detergent-insolubility **398**, 9-20
34. Garner, A. E., Smith, D. A., and Hooper, N. M. (2008) *Biophys J* Visualization of detergent solubilization of membranes: implications for the isolation of rafts **94**, 1326-1340
35. Dietrich, C., Bagatolli, L. A., Volovyk, Z. N., Thompson, N. L., Levi, M., Jacobson, K., and Gratton, E. (2001) *Biophys J* Lipid rafts reconstituted in model membranes **80**, 1417-1428
36. El Kirat, K., and Morandat, S. (2007) *Biochim Biophys Acta* Cholesterol modulation of membrane resistance to Triton X-100 explored by atomic force microscopy **1768**, 2300-2309
37. Ge, M., Field, K. A., Aneja, R., Holowka, D., Baird, B., and Freed, J. H. (1999) *Biophys J* Electron spin resonance characterization of liquid ordered phase of detergent-resistant membranes from RBL-2H3 cells **77**, 925-933
38. Sheets, E. D., Lee, G. M., Simson, R., and Jacobson, K. (1997) *Biochemistry* Transient confinement of a glycosylphosphatidylinositol-anchored protein in the plasma membrane **36**, 12449-12458
39. Rinia, H. A., Snel, M. M., van der Eerden, J. P., and de Kruijff, B. (2001) *FEBS Lett* Visualizing detergent resistant domains in model membranes with atomic force microscopy **501**, 92-96
40. Morandat, S., and El Kirat, K. (2006) *Langmuir* Membrane resistance to Triton X-100 explored by real-time atomic force microscopy **22**, 5786-5791

41. Shogomori, H., Hammond, A. T., Ostermeyer-Fay, A. G., Barr, D. J., Feigenson, G. W., London, E., and Brown, D. A. (2005) *J Biol Chem* Palmitoylation and intracellular domain interactions both contribute to raft targeting of linker for activation of T cells **280**, 18931-18942
42. Shogomori, H., and Brown, D. A. (2003) *Biol Chem* Use of detergents to study membrane rafts: the good, the bad, and the ugly **384**, 1259-1263
43. Schuck, S., Honsho, M., Ekroos, K., Shevchenko, A., and Simons, K. (2003) *Proc Natl Acad Sci U S A* Resistance of cell membranes to different detergents **100**, 5795-5800
44. Kurzchalia, T. V., Dupree, P., Parton, R. G., Kellner, R., Virta, H., Lehnert, M., and Simons, K. (1992) *J Cell Biol* VIP21, a 21-kD membrane protein is an integral component of trans-Golgi-network-derived transport vesicles **118**, 1003-1014
45. Roper, K., Corbeil, D., and Huttner, W. B. (2000) *Nat Cell Biol* Retention of prominin in microvilli reveals distinct cholesterol-based lipid micro-domains in the apical plasma membrane **2**, 582-592
46. Watanabe, S., Takahashi, N., Uchida, H., and Wakasugi, K. (2012) *J Biol Chem* Human neuroglobin functions as an oxidative stress-responsive sensor for neuroprotection
47. Madore, N., Smith, K. L., Graham, C. H., Jen, A., Brady, K., Hall, S., and Morris, R. (1999) *EMBO J* Functionally different GPI proteins are organized in different domains on the neuronal surface **18**, 6917-6926
48. Drobnik, W., Borsukova, H., Bottcher, A., Pfeiffer, A., Liebisch, G., Schutz, G. J., Schindler, H., and Schmitz, G. (2002) *Traffic* Apo AI/ABCA1-dependent and HDL3-mediated lipid efflux from compositionally distinct cholesterol-based microdomains **3**, 268-278
49. Braccia, A., Villani, M., Immerdal, L., Niels-Christiansen, L. L., Nystrom, B. T., Hansen, G. H., and Danielsen, E. M. (2003) *J Biol Chem* Microvillar membrane microdomains exist at physiological temperature. Role of galectin-4 as lipid raft stabilizer revealed by "superrafts" **278**, 15679-15684
50. Ismair, M. G., Hausler, S., Stuermer, C. A., Guyot, C., Meier, P. J., Roth, J., and Stieger, B. (2009) *Hepatology* ABC-transporters are localized in caveolin-1-positive and reggie-1-negative and reggie-2-negative microdomains of the canalicular membrane in rat hepatocytes **49**, 1673-1682
51. Eckhardt, E. R., Moschetta, A., Renooij, W., Goerdayal, S. S., van Berge-Henegouwen, G. P., and van Erpecum, K. J. (1999) *J Lipid Res* Asymmetric distribution of phosphatidylcholine and sphingomyelin between micellar and vesicular phases. Potential implications for canalicular bile formation **40**, 2022-2033
52. Ray, S., Taylor, M., Banerjee, T., Tatulian, S. A., and Teter, K. (2012) *J Biol Chem* Lipid Rafts Alter the Stability and Activity of the Cholera Toxin A1 Subunit
53. Saher, G., Rudolphi, F., Corthals, K., Ruhwedel, T., Schmidt, K. F., Lowel, S., Dibaj, P., Barrette, B., Mobius, W., and Nave, K. A. (2012) *Nat Med* Therapy of Pelizaeus-Merzbacher disease in mice by feeding a cholesterol-enriched diet
54. Hammond, A. T., Heberle, F. A., Baumgart, T., Holowka, D., Baird, B., and Feigenson, G. W. (2005) *Proc Natl Acad Sci U S A* Crosslinking a lipid raft component triggers liquid ordered-liquid disordered phase separation in model plasma membranes **102**, 6320-6325
55. Frazier, M. L., Wright, J. R., Pokorny, A., and Almeida, P. F. (2007) *Biophys J* Investigation of domain formation in sphingomyelin/cholesterol/POPC mixtures by fluorescence resonance energy transfer and Monte Carlo simulations **92**, 2422-2433
56. Heberle, F. A., Wu, J., Goh, S. L., Petruzielo, R. S., and Feigenson, G. W. (2010) *Biophys J* Comparison of three ternary lipid bilayer mixtures: FRET and ESR reveal nanodomains **99**, 3309-3318
57. Sengupta, P., Holowka, D., and Baird, B. (2007) *Biophys J* Fluorescence resonance energy transfer between lipid probes detects nanoscopic heterogeneity in the plasma membrane of live cells **92**, 3564-3574

58. Silvius, J. R. (2003) *Biophys J* Fluorescence energy transfer reveals microdomain formation at physiological temperatures in lipid mixtures modeling the outer leaflet of the plasma membrane **85**, 1034-1045
59. Sohn, H. W., Tolar, P., and Pierce, S. K. (2008) *J Cell Biol* Membrane heterogeneities in the formation of B cell receptor-Lyn kinase microclusters and the immune synapse **182**, 367-379
60. Zech, T., Ejsing, C. S., Gaus, K., de Wet, B., Shevchenko, A., Simons, K., and Harder, T. (2009) *EMBO J* Accumulation of raft lipids in T-cell plasma membrane domains engaged in TCR signalling **28**, 466-476
61. Gaus, K., Gratton, E., Kable, E. P., Jones, A. S., Gelissen, I., Kritharides, L., and Jessup, W. (2003) *Proc Natl Acad Sci U S A* Visualizing lipid structure and raft domains in living cells with two-photon microscopy **100**, 15554-15559
62. Owen, D. M., Magenau, A., Majumdar, A., and Gaus, K. (2010) *Biophys J* Imaging membrane lipid order in whole, living vertebrate organisms **99**, L7-9
63. Pralle, A., Keller, P., Florin, E. L., Simons, K., and Horber, J. K. (2000) *J Cell Biol* Sphingolipid-cholesterol rafts diffuse as small entities in the plasma membrane of mammalian cells **148**, 997-1008
64. Swamy, M. J., Ciani, L., Ge, M., Smith, A. K., Holowka, D., Baird, B., and Freed, J. H. (2006) *Biophys J* Coexisting domains in the plasma membranes of live cells characterized by spin-label ESR spectroscopy **90**, 4452-4465
65. Sampaio, J. L., Gerl, M. J., Klose, C., Ejsing, C. S., Beug, H., Simons, K., and Shevchenko, A. (2011) *Proc Natl Acad Sci U S A* Membrane lipidome of an epithelial cell line **108**, 1903-1907
66. Wenk, M. R. (2010) *Cell* Lipidomics: new tools and applications **143**, 888-895
67. Gerl, M. J., Sampaio, J. L., Urban, S., Kalvodova, L., Verbavatz, J. M., Binnington, B., Lindemann, D., Lingwood, C. A., Shevchenko, A., Schroeder, C., and Simons, K. (2012) *J Cell Biol* Quantitative analysis of the lipidomes of the influenza virus envelope and MDCK cell apical membrane **196**, 213-221
68. Baird, B., Sheets, E. D., and Holowka, D. (1999) *Biophys Chem* How does the plasma membrane participate in cellular signaling by receptors for immunoglobulin E? **82**, 109-119
69. Sheets, E. D., Holowka, D., and Baird, B. (1999) *J Cell Biol* Critical role for cholesterol in Lyn-mediated tyrosine phosphorylation of FcepsilonRI and their association with detergent-resistant membranes **145**, 877-887
70. Young, R. M., Holowka, D., and Baird, B. (2003) *J Biol Chem* A lipid raft environment enhances Lyn kinase activity by protecting the active site tyrosine from dephosphorylation **278**, 20746-20752
71. Chamberlain, L. H., Burgoyne, R. D., and Gould, G. W. (2001) *Proc Natl Acad Sci U S A* SNARE proteins are highly enriched in lipid rafts in PC12 cells: implications for the spatial control of exocytosis **98**, 5619-5624
72. Holzer, R. G., Park, E. J., Li, N., Tran, H., Chen, M., Choi, C., Solinas, G., and Karin, M. (2011) *Cell* Saturated fatty acids induce c-Src clustering within membrane subdomains, leading to JNK activation **147**, 173-184
73. Baumgart, T., Hammond, A. T., Sengupta, P., Hess, S. T., Holowka, D. A., Baird, B. A., and Webb, W. W. (2007) *Proc Natl Acad Sci U S A* Large-scale fluid/fluid phase separation of proteins and lipids in giant plasma membrane vesicles **104**, 3165-3170
74. Lingwood, D., Ries, J., Schwille, P., and Simons, K. (2008) *Proc Natl Acad Sci U S A* Plasma membranes are poised for activation of raft phase coalescence at physiological temperature **105**, 10005-10010

75. Korlach, J., Schwille, P., Webb, W. W., and Feigenson, G. W. (1999) *Proc Natl Acad Sci U S A* Characterization of lipid bilayer phases by confocal microscopy and fluorescence correlation spectroscopy **96**, 8461-8466
76. Kahya, N., Scherfeld, D., Bacia, K., Poolman, B., and Schwille, P. (2003) *J Biol Chem* Probing lipid mobility of raft-exhibiting model membranes by fluorescence correlation spectroscopy **278**, 28109-28115
77. Silvius, J. R., del Giudice, D., and Lafleur, M. (1996) *Biochemistry* Cholesterol at different bilayer concentrations can promote or antagonize lateral segregation of phospholipids of differing acyl chain length **35**, 15198-15208
78. Beattie, M. E., Veatch, S. L., Stottrup, B. L., and Keller, S. L. (2005) *Biophys J* Sterol structure determines miscibility versus melting transitions in lipid vesicles **89**, 1760-1768
79. Suzuki, K. G., Kasai, R. S., Hirosawa, K. M., Nemoto, Y. L., Ishibashi, M., Miwa, Y., Fujiwara, T. K., and Kusumi, A. (2012) *Nat Chem Biol* Transient GPI-anchored protein homodimers are units for raft organization and function
80. Pandit, S. A., Khelashvili, G., Jakobsson, E., Grama, A., and Scott, H. L. (2007) *Biophys J* Lateral organization in lipid-cholesterol mixed bilayers **92**, 440-447
81. Pandit, S. A., and Scott, H. L. (2007) *Methods Mol Biol* Atomistic and coarse-grained computer simulations of raft-like lipid mixtures **398**, 283-302
82. van Meer, G., Voelker, D. R., and Feigenson, G. W. (2008) *Nat Rev Mol Cell Biol* Membrane lipids: where they are and how they behave **9**, 112-124
83. Feigenson, G. W., and Buboltz, J. T. (2001) *Biophys J* Ternary phase diagram of dipalmitoyl-PC/dilauroyl-PC/cholesterol: nanoscopic domain formation driven by cholesterol **80**, 2775-2788
84. Pandit, S. A., Jakobsson, E., and Scott, H. L. (2004) *Biophys J* Simulation of the early stages of nano-domain formation in mixed bilayers of sphingomyelin, cholesterol, and dioleylphosphatidylcholine **87**, 3312-3322
85. Fastenberg, M. E., Shogomori, H., Xu, X., Brown, D. A., and London, E. (2003) *Biochemistry* Exclusion of a transmembrane-type peptide from ordered-lipid domains (rafts) detected by fluorescence quenching: extension of quenching analysis to account for the effects of domain size and domain boundaries **42**, 12376-12390
86. Garcia-Saez, A. J., Chiantia, S., and Schwille, P. (2007) *J Biol Chem* Effect of line tension on the lateral organization of lipid membranes **282**, 33537-33544
87. Xu, X., Bittman, R., Duportail, G., Heissler, D., Vilcheze, C., and London, E. (2001) *J Biol Chem* Effect of the structure of natural sterols and sphingolipids on the formation of ordered sphingolipid/sterol domains (rafts). Comparison of cholesterol to plant, fungal, and disease-associated sterols and comparison of sphingomyelin, cerebrosides, and ceramide **276**, 33540-33546
88. Xu, X., and London, E. (2000) *Biochemistry* The effect of sterol structure on membrane lipid domains reveals how cholesterol can induce lipid domain formation **39**, 843-849
89. Wang, J., Megha, and London, E. (2004) *Biochemistry* Relationship between sterol/steroid structure and participation in ordered lipid domains (lipid rafts): implications for lipid raft structure and function **43**, 1010-1018
90. Rog, T., Pasenkiewicz-Gierula, M., Vattulainen, I., and Karttunen, M. (2007) *Biophys J* What happens if cholesterol is made smoother: importance of methyl substituents in cholesterol ring structure on phosphatidylcholine-sterol interaction **92**, 3346-3357
91. Bagatolli, L., Gratton, E., Khan, T. K., and Chong, P. L. (2000) *Biophys J* Two-photon fluorescence microscopy studies of bipolar tetraether giant liposomes from thermoacidophilic archaebacteria Sulfolobus acidocaldarius **79**, 416-425

92. Kaiser, H. J., Surma, M. A., Mayer, F., Levental, I., Grzybek, M., Klemm, R. W., Da Cruz, S., Meisinger, C., Muller, V., Simons, K., and Lingwood, D. (2011) *J Biol Chem* Molecular convergence of bacterial and eukaryotic surface order **286**, 40631-40637
93. Haque, M., Hirai, Y., Yokota, K., and Oguma, K. (1995) *J Bacteriol* Steryl glycosides: a characteristic feature of the Helicobacter spp.? **177**, 5334-5337
94. Hirai, Y., Haque, M., Yoshida, T., Yokota, K., Yasuda, T., and Oguma, K. (1995) *J Bacteriol* Unique cholesteryl glucosides in Helicobacter pylori: composition and structural analysis **177**, 5327-5333
95. Lin, M., and Rikihisa, Y. (2003) *Infect Immun* Ehrlichia chaffeensis and Anaplasma phagocytophilum lack genes for lipid A biosynthesis and incorporate cholesterol for their survival **71**, 5324-5331
96. Smith, P. F. (1971) *J Bacteriol* Biosynthesis of cholesteryl glucoside by Mycoplasma gallinarum **108**, 986-991
97. Benach, J. L., Bosler, E. M., Hanrahan, J. P., Coleman, J. L., Habicht, G. S., Bast, T. F., Cameron, D. J., Ziegler, J. L., Barbour, A. G., Burgdorfer, W., Edelman, R., and Kaslow, R. A. (1983) *N Engl J Med* Spirochetes isolated from the blood of two patients with Lyme disease **308**, 740-742
98. Johnson, R. C. (1977) *Annu Rev Microbiol* The spirochetes **31**, 89-106
99. Ben-Menachem, G., Kubler-Kielb, J., Coxon, B., Yergey, A., and Schneerson, R. (2003) *Proc Natl Acad Sci U S A* A newly discovered cholesteryl galactoside from Borrelia burgdorferi **100**, 7913-7918
100. LaRocca, T. J., Crowley, J. T., Cusack, B. J., Pathak, P., Benach, J., London, E., Garcia-Monco, J. C., and Benach, J. L. (2010) *Cell Host Microbe* Cholesterol lipids of Borrelia burgdorferi form lipid rafts and are required for the bactericidal activity of a complement-independent antibody **8**, 331-342
101. LaRocca, T. J., Holthausen, D. J., Hsieh, C., Renken, C., Mannella, C. A., and Benach, J. L. (2009) *Proc Natl Acad Sci U S A* The bactericidal effect of a complement-independent antibody is osmolytic and specific to Borrelia **106**, 10752-10757
102. Crane, J. M., and Tamm, L. K. (2004) *Biophys J* Role of cholesterol in the formation and nature of lipid rafts in planar and spherical model membranes **86**, 2965-2979
103. Cheng, H. T., Megha, and London, E. (2009) *J Biol Chem* Preparation and properties of asymmetric vesicles that mimic cell membranes: effect upon lipid raft formation and transmembrane helix orientation **284**, 6079-6092
104. Dietrich, C., Volovyk, Z. N., Levi, M., Thompson, N. L., and Jacobson, K. (2001) *Proc Natl Acad Sci U S A* Partitioning of Thy-1, GM1, and cross-linked phospholipid analogs into lipid rafts reconstituted in supported model membrane monolayers **98**, 10642-10647
105. Morandat, S., and El Kirat, K. (2007) *Langmuir* Real-time atomic force microscopy reveals cytochrome c-induced alterations in neutral lipid bilayers **23**, 10929-10932
106. Heerklotz, H. (2002) *Biophys J* Triton promotes domain formation in lipid raft mixtures **83**, 2693-2701
107. Heerklotz, H., Szadkowska, H., Anderson, T., and Seelig, J. (2003) *J Mol Biol* The sensitivity of lipid domains to small perturbations demonstrated by the effect of Triton **329**, 793-799
108. Kleemann, W., and McConnell, H. M. (1976) *Biochim Biophys Acta* Interactions of proteins and cholesterol with lipids in bilayer membranes **419**, 206-222
109. Lentz, B. R., Barenholz, Y., and Thompson, T. E. (1976) *Biochemistry* Fluorescence depolarization studies of phase transitions and fluidity in phospholipid bilayers. 2 Two-component phosphatidylcholine liposomes **15**, 4529-4537
110. Chattopadhyay, A., and London, E. (1984) *Anal Biochem* Fluorimetric determination of critical micelle concentration avoiding interference from detergent charge **139**, 408-412

111. Wenz, J. J., and Barrantes, F. J. (2003) *Biochemistry* Steroid structural requirements for stabilizing or disrupting lipid domains **42**, 14267-14276
112. Alanko, S. M., Halling, K. K., Maunula, S., Slotte, J. P., and Ramstedt, B. (2005) *Biochim Biophys Acta* Displacement of sterols from sterol/sphingomyelin domains in fluid bilayer membranes by competing molecules **1715**, 111-121
113. Chattopadhyay, A., and London, E. (1987) *Biochemistry* Parallax method for direct measurement of membrane penetration depth utilizing fluorescence quenching by spin-labeled phospholipids **26**, 39-45
114. Ayuyan, A. G., and Cohen, F. S. (2008) *Biophys J* Raft composition at physiological temperature and pH in the absence of detergents **94**, 2654-2666
115. Honerkamp-Smith, A. R., Cicuta, P., Collins, M. D., Veatch, S. L., den Nijs, M., Schick, M., and Keller, S. L. (2008) *Biophys J* Line tensions, correlation lengths, and critical exponents in lipid membranes near critical points **95**, 236-246
116. Staneva, G., Seigneuret, M., Koumanov, K., Trugnan, G., and Angelova, M. I. (2005) *Chem Phys Lipids* Detergents induce raft-like domains budding and fission from giant unilamellar heterogeneous vesicles: a direct microscopy observation **136**, 55-66
117. Ben-Menachem, G., Bystrom, T., Rechnitzer, H., Rottem, S., Rilfors, L., and Lindblom, G. (2001) *Eur J Biochem* The physico-chemical characteristics of the phosphocholine-containing glycoglycerolipid MfGL-II govern the permeability properties of Mycoplasma fermentans **268**, 3694-3701
118. Burgdorfer, W., Barbour, A. G., Hayes, S. F., Benach, J. L., Grunwaldt, E., and Davis, J. P. (1982) *Science* Lyme disease-a tick-borne spirochetosis? **216**, 1317-1319
119. Motaleb, M. A., Corum, L., Bono, J. L., Elias, A. F., Rosa, P., Samuels, D. S., and Charon, N. W. (2000) *Proc Natl Acad Sci U S A* Borrelia burgdorferi periplasmic flagella have both skeletal and motility functions **97**, 10899-10904
120. LaRocca, T. J., and Benach, J. L. (2008) *Curr Top Microbiol Immunol* The important and diverse roles of antibodies in the host response to *Borrelia* infections **319**, 63-103
121. Belisle, J. T., Brandt, M. E., Radolf, J. D., and Norgard, M. V. (1994) *J Bacteriol* Fatty acids of Treponema pallidum and Borrelia burgdorferi lipoproteins **176**, 2151-2157
122. Jones, J. D., Bourell, K. W., Norgard, M. V., and Radolf, J. D. (1995) *Infect Immun* Membrane topology of Borrelia burgdorferi and Treponema pallidum lipoproteins **63**, 2424-2434
123. Radolf, J. D., Goldberg, M. S., Bourell, K., Baker, S. I., Jones, J. D., and Norgard, M. V. (1995) *Infect Immun* Characterization of outer membranes isolated from Borrelia burgdorferi, the Lyme disease spirochete **63**, 2154-2163
124. Stubs, G., Fingerle, V., Wilske, B., Gobel, U. B., Zahringer, U., Schumann, R. R., and Schroder, N. W. (2009) *J Biol Chem* Acylated cholesteryl galactosides are specific antigens of Borrelia causing lyme disease and frequently induce antibodies in late stages of disease
125. Schroder, N. W., Schombel, U., Heine, H., Gobel, U. B., Zahringer, U., and Schumann, R. R. (2003) *J Biol Chem* Acylated cholesteryl galactoside as a novel immunogenic motif in Borrelia burgdorferi sensu stricto **278**, 33645-33653
126. Trott, D. J., Alt, D. P., Zuerner, R. L., Wannemuehler, M. J., and Stanton, T. B. (2001) *Anim Health Res Rev* The search for Brachyspira outer membrane proteins that interact with the host **2**, 19-30
127. London, E. (2002) *Curr Opin Struct Biol* Insights into lipid raft structure and formation from experiments in model membranes **12**, 480-486
128. Harder, T. (2012) *Frontiers in immunology* The T Cell Plasma Membrane Lipid Bilayer Stages TCR-proximal Signaling Events **3**, 50

129. Pierce, S. K., and Liu, W. (2010) *Nature reviews. Immunology* The tipping points in the initiation of B cell signalling: how small changes make big differences **10**, 767-777
130. Owen, D. M., Magenau, A., Williamson, D., and Gaus, K. (2012) *BioEssays : news and reviews in molecular, cellular and developmental biology* The lipid raft hypothesis revisited - New insights on raft composition and function from super-resolution fluorescence microscopy **34**, 739-747
131. Megha, Bakht, O., and London, E. (2006) *J Biol Chem* Cholesterol precursors stabilize ordinary and ceramide-rich ordered lipid domains (lipid rafts) to different degrees. Implications for the Bloch hypothesis and sterol biosynthesis disorders **281**, 21903-21913
132. Buranda, T., Wu, Y., Perez, D., Chigaev, A., and Sklar, L. A. (2010) *J Phys Chem B* Real-time partitioning of octadecyl rhodamine B into bead-supported lipid bilayer membranes revealing quantitative differences in saturable binding sites in DOPC and 1:1:1 DOPC/SM/cholesterol membranes **114**, 1336-1349
133. Loura, L. M., Fedorov, A., and Prieto, M. (2001) *Biochim Biophys Acta* Exclusion of a cholesterol analog from the cholesterol-rich phase in model membranes **1511**, 236-243
134. Bakht, O., Pathak, P., and London, E. (2007) *Biophys J* Effect of the structure of lipids favoring disordered domain formation on the stability of cholesterol-containing ordered domains (lipid rafts): identification of multiple raft-stabilization mechanisms **93**, 4307-4318
135. Simon-Plas, F., Perraki, A., Bayer, E., Gerbeau-Pissot, P., and Mongrand, S. (2011) *Curr Opin Plant Biol* An update on plant membrane rafts **14**, 642-649
136. Pathak, P., and London, E. (2011) *Biophys J* Measurement of lipid nanodomain (raft) formation and size in sphingomyelin/POPC/cholesterol vesicles shows TX-100 and transmembrane helices increase domain size by coalescing preexisting nanodomains but do not induce domain formation **101**, 2417-2425
137. Wigglesworth, V. B. (1948) *Biol Rev Camb Philos Soc* The insect cuticle **23**, 408-451